

AD-A145 365

(2)

AGARD-LS-135

AGARD-LS-135

AGARD

ADVISORY GROUP FOR AEROSPACE RESEARCH & DEVELOPMENT

7 RUE ANCELLE 92200 NEUILLY SUR SEINE FRANCE

AGARD LECTURE SERIES No.135

Advanced Technology for SAM Systems Analysis Synthesis and Simulation

DATE
SEP 07 1984
S E D

NORTH ATLANTIC TREATY ORGANIZATION



DISTRIBUTION AND AVAILABILITY
ON BACK COVER

1984 100 100 100 100 100

DTIC FILE COPY

NORTH ATLANTIC TREATY ORGANIZATION
ADVISORY GROUP FOR AEROSPACE RESEARCH AND DEVELOPMENT
(ORGANISATION DU TRAITE DE L'ATLANTIQUE NORD)

AGARD Lecture Series No.135
ADVANCED TECHNOLOGY FOR SAM SYSTEMS
ANALYSIS SYNTHESIS AND SIMULATION

Accession For	
NTM: GRA&I	
Date: 1984	
Type: Standard	
Title: Advanced Technology for SAM Systems	
Author: Various	
Subject: Analysis, Synthesis, and Simulation	
Classification:	
Availability Codes	
Part	Avail and/or Special
A-1	

0816
COPY
REPRODUCED
2

REPRODUCED FROM
BEST AVAILABLE COPY

The material in this publication was assembled to support a Lecture Series under the sponsorship of the Guidance and Control Panel and the Consultant and Exchange Programme of AGARD presented on 25-26 June 1984 at Porz-Wahn (Cologne), Germany; on 28-29 June 1984 in Rome, Italy and on 2-3 July 1984 in London, UK.

THE MISSION OF AGARD

The mission of AGARD is to bring together the leading personalities of the NATO nations in the fields of science and technology relating to aerospace for the following purposes:

- Exchanging of scientific and technical information;
- Continuously stimulating advance in the aerospace sciences relevant to strengthening the common defence posture;
- Improving the co-operation among member nations in aerospace research and development;
- Providing scientific and technical advice and assistance to the North Atlantic Military Committee in the field of aerospace research and development;
- Rendering scientific and technical assistance, as requested, to other NATO bodies and to member nations in connection with research and development problems in the aerospace field;
- Providing assistance to member nations for the purpose of increasing their scientific and technical potential;
- Recommending effective ways for the member nations to use their research and development capabilities for the common benefit of the NATO community.

The highest authority within AGARD is the National Delegates Board consisting of officially appointed senior representatives from each member nation. The mission of AGARD is carried out through the Panels which are composed of experts appointed by the National Delegates, the Consultant and Exchange Programme and the Aerospace Applications Studies Programme. The results of AGARD work are reported to the member nations and the NATO Authorities through the AGARD series of publications of which this is one.

Participation in AGARD activities is by invitation only and is normally limited to citizens of the NATO nations.

The content of this publication has been reproduced
directly from material supplied by AGARD or the authors.

Published May 1984

Copyright © AGARD 1984
All Rights Reserved

ISBN 92-835-0353-8



Printed by Specialised Printing Services Limited
40 Chigwell Lane, Loughton, Essex IG10 3TZ

LIST OF SPEAKERS

Lectur: Series Director: Mr M.Paulet

Direction Technique
Thomson-CSF (DSE)
1 Rue des Mathurins
92220 Bagneux
France

SPEAKERS

Mr R.C.Brown and Mr G.Santi
Selenia
Industria Elettroniche Associate S.p.A.
Via Tiburtina KM 12.400
00131 Rome
Italy

Mr A.Desmerger
Département RCM
Division Avionique
Thomson CSF
178 Bd. Gabriel Péri
92240 Malakoff
France

Mr J-L.Durieux
C.E.T.A.
28 rue de Belat
16000 Angouleme
France

Mr G.Selince
Groupe Etudes Futures
Division des Engins Tactiques
SNIAS (Aérospatiale)
2. Rue Béranger
92320 Châtillon sous Bagneux
France

Dr D.East
Electronics and Electrical
Engineering Department
RMCS, (Royal Military College of Science)
Shrivenham, Swindon
Wilt., SN6 8LA
UK

Mr J-F.Gondet
Matra B.M. R & D
B.P. 1
35 Avenue Louis Bréguet
78140 Velizy
France

Mr K.Grider
Systems Simulation and Development
DRS MR RD
US Army Missile Command
Redstone Arsenal
Huntsville, Alabama 35809
USA

Dr M.Held
Messerschmitt-Bölkow-Blohm GmbH
Abt. AG41
D-8898 Schröbenhausen
Germany

CONTENTS

	Page
LIST OF SPEAKERS	iii
TECHNIQUES AVANCEES POUR LES SYSTEMES DE MISSILES SOL-AIR ANALYSE, SYNTHESE ET SIMULATION ADVANCED TECHNOLOGY FOR S.A.M. SYSTEMS ANALYSIS, SYNTHESIS AND SIMULATION by M.Paulet	1
METHODOLOGIE DE LA CONCEPTION DES SYSTEMES D'ARMES FUTURS by J.F.Gondet	2
SOME ASPECTS OF GUIDANCE LOOP DESIGN FOR SAM SYSTEMS by D.J.East	3
TERMINAL CONTROL FOR COMMAND TO LINE OF SIGHT GUIDED MISSILE by J-L.Durieux	4
UN NOUVEAU CONCEPT DE PILOTAGE DES MISSILES APPLICATION AUX SOL-AIR by G.Selince	5
SEEKER SYSTEMS SIMULATION, PRESENT CAPABILITY AND FUTURE TECHNOLOGY by K.V.Grider	6
MISSILE SYSTEM FOR LOW ALTITUDE AIR DEFENCE by R.Brown and G.Santi	7
HOMING HEAD IMPERFECTIONS ALTERING MISSILE GUIDANCE by M.Desmeger	8
Paper 9 withdrawn	
WARHEADS FOR SAM SYSTEMS by M.Held	10

TECHNIQUES AVANCEES POUR LES SYSTEMES DE MISSILES SOL-AIR
ANALYSE, SYNTHESE ET SIMULATION

par

Marc Paulot
Thomson-CSF
Division Systèmes Electroniques
1 rue des Mathurins
92220 Bagneux
France

Cette série de conférences, proposée et soutenue par le Panel de Guidage et de Pilotage de l'AGARD, réalisée au titre du Programme d'Echanges et de Consultations, sera consacrée à examiner l'impact des techniques et technologies nouvelles dans les systèmes de missiles sol-air. Les exposés se placeront au triple point de vue de l'analyse, de la synthèse et de la simulation des systèmes. Mais le sujet étant immense, ils se limiteront pour l'essentiel aux aspects de guidage et de pilotage des missiles.

Immense, le sujet l'est d'abord par son importance. Certains événements des dernières années ont mis en évidence que dans toute forme de bataille, face à des moyens d'attaque de plus en plus diversifiés et efficaces, les systèmes de défense jouaient et seraient appelés à jouer un rôle décisif. Il est même clair que tout agresseur chercherait d'abord à neutraliser les SAM de la défense, en les détruisant dès les premières heures, en les brouillant ou en les leurrant. Le problème est de savoir quel niveau de pertes entraînent pour l'assaillant ces tentatives de neutralisation, et quelle est leur efficacité. Les systèmes de défense sont forcément soumis à un processus de perfectionnements constants et, sous peine d'obsolescence rapide, se doivent d'intégrer sans retard les avancées techniques et technologiques disponibles.

Les décideurs sont malheureusement, dans ce domaine encore plus que dans d'autres, confrontés à des contraintes qui ont toutes chances de se faire de plus en plus pesantes :

- c'est d'abord le coût grandissant de développement des systèmes : les volumes financiers en cause imposent de ne pas se tromper dans les choix essentiels, et rendent les solutions de rattrapage difficiles et incertaines ; il s'écoule de l'ordre de sept années entre les premières décisions et la fabrication de série pour un grand programme : la prévision technologique doit être clairvoyante et les risques techniques correctement évalués ; n'en pas prendre est se condamner à réaliser un système prématurément vieilli ; en prendre de déraisonnables est une assurance d'échec ;
- en même temps, la progression et le renouvellement des techniques se font de plus en plus rapides : elles ne cessent de naître, de se développer, de se périmer, souvent de renaitre : en matière de capteurs d'informations, le radar et les procédés électro-optiques ont engagé une course poursuite ; pour le guidage des missiles, télécommande et autoguidage se concurrencent et font l'objet de modes, mais aussi de perfectionnements successifs ; en ce qui concerne le pilotage, les commandes aérodynamiques rivalisent avec les jets de gaz ; enfin, pour limiter là cette énumération, les structures de traitement de l'information se font incroyablement petites et puissantes, ouvrant sans cesse des perspectives nouvelles.

C'est parmi ce foisonnement des techniques et des technologies que les choix décisifs, à l'aube d'un grand programme, doivent être faits, sachant qu'ils engagent des sommes considérables et qu'ils conditionnent irréversiblement la réussite. Heureusement, pour le salut des pauvres décideurs, Dieu crée la simulation. Grâce à elle un système peut être essayé avant d'exister, dans ses composants et dans son ensemble. Les méthodes et les moyens de simulation, où les calculateurs numériques jouent un rôle essentiel, ont connu, ces dernières années, un essor considérable. On peut distinguer les simulations techniques où les composants du système, capteurs d'informations, pointeurs, missiles, processeurs de traitement des informations, sont représentés d'une manière fine, et les simulations tactiques où le système est évalué face à une menace et dans un environnement simulé. Un effort de plus en plus grand doit être fait pour mettre entre les mains de ceux qui ont à prendre des décisions des outils et des aides de nature opérationnelle, financière et technique. Ainsi peut-on espérer qu'en résultent les choix les meilleurs.

Trois des neuf exposés qui composent ces "Lecture Séries" seront consacrés à la méthodologie de développement des systèmes de défense, et aux simulations intégrant ou non des éléments réels. Les autres traiteront des perfectionnements apportés aux missiles dans leur guidage, leur pilotage et leur charge militaire.

On ne saurait regretter que les conférences n'abordent pas les problèmes complexes des capteurs d'information et du traitement des données. Le programme réparti sur deux journées est déjà fort chargé et mieux vaut être incomplet que superficiel. Nul pas que ces domaines ne fassent l'objet d'évolutions très rapides, au contraire. Chacun d'entre eux pourrait être le thème d'une nouvelle série de conférences. Citons quelques exemples en échantillonnant très sommairement :

- les antennes à balayage électronique abolissent la distinction entre radars de veille et radars de poursuite et font des radars multifonctions les senseurs tous temps capables à la fois de détecter les objectifs dans un environnement difficile, y compris dans des conditions de brouillage sévères, et de les poursuivre ensuite, quel que soit leur nombre, en faisant sur eux des mesures de localisation précises ;
- les antennes synthétiques plaquées sur la structure d'un missile fournissent des performances bien supérieures à celles d'une petite antenne classique et, en même temps, permettent de donner à l'avant du missile la forme optimale que requiert l'aérodynamique ;
- le développement enfin rapide des lasers dans le sens d'une miniaturisation poussée, de puissances accrues, de fréquences de répétition élevées étend le champ des applications ; il est maintenant possible, sous condition d'une visibilité météorologique convenable, de faire des mesures précises sur un objectif à 15 km au moins ;
- les progrès très remarquables de l'imagerie infrarouge, qui utilise des barrettes ou des matrices, CCD ou non, au nombre de cellules détectrices de plus en plus élevé, permettent aux techniques électro-optiques de rivaliser avec le radar et de le compléter, dans le domaine courte et très courte portée, tant pour la recherche des cibles que pour leur poursuite au sol ou dans les autodirecteurs.
- enfin les microprocesseurs modernes apportent sous un volume très réduit des puissances de calcul considérables tant dans les matériels au sol que dans les missiles pour le traitement du signal et tous les problèmes de filtrage et de commande ; c'est grâce à eux en particulier qu'il est possible de mettre à bord des autopilotes digitaux adaptatifs qui augmentent considérablement les performances des missiles dans de larges plages de vitesse et d'altitude ; d'ailleurs plusieurs des exposés qui suivent supposent que des moyens de calcul assez importants sont disponibles tant pour les problèmes de guidage que de pilotage et, bien entendu aussi, dans un autre ordre de grandeur, pour toutes les questions de simulation.

Le premier sujet, exposé par Monsieur GONDET (Société MATRA, FRANCE), pose le problème essentiel déjà mentionné de la méthodologie de conception des systèmes nouveaux. Le conférencier s'applique à montrer le mécanisme des choix qui ont présidé au développement du système très courte portée MISTRAL. Dans un tel cas, des études comparatives multicritères permettent de sélectionner les systèmes les plus intéressants, et d'identifier les actions qui doivent être lancées avant le démarrage du programme pour lever certains risques majeurs. Des études d'analyse des ressources et des études de marché définissent les choix budgétaires les plus rationnels. Le décideur peut alors retenir le programme le plus approprié et arrêter sa planification.

Très technique, la conférence du Dr EAST (Royal Military College of Science, UNITED KINGDOM) traite des structures des boucles de guidage et compare les lois d'alignement télécommandées avec les lois de navigation des missiles autoquidés. Dans les structures en alignement, le Dr EAST montre qu'il est possible et indispensable d'utiliser en commande directe les accélérations cinématiques calculées, et de réduire au minimum nécessaire les bandes passantes des boucles de guidage et de pilotage. Une méthode de conception aidée par calculateur est exposée, pour obtenir des caractéristiques optimales et adaptatives, grâce à des structures qui tolèrent des commutations de leurs coefficients.

La conférence de Monsieur DURIEUX (CETA, FRANCE) revient sur la comparaison entre systèmes télécommandés et autoguidés. En phase terminale, à la condition que la distance missile - but soit mesurée, toute loi de guidage souhaitable peut être réalisée par télécommande. Si l'on compare les procédés de téléguidage et d'autoguidage en navigation proportionnelle classique, il apparaît une limite en distance en-deçà de laquelle le téléguidage résiste mieux aux manœuvres de la cible que l'autoguidage, ceci étant dû à la bande passante limitée de l'autodirecteur. Si l'on met en oeuvre, dans les deux cas, une loi de commande optimale, cette limite existe encore, mais elle n'est due qu'aux imperfections technologiques de l'autodirecteur.

Monsieur SELINCE (Aérospatiale, FRANCE) expose une conception nouvelle du pilotage des missiles sol-air. Le dispositif baptisé "PIF,PAF" combine l'action de jets de gaz qui créent des forces de commande latérales au niveau du centre de gravité du missile avec celle de gouvernes aérodynamiques classiques. Les avantages des deux procédés se cumulent, et l'on obtient un temps de réponse très court et des accélérations latérales importantes même à faible vitesse et haute altitude, la rapidité d'exécution du PIF comblant l'erreur dynamique de l'asservissement PAF. Il en résulte une diminution importante de la distance de passage contre des cibles très manœuvrantes.

En début de deuxième journée, le Docteur GRIDER (US Army Missile Laboratory) revient sur le problème des choix techniques et des méthodes de développement pour des systèmes modernes sophistiqués utilisant des missiles guidés. Il montre comment des simulateurs permettent de tester le système et en particulier le missile et son autodirecteur dans leur environnement complet électro-optique, infrarouge et hyperfréquences, avec une représentation dynamique de l'engagement de la cible par le missile ; ces simulations remplacent et complètent les essais en vol qui deviendraient d'un coût

total prohibitif s'ils constituaient les seuls instruments de développement, en particulier lorsqu'il faut mesurer l'efficacité de contre mesures ou de contre-contre mesures. Les décisions dans le programme, les modifications de conception, les améliorations, l'évaluation du système peuvent être analysées et étayées grâce à des milliers d'essais simulés, en boucle ouverte ou fermée, avec introduction ou non des éléments matériels du système.

L'exposé de Monsieur SANTI (SELENIA Industrie, ITALIE) montre précisément comment les techniques de simulation mettant en oeuvre à la fois des calculateurs numériques et des éléments réels ont permis de développer et d'évaluer le système de défense courte portée SPADA.

Monsieur DESMERCER (THOMSON-CSF, FRANCE) et le Docteur BATY (B.D.M. Corporation, U.S.A.) traitent des autodirecteurs électromagnétiques et des phénomènes qui induisent des erreurs dans la mesure des paramètres de la cible. Le premier exposé s'intéresse surtout aux inévitables imperfections d'un autodirecteur, les énumère et en analyse les conséquences. Le deuxième examine les effets de contre mesures qui utilisent les caractéristiques de réflexion des terrains.

Enfin le Docteur HELD (M.B.B., R.F.A.) approfondit ce qui constitue l'ultime finalité d'un système de missiles guidés, c'est-à-dire la valeur de la charge militaire. Son exposé montre les évolutions techniques en cours, et les perspectives dans le domaine délicat d'une parfaite adéquation entre la précision du guidage, l'exactitude de la fusée de proximité et l'efficacité de la charge explosive.

Ainsi ces exposés, mettant en relief les diverses facettes des systèmes de missiles sol-air, brossent une vaste fresque de la progression des techniques et des technologies dans ce domaine. Face aux armes d'attaque les plus performantes et les plus sophistiquées, la défense a le devoir et le pouvoir d'être efficace et étanche. Les perfectionnements, aussi bien dans les concepts que dans les réalisations, relancent pour demain l'antique débat de la lance et de la cuirasse.

ADVANCED TECHNOLOGY FOR S.A.M. SYSTEMS
ANALYSIS, SYNTHESIS AND SIMULATION

by

Marc Poulet
Thomson-CSF
Division Systèmes Electroniques
1 rue des Mathurins
92220 Bagneux
France

The present lecture series, sponsored by the Guidance and Control Panel of AGARD and implemented by the Consultant and Exchange Programme is devoted to the introduction of new technologies in Surface to Air Missile Systems. The lectures will use the three points of view of analysis, synthesis and simulation, but, due to the magnitude of the subject, they are mainly concerned with the sole aspects of missile guidance and control.

The magnitude of the subject appears first in its importance. Events of the last few years have shown that, in any form of battle, the defence systems have played, and will play, a decisive rôle vis à vis to more and more diversified and efficient attack means. Further, it is clear that the attacker will first seek to neutralize the defence SAM, either by destroying them in the first hours of the battle or by jamming or deceiving them. The question is then to assess the level of losses suffered by the attacker during the neutralizing attempt, and its effectiveness. Therefore, the defence systems are of necessity the object of an endless improvement process and, at the risk of obsolescence, have to include without delay the available advanced technologies.

In this field, still more than in others, decision makers are unfortunately subject to constraints which in all likelihood will become heavier and heavier :

- firstly the increasing development cost : financial bulks involved command to make no error in the essential choices and make difficult and uncertain any corrective action ; for any sizeable project, about seven years are required from first decision to mass production, so that shrewdness is a must in the technological foresight and the risk assessment ; for to take no risk is to doom oneself to produce an already obsolete system, and to take unreasonable risks warrants failure ;
- in parallel, progress and renewal of technologies go faster and faster : they unceasingly arise, grow, become out-dated and often arise again. For instance, in the field of sensors, microwaves and optronics are racing one against the other ; in the field of missile guidance, command and homing are competing, come into and go out of fashion, but are also constantly improved ; in the field of control, thrust vector control rivals with aerodynamic control surfaces and, to close this list, data processing tools are becoming incredibly small and powerful, creating every day new prospects.

It is among this profusion of techniques and technologies that, at the dawn of a project, the decisive choices have to be made, knowing that they engage large amounts of money and determine irreversibly failure or success. Fortunately, for the salvation of unhappy decision makers, God created Simulation. Thanks to simulation, a system can be assessed without existing, in its parts as well as in its whole. Simulation methods and tools, where digital computers play the leading part, have experienced these last years extensive developments. It is possible to distinguish between technical simulations, where system parts, such as sensors, trackers, missiles, data processors, are modelised in detail and tactical simulations, where the system is assessed against a simulated threat and in a simulated environment. Greater and greater efforts have to be made to give the decision makers tools and assistance for technical, operational and financial assessment. The taking of proper decisions is at this cost.

Out of the nine lectures of the present series, three are concerned with the methodology to be used in system development and with simulations making use - or not - of actual hardware. The other lectures deal with improvements brought to missiles for guidance, control and warhead.

We should not regret that subjects as sensors or data processors are ignored. Our two day agenda is already well filled and lack of completeness is preferable to lack of depth. This does not mean that the mentioned fields are not subject to fast evolution, far from it. Indeed, each of them could be the matter for a new series of lectures. Let us list a brief example :

- electronic scan antennas suppress the conventional distinction between search and tracking radars, and make of multifunction radars the all weather sensors capable of detecting targets in difficult environments, this including heavy jamming, and of tracking a large number of them while allowing precise localization measurements ;

- synthetic aperture antennas plated on missile bodies provide performances well above those of a small conventional antenna with the additional advantage of allowing the best aerodynamical shaping of the missile front end ;
- the long sought for but now fast development of lasers in the way of miniaturization, increased power and high repetition frequency extends their utilization domain ; it becomes now possible, subject to proper meteorological visibility, to obtain precise measurements of a 15 km distant target ;
- remarkable progress of infrared displays, using linear or rectangular arrays, C.C.D. or not, with an increasing number of detecting cells, make the electro-optical techniques the rival of radar or its complement in short or very short range systems, for detection as well as for ground and on-board tracking ;
- lastly, modern microprocessors offer under very reduced volume a considerable computation power used in ground or missile equipments for signal and data processing ; for instance, they make possible the implementation of adaptive autopilots providing satisfactory missile performances in a wide range of speeds and altitudes ; in fact, several of the lectures assume the availability of large computation means for solving guidance and control problems, as well as, but here with an other order of magnitude, for simulation.

Mr CONDET (Société MATRA, FRANCE) deals with the first topic, already mentioned, of the methodology for the design of a new system. The author describes the mechanism used for the choices made in the development of the very short range system MISTRAL. In this exemple, comparative studies, based on a number of criteria, lead to select the most promising candidate systems and to identify the preliminary actions necessary to remove some of the major risks. Ressource analysis and market studies determine the most rational budgetary choices. The decision maker can then pick up the most suitable project and determine its plan.

Of a highly technical nature, the lecture of Dr EAST (Royal Military College of Science, UNITED KINGDOM) deals with the structure of guidance loops and compares the command line of sight laws with the navigation laws used in homing missiles. For the line of sight structures, Dr EAST shows that it is both possible and mandatory to feed forward computed kinematic accelerations and to narrow as much as possible the bandwidth of the guidance and control loops. A computer aided design method is indicated, for achieving optimum adaptive characteristics, thanks to coefficient switching robust structures.

Comparison between command and homing systems is also the concern of Mr. DURIEUX (CETA, FRANCE). In terminal phase, and under the condition that the missile to target range be available, any desired guidance law can be implemented with a command technique. Comparing the two techniques - command and homing - for the well known proportional navigation, a border line is defined, beyond which command is less sensitive to target manoeuvres than homing, due to the limited bandwidth of the homing head. If, in both cases, an optimal command law is used, such a limit still exists, but results then only from imperfections in homing head hardware.

Mr SELINCE (AEROSPATIALE, FRANCE) describes a new concept in the control of surface-to-air missiles. The "PIF,PAF" system associates to conventional control surfaces the action of gas jets creating lateral forces applied near the missile center of gravity. The advantages of the two devices are then cumulated, leading to very short response time and large lateral accelerations, even at low speed or high altitude, as the PIF rapidity makes up for the PAF dynamic error. The result is a notable decrease of miss distance against highly manoeuvring targets.

At the beginning of the second day, Dr GRIDIER (US Army Missile Laboratory) comes back to the problem of technical choices and development methods for modern and sophisticated systems using guided missiles. He shows how simulators can be used to test the system or the missile and its seeker in their complete electro-optical, infrared and microwave environment, with a dynamic representation of the engagement. Such simulations supplement and even replace flight testing which, used alone for development, would lead to a prohibitive cost, especially when counter or counter-countermeasures are concerned. Decisions to be taken during the development, reorientations of designs, improvements, system assessment are then studied and supported by thousands of simulated tests in open or closed loop, with or without actual hardware.

Almost as an illustration, the lecture of Dr SANTI (SELENIA Industrie, ITALIA) shows how simulation techniques including digital computers and actual hardware have been used in the development and the assessment of the short range system SPADA.

Mr DESMERGER (THOMSON-CSF, FRANCE) and Dr BATY (B.D.M. Corporation, U.S.A.) deal both with microwave homing heads and phenomena leading to errors in target parameters measurements. The first lecture is mainly concerned with unavoidable seeker imperfections, gives their list and analyses their consequences. The second lecture describes the effectiveness of terrain bounce countermeasures.

Lastly, Dr HELD (M.B.B., R.F.A.) studies thoroughly the ultimate finality of a guided missile system, namely the warhead. His lecture describes the present technical evolution and the prospects in the sensitive area of perfect adaptation between guidance accuracy, proximity fuze precision and warhead effectiveness.

All these lectures, with their display of SAM systems various facets, draw a wide picture of the technological progress in this domain. Against the most powerful and sophisticated attack weapons, defence must and can be efficient and tight. Improvements in concept as well as in design reopen for tomorrow the ancient contest between the armour and the spear.

METHODOLOGIE DE LA CONCEPTION DES SYSTEMES D'ARMES FUTURS

Exemple des Systèmes Sol-Air Très Courte Portée

Par

J.F. GONDET
 Chef du Département d'Analyse de Systèmes Militaires
 Direction Recherche et Développement
 S.A. MATRA - 37 Avenue Louis Bréguet - 78140 VELIZY - FRANCE

RESUME

Après avoir décrit l'ensemble et l'enchaînement des études qu'il est souhaitable de réaliser avant de lancer le développement d'un système d'armes nouveau, l'exposé se focalisera sur une des étapes importantes de cette démarche constituée par des études comparatives multicritères de systèmes envisageables pour répondre au problème opérationnel posé.

Afin d'illustrer leur méthodologie, une étude paramétrique de systèmes d'armes Sol-Air Très Courte Portée (SATCP) dont certaines conclusions ont été prises en compte pour la définition du système MISTRAL est ensuite présentée.

1 INTRODUCTION

Pour remplir une mission donnée, il existe bien souvent un certain nombre de solutions techniques potentielles capables de répondre au problème posé et il est important de disposer d'une méthodologie d'Analyse de Systèmes adaptée de façon à pouvoir effectuer les choix judicieux avant le lancement du programme de développement, c'est-à-dire avant d'engager des volumes financiers importants.

En effet, l'Analyse de Système a pour but principal d'aider le responsable d'une décision à choisir une ligne de conduite, en examinant de façon systématique tous les aspects de son problème, en recherchant les objectifs visés et les solutions possibles, en les comparant à la lumière de leurs conséquences, en utilisant un processus approprié pour porter un jugement éclairé sur le problème.

C'est ainsi qu'avant le lancement d'un programme militaire, un certain nombre d'études d'Analyse de Systèmes sont nécessaires pour éclairer le décideur.

Ces études préliminaires, que nous présenterons au chapitre suivant, sont aussi bien de nature opérationnelle, financière que technique. Parmi ces dernières, il en est une qui constitue une étape importante dans le processus de décision puisqu'elle élabore de façon rationnelle les éléments de choix et identifie les actions qui doivent être nécessairement poursuivies afin de minimiser les risques de développement du système. C'est cette étape que nous avons choisie de présenter dans la suite de l'exposé, en prenant comme application une comparaison multicritère de systèmes SATCP.

2 ETUDES D'ANALYSE DE SYSTEMES PRELIMINAIRES AU LANCEMENT D'UN PROGRAMME

L'enchaînement des études constituant les différentes étapes de l'analyse globale préliminaire au lancement d'un programme est illustrée sur la figure N° 1.

Nous y trouvons en amont des études de prospective technologique qui servent principalement à asseoir la faisabilité des sous-systèmes envisageables pour réaliser les fonctions du système compte tenu de l'horizon de mise en service souhaité. Ces analyses prospectives permettent de réaliser un premier tri des techniques qui pourront être utilisées pour remplir certaines fonctions du système et, pour les sous-systèmes retenus, de fixer une plage de valeurs possibles des performances intrinsèques pouvant être obtenues. Certaines d'entre elles sont bien entendu assorties d'un risque technique (faisabilité conditionnelle) qui devra être pris en considération au moment de l'élaboration du programme de développement et de l'identification des actions qui doivent être initialisées avant celui-ci (développements exploratoires) si le système jugé le plus prometteur au terme de l'analyse globale fait appel à ces techniques.

Ces études prospectives servent d'autre part à définir la menace potentielle par extrapolation à l'horizon considéré de la menace actuelle, dont l'évaluation est un thème permanent d'études dans le cadre de l'analyse du contexte stratégique. En effet, cette projection dans le futur de la menace est le plus souvent effectuée en supposant que la technologie de l'adversaire potentiel va suivre la même évolution que la nôtre.

L'analyse du contexte stratégique sert d'autre part à définir la mission que devra réaliser le futur système d'armes.

Possédant alors une bonne connaissance des trois facteurs que sont le besoin militaire, l'environnement ennemi et les possibilités technologiques, il est alors possible de définir une première ébauche de systèmes envisageables répondant à la mission compte tenu de la menace.

L'efficacité opérationnelle de ces systèmes est ensuite évaluée au moyen de simulations. Ce critère d'"efficacité" comprend bien sûr l'efficacité intrinsèque du système d'armes en termes de probabilité de destruction mais aussi des facteurs tels que la vulnérabilité, la capacité tous temps, la fiabilité, la versatilité, etc.... Ces évaluations servent d'une part à optimiser certains paramètres de définition des systèmes et d'autre part à élaborer un catalogue des performances des systèmes ainsi optimisés.

Parallèlement à cette procédure itérative, l'évaluation des coûts (développement, production et exploitation) de ces différents systèmes est effectuée ce qui permet de les comparer sous l'aspect coût/efficacité. Cette analyse est complétée par des études de sensibilité des résultats à certains paramètres ayant été jugés comme secondaires lors de l'analyse préliminaire.

Ces études comparatives multicritères permettent d'une part de sélectionner le ou les systèmes jugés les plus intéressants compte tenu des critères d'appréciation et d'autre part d'identifier les actions qui doivent impérativement être lancées préalablement au démarrage du programme de façon à lever certains risques techniques majeurs.

Parallèlement à cette évaluation à caractère technique, des études d'analyse des ressources et des études de marché permettront d'effectuer une étude de rationalisation des choix budgétaires.

Compte tenu de ces éléments financiers et des résultats de l'analyse comparative des systèmes possibles, le décideur pourra alors, en toute connaissance de cause, choisir le programme le plus approprié et définir sa planification.

3 COMPARAISON MULTICRITÈRE DE SYSTEMES SOL-AIR TRES COURTE PORTEE (SATCP)

3.1 BUT DE L'ETUDE

L'étude que nous avons choisi de présenter afin d'illustrer la méthodologie générale est une comparaison multicritères de systèmes Sol-Air guidés à Très Courte Portée. Il s'agissait d'effectuer une étude paramétrique à l'horizon 1985-1990 de la faisabilité et de l'efficacité de ces systèmes ainsi que d'évaluer leurs coûts.

L'ensemble des travaux était destiné à :

- établir la faisabilité technique des solutions envisagées,
- évaluer l'efficacité intrinsèque des solutions possibles,
- estimer le coût global (recherche et développement, équipement et exploitation) du programme correspondant à chaque solution possible,
- comparer les résultats obtenus dans la perspective d'une prise de décision sur la base d'une comparaison des diverses solutions d'un point de vue coût-éfficacité et de fournir ainsi les éléments permettant un choix judicieux des types de systèmes SATCP les mieux adaptés au contexte d'emploi opérationnel prévu,
- recommander le programme de recherches préliminaires qu'il serait nécessaire d'entreprendre pour disposer, à l'horizon considéré, des techniques indispensables à la réalisation des systèmes les plus intéressants mis en évidence par la comparaison coût-éfficacité,
- être intégré dans une étude générale de défenses anti-aériennes à basse et très basse altitude du champ de bataille.

3.2 METHODOLOGIE DE L'ETUDE

L'étude a été organisée en quatre phases selon le schéma, désormais classique pour une étude coût-éfficacité, présenté sur la figure N° 2.

Phase 1 : Définition du problème et des hypothèses de base ; recueil des données.

Au cours de cette phase de formulation du problème on s'attache plus particulièrement à définir et analyser d'une part les spécifications et conditions opérationnelles et d'autre part les critères de comparaison qui seront utilisés par la suite. Enfin, on identifie les fonctions du système et les solutions techniques capables de les réaliser.

Phase 2 : Etudes de faisabilité ; modélisations des sous-systèmes.

A la suite de l'inventaire technologique réalisé précédemment on étudie la faisabilité et on modélise les performances intrinsèques de ces sous-systèmes à l'horizon considéré pour la mise en service du système.

Phase 3 : Modélisation des systèmes ; évaluation de l'efficacité et du coût.

Cette étape commence par une définition des systèmes possibles qui sont ensuite évalués suivant les critères (principalement efficacité et coût) définis au cours de la première phase.

Phase 4 : Comparaison des systèmes ; conclusions et recommandations.

A partir des résultats de l'évaluation des performances des systèmes, on réalise une synthèse ayant pour but :

- de comparer les divers types de systèmes Sol-Air suivant les critères adoptés, de façon à identifier les systèmes les plus intéressants,
- de dégager les axes d'efforts et de recherche qu'il serait nécessaire d'entreprendre pour pouvoir disposer, à l'horizon considéré, des systèmes précédemment définis.

3.3 1ère Phase : FORMULATION DU PROBLEME

Pour mener à bien cette étude, il a été nécessaire dès le départ de faire un certain nombre d'hypothèses et de définir les critères à utiliser pour évaluer et comparer les systèmes d'armes Sol-Air Très Courte Portée.

Les travaux effectués au cours de cette première phase de l'étude ont donc comporté :

- un recueil des données et une définition des conditions opérationnelles,
- la définition des critères d'évaluation des systèmes SATCP,
- un inventaire des solutions possibles pour les sous-systèmes des systèmes Sol-Air à Très Courte Portée.

3.3.1 RECUEIL DES DONNEES ET DEFINITION DES CONDITIONS OPERATIONNELLES

Au cours de cette phase nous nous sommes efforcés de définir, en accord avec les opérationnels, les points suivants :

- les contraintes principales que doivent respecter les systèmes :
 - . transportables à dos d'homme
 - . portée opérationnelle maximale à très basse altitude : 5 km
 - . munition guidée
- les menaces devant être engagées par ces systèmes et qui ont été définies par quatre types d'aéronefs :
 - . hélicoptère lourd de combat
 - . chasseur bombardier
 - . avion de combat léger
 - . drone.

Ces menaces ont été définies aussi bien par leurs caractéristiques dimensionnelles et cinématiques que par leurs signatures dans différentes longueurs d'onde.

- l'environnement dans lequel les systèmes SATCP sont susceptibles d'évoluer. En particulier un recueil statistique des conditions météorologiques prévalant en Centre Europe a été effectué. Deux données très importantes ont été dégagées de ces investigations :
 - . la visibilité météorologique horizontale (figure 3) moyenne dans la région Centre Europe n'est que de 7 km, une visibilité météorologique supérieure à 17 km ayant une probabilité d'apparition de 10 %.
 - . les distances d'intervisibilité entre le sol et un aéronef volant à 100 mètres d'altitude sont très rarement supérieures à 3 km.

3.3.2 DEFINITION DES CRITERES D'EVALUATION DES SYSTEMES SATCP

Afin de pouvoir orienter les modélisations de la phase 2 en fonction des évaluations qui devront être faites au cours de la phase 3, une liste de critères de comparaison a été établie dès le début de l'étude.

Ces critères sont d'ordre quantitatifs, semi-quantitatifs ou qualitatifs. La liste suivante a été établie :

- 1 - Domaines de tir et d'interception
- 2 - Pourcentage du temps pendant lequel le système est utilisable
- 3 - Probabilité unitaire de destruction de la cible
- 4 - Servitudes de mise en œuvre (délais de mise en service, durée du rechargement)
- 5 - Probabilité globale de destruction d'une cible traversant le domaine d'action
- 6 - Portabilité/épaulabilité (masse et encombrement)
- 7 - Coût

- 8 - Polyvalence vis à vis des objectifs principaux
- 9 - Aptitude à remplir d'autres missions marginales (anti-char, combat hélicoptère-hélicoptère)
- 10 - Horizon de la mise en service des systèmes
- 11 - Discrétion d'utilisation
- 12 - Résistance aux CM (IR, EM, ...).

3.3.3 INVENTAIRE DES FONCTIONS ET SOLUTIONS TECHNIQUES

A la fin de la phase de formulation du problème un premier inventaire des principales fonctions remplies par un système SATCP a été dressé. Une vingtaine de fonctions ont ainsi pu être identifiées qui ont été classées en fonctions "système" et "missile" comme l'indique le tableau N°1 ci-dessous :

<u>FONCTIONS SYSTEME</u>		<u>FONCTIONS MISSILE</u>
LANCER	{ IMPLANTATION LANCEUR	AERODYNAMIQUE
ALERTE		PILOTAGE
IDENTIFICATION		NAVIGATION
ACQUISITION		STRUCTURE
EVALUATION		PROPELLAGE
POURSUITE	{ OBJECTIF MISSILE	{ EJECTION PROPELLAGE PRINCIPALE
ILLUMINATION		ARMEMENT
GUIDAGE	{ MODE DE GUIDAGE ELABORATION DES ORDRES	{ CHARGE MILITAIRE MISE A FEU
RALLIEMENT		ENERGIE
TRANSMISSION		

Tableau N° 1 : Fonctions d'un système SATCP

Pour chacune de ces fonctions, un inventaire des sous-systèmes a priori envisageables pour les assurer a été réalisé, de façon la plus exhaustive possible à ce stade de l'étude. Ces fonctions sont répertoriées sur la figure N° 7.

3.4 2ème Phase : ETUDES DE FAISABILITE ET MODELISATION DES PERFORMANCES DES SOUS-SYSTEMES

Les études de faisabilité et de modélisation effectuées pour chacun des sous-systèmes susceptibles de remplir une fonction dans un système Sol-Air à Très Courte Portée ont permis de choisir le ou les sous-systèmes dont le niveau technique et les performances, actuels et futurs, permettent d'envisager leur utilisation dans ces systèmes d'armes à l'horizon 1985-1990.

Nous donnons ci-après quelques exemples de résultats sur les sous-systèmes principaux.

3.4.1 DETECTION VISUELLE

L'œil humain restera un système de détection utilisé dans la grande majorité des systèmes et ce, quelque soit l'horizon.

Les travaux effectués ont consisté à modéliser le processus de détection visuelle d'un objectif aérien en validant cette modélisation par comparaison des résultats de la simulation à des résultats expérimentaux. La figure N° 5 illustre la bonne représentativité du modèle. L'exploitation de celui-ci a ensuite permis de mettre en évidence les points suivants :

- il est très intéressant et sans doute primordial de pouvoir affecter au servant des secteurs de recherche plus petits que $30^\circ \times 5^\circ$ voire $15^\circ \times 5^\circ$, d'où l'importance des moyens de préalerte.
- les distances de détection visuelle à l'œil nu sont toujours faibles. Les distances de détection d'un chasseur bombardier avec un champ de recherche de $10^\circ \times 5^\circ$ pour une probabilité de détection de 0,9 et par une visibilité météorologique de 7 km sont inférieures à 2 km.

- l'utilisation d'une lunette grossissante permet d'améliorer ces distances de détection. Ainsi dans le cas d'un chasseur bombardier à Mach 0,7 et pour les mêmes conditions ($\Psi \times \Psi = 10^\circ \times 5^\circ$; VM = 7 km) on trouve les portées suivantes (en km) :

Grossissement	Oeil nu	2	5	8	10
P _d = 0,9	1,75	2,55	3,5	3,8	4
P _d = 0,5	2,65	3,5	4,45	4,95	5,1

Tableau N° 2 : Distances de détection visuelle avec lunette grossissante (cible chasseur bombardier)

3.4.2 SYSTEMES T.V.

Deux utilisations de la télévision sont a priori envisageables dans le cadre des systèmes d'armes SATCP :

- pointage automatique d'un faisceau sur la cible,
- autodirecteur du missile.

Que ce soit pour l'une ou l'autre des applications, ces systèmes devront réaliser une corrélation optique automatique nécessitant cependant une visualisation préalable pour détecter, acquérir et accrocher l'autotraqueur T.V. sur la cible.

L'étude de faisabilité avait conclu que grâce à l'utilisation possible des techniques C.C.D. et à la miniaturisation des composants, des autodirecteurs T.V. implantables dans un missile de calibre minimum 100 mm étaient envisageables à l'horizon considéré mais devaient être associés à des postes de tir sophistiqués.

3.4.3 GUIDAGE I.R.

En fonction de l'horizon de mise en service, deux types de détecteur ont été identifiés :

- A l'horizon 85, utilisation soit des détecteurs monocellules classiques, soit des autodirecteurs à cellules en croix qui améliorent la précision du guidage (bruit d'écartométrie plus faible) et les portées de détection (meilleur traitement du signal).
- A l'horizon 1990, utilisation de matrices C.I.D.

Pour des cellules en Antimoniure d'Indium, la figure N° 6 compare les portées de détection atteignables soit avec un autodirecteur monocellule, soit avec des autodirecteurs multicellules, l'un étant composé de quatre cellules en croix, l'autre ayant une sensibilité 10 fois plus élevée par augmentation du nombre de cellules, de leur déTECTIVITÉ et par amélioration du traitement du signal.

3.4.4 TECHNIQUES LASER

Les études de faisabilité ont montré que la réalisation d'un système d'autoguidage semi-actif laser respectant les contraintes imposées par les systèmes SATCP était possible aux horizons considérés.

En effet, la faisabilité d'un émetteur portable émettant à la longueur d'onde 1,06 μ (YAG dopé au Néodyme) était acquise et d'autre part l'autodirecteur correspondant était réalisable dans un diamètre de 100 mm pour obtenir la portée suffisante (figure 7).

Une autre application des techniques laser est le guidage sur faisceau qui a semblé réalisable à condition d'utiliser un émetteur constitué de diodes laser afin de le rendre portable, voire épaisse. Ce système, compte tenu des caractéristiques des diodes réceptrices devait, pour pouvoir fournir les portées opérationnelles souhaitées par faible visibilité météorologique, être utilisé sur des missiles équipés de propulseurs émettant très peu de fumées, comme le montre la figure 7.

3.4.5 TECHNIQUES ELECTROMAGNETIQUES

Aux horizons considérés, les techniques EM pouvaient être utilisées de deux façons dans le cadre du SATCP :

- radar de préalerte et désignation d'objectif,
- poursuite et illumination de la cible.

Dans le cas de cette dernière application, l'illuminateur associé à un missile guidé grâce à un autodirecteur électromagnétique semi-actif devait être réalisé en technologie état solide pour être transportable ce qui conduisait à des puissances très limitées, mais néanmoins exploitables. Quant à l'autodirecteur, compte tenu des faibles calibres des missiles envisagés, il devait être du type antenne synthétique comme le montrent des études antérieures effectuées par d'autres sociétés.

3.4.6 PROPULSION

Deux types de propulsion avaient été envisagés :

- le moteur fusée à poudre
- le statoréacteur solide rustique ablatable.

Cette dernière solution prometteuse de par ses performances intrinsèques en termes de portée et vitesse sur trajectoire n'a cependant pas été retenue pour la phase d'évaluation principalement à cause du problème posé par la nécessité de surcalibrer le tube de lancement pour loger les entrées d'air et de la faisabilité très incertaine de cette solution dans de petits calibres.

Par contre, l'état de la technologie des propérgols solides permettait de résoudre correctement la plupart des problèmes de propulsion relatifs aux systèmes SATCP envisageables, qu'il s'agisse :

- de l'éjection à moyenne (50 m/s) ou grande vitesse (250 m/s),
- de l'étage d'accélération,
- de l'étage de croisière.

Il convenait toutefois de signaler :

- 1) l'intérêt présenté, pour l'application SATCP, par les propérgols à grande vitesse de combustion ($v > 50$ mm/s) et très énergétiques (étage de croisière à combustion frontale) ;
- 2) la faiblesse de la panoplie des compositions discrètes, faiblesse d'abord du point de vue énergétique et ensuite du point de vue des vitesses de combustion (et/ou des exposants de pression).

Un effort particulier de développement devait donc être envisagé si les systèmes retenus exigeaient impérativement cette condition.

3.4.7 ARMEMENT

Après un inventaire exhaustif des charges militaires envisageables pour les missiles SATCP, il est apparu que des charges à éclats préfragmentés constituaient la solution préférentielle, chaque éclat ayant une masse unitaire inférieure à 1,5 g.

Les masses maximales de charge militaire envisageables dans les différents calibres sont les suivantes :

\varnothing (mm)	70	80	90	100
Mo (kg)	1,7	2,4	3,5	5,5

L'utilisation d'une fusée de proximité électrostatique semblait être la meilleure solution dans les cas où la charge militaire est suffisamment grosse pour que l'impact ne soit pas systématiquement nécessaire pour endommager la cible. Pour les grosses charges militaires et les distances de passage plus élevées, une fusée de proximité laser semblait la voie la plus prometteuse.

3.4.8 CELLULE PILOTEE

Les configurations aérodynamiques les mieux adaptées semblaient être la configuration canard et la configuration aile longue. En effet, la première se prête très bien aux chaînes de pilotage simplifiées (retour en braquage, pilotage en couple, missile en autorotation), tandis que la version aile longue est mieux adaptée à des missiles sophistiqués, très manœuvrables, pilotés suivant les trois axes. Cependant, le choix définitif entre les différentes versions et les chaînes de pilotage associées dépendraient avant tout des choix du système en matière de calibre et donc de coût.

En ce qui concerne la loi de navigation, son choix était lié au système de guidage utilisé qui pouvait être soit :

- une télécommande manuelle,
- un guidage sur faisceau,
- un autoguidage.

Le modèle de simulation dynamique mis au point au cours de cette étude a ensuite permis d'évaluer les distances de passage obtenues.

Dans le cas de la télécommande manuelle, le comportement de l'opérateur humain a été modélisé sous forme d'une erreur de pointage en fonction du temps, à partir de résultats d'expérimentations effectuées sur des systèmes similaires. En effet, la modélisation analytique des performances en poursuite du tireur est trop liée à la définition ergonomique de son poste de tir et à sa fonction prédition, éléments qu'il était impossible de prendre en compte dans une telle étude.

3.4.9 CONCLUSION

Au cours de cette deuxième phase nous avons donc réalisé :

- un premier tri des techniques pouvant être mises en oeuvre pour remplir les fonctions d'un système SATCP,
- un catalogue des performances intrinsèques des sous-systèmes intéressants et/ou la mise en place des modèles de simulation permettant de les déterminer.

3.5 3ème Phase : DEFINITION ET EVALUATION DES SYSTEMES

3.5.1 DEFINITION DES SYSTEMES

Afin de faciliter la nomenclature des systèmes SATCP envisageables, nous avons établi un graphe des structures de systèmes organisé autour des trois fonctions qui définissent de manière déterminante la physionomie du système, à savoir :

- la poursuite de l'objectif,
- la poursuite du missile,
- la mode de guidage du missile.

En effectuant ainsi toutes les combinaisons possibles de sous-systèmes retenus et en prenant bien entendu un sous-système par fonction, nous avons réussi à mettre en évidence une quarantaine de structures de base. Bien entendu, toutes ces structures de base qui apparaissent ainsi a priori ne présentent pas toutes le même niveau d'intérêt et certaines ne figureront que parce que le procédé d'élaboration de ces structures les avait mises en évidence faute de quoi elles n'auraient pas été citées tant leur nature les rendait a priori peu attrayantes ou à l'évidence moins intéressantes qu'une structure voisine.

C'est ainsi que, si a priori, il n'est pas inenvisageable d'associer une poursuite radar de l'objectif et un guidage du missile sur faisceau laser, il paraît quand même plus sain techniquement et opérationnellement d'associer poursuite et faisceau radar d'une part poursuite optique et faisceau laser d'autre part ne serait-ce que par souci d'homogénéité des comportements en fonction des conditions de visibilité.

A ce stade de l'étude il s'agissait donc, avant d'entamer l'évaluation, de choisir parmi les structures de base les classes de systèmes intéressantes et au sein de chacune d'entre elles des solutions caractéristiques représentatives au niveau des dimensions, des types de cellule pilotée, des lois de vitesse, etc..., tous paramètres qui sont a priori susceptibles de varier d'un système à l'autre.

C'est ainsi que parmi les quarantes structures identifiées, nous avons choisi, en accord avec le client, sept classes de systèmes dont l'évaluation puis la comparaison semblaient particulièrement intéressantes.

Après avoir effectué une analyse des contraintes que le concept même de chaque système faisait subir sur les principaux sous-systèmes compte tenu des résultats des études de faisabilité, nous avons défini au sein de chaque classe de systèmes une ou plusieurs versions de base représentatives et éventuellement une ou plusieurs options. La sélection de ces versions qui ont ensuite fait l'objet des évaluations a été opérée en assemblant des sous-systèmes homogènes entre eux au vu de critères qualitatifs et/ou quantitatifs.

Afin de ne pas alourdir l'étude, la validation de l'intérêt de certains sous-systèmes (déviation de jet, tir canon, tir avec avance, aérodynamique du type aile longue, ...) a été effectuée sur un des systèmes auquel il paraissait bien adapté a priori.

Compte tenu de cette analyse, onze versions de base ont été retenues pour l'évaluation des systèmes et sont présentées sur la Figure N° 8.

3.5.2 EVALUATIONS DES SYSTEMES

Ayant effectué ce premier travail nous avons donc ensuite évalué ces différents systèmes suivant les critères quantitatifs définis au début de l'étude, cette évaluation étant effectuée système par système. Auparavant, les performances de détection visuelle de cibles aériennes par un opérateur humain ont fait l'objet d'une étude car ce processus d'acquisition de la cible est commun à un grand nombre de systèmes.

L'évaluation des systèmes a ensuite consisté pour chacun d'entre eux à :

- effectuer un devis de masse,
- évaluer les lois de vitesse et distance parcourue,
- évaluer les domaines de tir cinématiques,
- évaluer les domaines de tir dynamiques et donc les distances de passage,
- évaluer les probabilités de destruction compte tenu des distances de passage et de la masse de la charge militaire,
- évaluer les performances des systèmes de guidage du point de vue des portées d'utilisation,
- évaluer les délais de réaction dans diverses utilisations opérationnelles,
- évaluer les domaines de tir opérationnels compte tenu des résultats précédents,
- évaluer les coûts de recherche et développement ainsi que les coûts de série, pour une série de 5 000 missiles et de 500 postes de tir.

A la fin de cette phase d'évaluation, nous avons donc disposé :

- de comparaisons partielles de certains concepts de sous-systèmes,
- d'un catalogue des performances des différents systèmes qui nous a permis ensuite de les comparer critère par critère.

Nous n'en donnons ici que les principaux résultats pour illustrer le type de sorties de telles études.

3.5.2.1 Conclusion générales sur les structures de base

Ces conclusions générales sur les sous-systèmes de base étant valables en général pour l'ensemble des systèmes considérés, elles ont donné lieu à des recommandations applicables à la fin de l'étude aux systèmes jugés les plus intéressants. C'est ainsi que l'on a identifié les besoins suivants :

a). détection visuelle

- nécessité, pour engager les cibles secteur avant, d'une désignation d'objectif précise,
- nécessité, pour avoir des portées suffisantes dans ces conditions, d'effectuer l'acquisition avec une lunette grossissante.

b). cellule pilotée

- l'aile longue présente peu d'intérêt en termes de manœuvrabilité et beaucoup d'inconvénients en termes d'encombrement,
- grande sensibilité de la portée du vecteur à la forme de la pointe avant d'où l'intérêt des formes hémiconiques ou des irdômes pyramidaux pour les systèmes à guidage électro-optique.
- le pilotage un axe en autorotation nécessite des tirs avec avance en azimut pour compenser la plus faible manœuvrabilité obtenue qu'avec les systèmes twist and steer qui ont de très bonnes performances en distance courte.

c). Propulsion

- sur les cibles immobiles stationnaires il est indispensable d'avoir une vitesse d'éjection suffisante faute de quoi il est nécessaire de procurer une élévation élevée en site pour contrer les effets de la pesanteur, ce qui dégrade les performances à courte portée.
- l'éjection par effet canon doit procurer des accélérations inférieures à 500 g pour rester compétitive avec les autres solutions au niveau des dimensions du système et dans ce cas elle n'apporte aucune amélioration au niveau des distances courtes du domaine d'action.

d). Épaulabilité/Portabilité

Du point de vue des masses, la limite entre l'épaulabilité et la portabilité semble se situer entre les calibres 70 mm et 80 mm, les systèmes de calibre 100 mm n'étant plus guère portables.

3.5.2.2 Performances des systèmes

Les évaluations ont été effectuées *système par système*, ce qui a permis de dresser, pour chacun d'entre eux, un catalogue exhaustif de leurs performances.

A l'aide du catalogue des performances de chacun des systèmes nous avons ensuite comparé ces systèmes critère par critère en essayant à chaque fois de synthétiser et schématiser de façon la plus claire possible les caractéristiques de chaque système.

Toujours dans un souci de concision, les variantes de certains systèmes n'ont été prises en compte que dans la mesure où, face à un certain critère, elles se démarquaient par rapport à la version de base.

Afin de faciliter la compréhension de cet exposé, nous présentons directement les résultats de cette comparaison sur les critères quantitatifs, bien que celle-ci n'ait été effectuée qu'au début de la quatrième phase de l'étude.

a) Domaines de tir

La comparaison des domaines de tir a été effectuée en considérant les performances "dynamiques" des vecteurs, sans faire intervenir de limitations opérationnelles. Ces domaines de tir face à un chasseur bombardier sont représentés, à titre d'exemple, sur la figure N° 9.

Il ressort de l'examen de ces domaines que ce sont les systèmes à autoguidage infrarouge qui présentent les meilleures distances courtes, surtout s'ils sont équipés d'un pilotage deux axes. Les systèmes à autoguidage laser semi-actif peuvent également procurer de bonnes performances.

Par contre, les limites longues de ces systèmes sont relativement faibles. Les systèmes à autoguidage I.R. auront des distances longues supérieures ou égales à celles des missiles guidés en alignement sur faisceau laser pourvu que l'aérodynamique de leur pointe avant permette de diminuer la traînée, c'est à dire qu'ils soient équipés d'un hémisphère ou mieux encore d'un irdôme pyramidal.

Enfin, notons qu'une dérobade de la cible dégrade fortement les limites courtes des systèmes guidés en alignement, beaucoup plus que celles des systèmes autoguidés.

b) Pourcentage du temps d'utilisation des systèmes

Le pourcentage du temps d'utilisation des différents systèmes en fonction de la distance de tir a été déterminé en tenant compte :

- des limites de détection visuelle en fonction de la visibilité météorologique horizontale V_M
- des limites de portée d'utilisation des systèmes de guidage en fonction de V_M
- des délais de réaction des systèmes
- des statistiques de visibilité météorologique horizontale sur la zone Centre-Europe
- des domaines de tir dynamiques des systèmes.

Ce pourcentage de temps d'utilisation a été évalué soit sur un avion volant à Mach 0,7 en présentation frontale (figure 10), soit sur un hélicoptère stationnaire se démasquant 20 secondes (figure 11).

Mises à part pour les faibles distances de tir où dans ce cas les systèmes autoguidés permettent une utilisation sur une durée beaucoup plus grande du fait des performances intrinsèques des vecteurs, on peut remarquer que les pourcentages d'utilisation des différents systèmes sont peu différents aux grandes portées.

En fait, les différences proviennent de deux causes :

- les délais de réaction qui sont légèrement différents d'un système à l'autre
- l'utilisation ou non d'une lunette grossissante pour l'acquisition visuelle.

La détection visuelle de la cible étant un processus très contraignant, toutes les différences entre systèmes sont "nivélées" par ses médiocres performances et finalement le pourcentage du temps d'utilisation des systèmes à des portées supérieures à 2 km dépend surtout de la façon dont s'opère l'acquisition visuelle de la cible. On peut tenter de résumer la comparaison de la façon suivante :

- pour des distances de tir inférieures à 2 km, il existe un net avantage pour les systèmes autoguidés, surtout infrarouges.
- au delà de 2 km, le pourcentage d'utilisation dépend surtout du type d'acquisition visuelle qui est effectuée (grossissement ou non). Cependant, pour rester compétitifs au niveau de ce critère, les systèmes autoguidés I.R. devront être équipés d'un autodirecteur sophistiqué de grande sensibilité.

c) Probabilité unitaire de destruction

Si l'on met de côté les notions de fiabilité, la probabilité unitaire de destruction dépend principalement de la nature et de la masse de la charge militaire, du fonctionnement de la fusée de proximité compte tenu de la géométrie de la présentation terminale, de la distance de passage et de la vulnérabilité de la cible.

Dans le cas présent, la détermination de ces relations est impossible à obtenir avec un degré de confiance suffisant par des méthodes simples, donc globales, étant donné que les masses de charge sont faibles et que vis à vis des distances de passage obtenues, la cible ne peut être considérée comme ponctuelle, bien au contraire.

Une première mesure de l'efficacité relative des différents systèmes est donc l'écart-type de la distance de passage (supposée être distribuée suivant un loi de Rayleigh centrée). Nous avons donc représenté, pour un avion évoluant à Mach 0,7 à une distance nodale de 1 km, l'évolution de ces distances de passage en fonction de l'abscisse du point de tir (figure 12), le même paramètre ayant été représenté face à l'hélicoptère stationnaire (figure 13).

Ce sont les systèmes autoguidés I.R. qui présentent en général les distances de passage les plus faibles, les systèmes guidés en alignement ou autoguidés laser semi-actifs ayant une distance de passage qui augmente assez rapidement aux grandes distances étant donné les erreurs qui sont liées à la poursuite de la cible.

En parallèle, un modèle d'efficacité terminale de charges militaires a été utilisé pour fournir, face aux différentes cibles représentées sous forme d'une décomposition géométrique et d'éléments vulnérables quantifiés, les probabilités de destruction en fonction de l'écart-type de la distance de passage, et ce pour plusieurs masses de charges militaires à éclats (voir un exemple figure 14).

A l'aide de ces données, il est alors possible de graduer les domaines de tir non plus en distances de passage, mais en probabilités de destruction.

d) Performances opérationnelles

Les figures 15 et 16 représentent, pour deux valeurs de la visibilité météorologique horizontale, des domaines de tir opérationnels obtenus en tenant compte des délais de réaction, des portées de détection visuelle, des portées du système de guidage et des performances dynamiques des missiles.

Pour synthétiser et comparer les performances des différents systèmes suivant les critères envisagés nous avons finalement évalué les valeurs des différents paramètres principaux caractérisant les aptitudes opérationnelles de chacun des systèmes en nous plaçant dans des conditions de tir non plus paramétriques mais fixées. Par exemple, les deux tableaux ci-après fournissent certaines de ces performances dans deux cas :

- interception d'un hélicoptère se démasquant pendant 20 secondes à 4 km (Tableau N° 3)
- interception d'un avion en présentation frontale à 3 km (Tableau N° 4).

SYSTEMES		Pourcentage du temps d'utilisation	Distance de passage (m)	Probabilité de destruction
Autoguidage I.R. Ø = 90 mm	A.D. monocellule	0		
	- AD sophistiqué - lunette grossissante	0,55	0,5	1
Guidage sur faisceau laser	Ø = 70 mm	0,07	1,96	0,1
	Ø = 90 mm - pointage automatique - lunette grossissante	0,5	0,78	0,84
Autoguidage laser semi-actif	Pointage automatique + lunette grossissante	0,38	0,88	0,9

Tableau N° 3 : Cible hélicoptère se démasquant 20 s à 4 km

SYSTEMES		Pourcentage du temps d'utilisation	Distance de passage (m)	Probabilité de destruction
Autoguidage I.R. $\theta = 90 \text{ mm}$	A.D. de référence monocellule	0		
	- AD sophistiqué - lunette grossissante	0,40	0,5	1
Guidage sur faisceau laser	$\theta = 70 \text{ mm}$	0,225	1,26	0,31
	$\theta = 90 \text{ mm}$ - pointage automatique - lunette grossissante	0,375	1,12	0,57
Autoguidage laser semi-actif	Pointage automatique + lunette grossissante	0,39	1	0,8

Tableau N° 4 : Cible avion interceptée à 3 km

e) Masse des missiles et des systèmes

En faisant varier la masse des missiles, nous avons calculé pour chaque calibre la portée correspondante. On s'aperçoit que à calibre et à portée donnés, les missiles guidés en alignement sont plus légers que les missiles autoguidés (figure 17), tandis qu'au niveau des systèmes les masses sont comparables (figure 18), les postes de tir des systèmes guidés en alignement étant plus lourds que ceux des systèmes à autoguidage I.R.

Quoi qu'il en soit, cette comparaison des masses ne constitue pas un critère de choix si l'on effectue des comparaisons calibre par calibre. Ce que l'on peut dégager de ces graphiques est que :

- les systèmes de calibre 70 mm sont épaulables,
- les systèmes de calibre 80 mm pourraient être épaulables mais leur portée serait très faible,
- les systèmes de calibre 90 mm sont transportables en un ou deux fardeaux,
- les systèmes de calibre 100 mm sont très difficilement transportables et doivent pratiquement être implantés sur véhicule.

En corollaire de ces constatations, il s'ensuit que :

- les systèmes à autoguidage I.R. ou à télécommande en alignement peuvent exister en versions épaulables, transportables ou montés sur véhicule,
- les systèmes guidés sur faisceau laser peuvent être épaulables éventuellement dans une version uniquement anti-hélicoptère mais seront plutôt transportables ou montés sur véhicule,
- les systèmes à autoguidage laser semi-actif ou à autoguidage T.V. ou électromagnétiques seront très difficilement transportables et devront sans doute être installés sur véhicule.

f) Coût des systèmes

Les coûts de série pour une série de référence de 5 000 missiles et de 500 postes de tir ainsi que les coûts de recherche et développement ont été évalués pour chaque système.

Ces coûts ont ensuite été comparés en valeur relative en prenant comme base le système à télécommande manuelle en calibre 70 mm qui présente le plus faible coût d'équipement total (5 000 missiles + 500 postes de tir + R et D). On s'aperçoit alors que les systèmes guidés en alignement sur faisceau laser représentent un coût global d'équipement inférieur au coût des systèmes autoguidés infrarouge de même calibre (30 % plus chers). En effet, si le coût des postes de tir des systèmes guidés en alignement sur faisceau laser est presque 3 fois plus élevé que celui des systèmes à autoguidage infrarouge, il n'en reste pas moins vrai que les missiles de ces derniers systèmes étant en contre-partie 80 % plus chers, ceci donne un coût global plus élevé étant donné qu'il n'y a que 500 postes de tir pour 5 000 missiles.

On peut supposer que tant que le rapport entre le nombre de missiles et le nombre de postes de tir sera de 10, cet écart de 30 % subsistera quelles que soient les séries en considérant des coefficients d'apprentissage identiques.

Quant aux coûts globaux des autres systèmes autoguidés (laser et T.V.) ils sont 2 à 2,5 fois plus élevés que les coûts des systèmes guidés en alignement étant donné que non seulement le missile mais aussi le poste de tir sont chers.

Nous n'avons pas évalué, pour diverses raisons, le coût de la phase d'exploitation et de vie opérationnelle du système. Ces coûts représentent en général un pourcentage assez élevé du coût total et d'autre part l'expérience montre qu'assez souvent ce sont les systèmes qui sont les plus simples et donc les moins chers à l'achat qui coûtent le plus en phase de vie opérationnelle à cause par exemple des programmes d'entraînement qui sont plus étoffés.

3.6 4ème Phase : CONCLUSIONS/RECOMMANDATIONS

3.6.1 COMPARAISON DES SYSTEMES

Cette phase de synthèse a permis de comparer quantitativement et qualitativement les différentes solutions envisagées face à une dizaine de critères. Les comparaisons quantitatives ont été présentées au chapitre précédent dans la rubrique évaluation. Quant aux comparaisons qualitatives elles ont donné lieu à des jugements relatifs compte tenu des critères suivants :

- polyvalence des systèmes,
- horizon de mise en service,
- risques de développement,
- discréption d'utilisation,
- résistance aux contre-mesures.

3.6.2 CONCLUSIONS SUR LES SYSTEMES

3.6.2.1 Systèmes à autoguidage I.R.

Les systèmes à autoguidage infrarouge offrent de bonnes performances à courte portée, que ce soit avec un pilotage twist and steer ou avec un missile en autorotation piloté sur un axe si un angle d'avance est donné au départ (cf figure 7). Les portées d'accrochage des autodirecteurs infrarouges sur les cibles étudiées semblent pouvoir être portées à un niveau de performances suffisant pour ne pas limiter opérationnellement la portée du système (figure 5).

Finalement, il semble se dégager deux classes possibles de systèmes autoguidés infrarouges :

- une classe de missiles de calibre 90 mm, transportables mais non épaulables et dont l'utilisation optimale pourrait être la défense des points sensibles par intégration dans un système comprenant des moyens de préalerte performants ;
- une classe de missiles de calibre 70 mm, ayant une capacité d'attaque avant limitée (autodirecteur et viseur plus rustique) mais ayant l'avantage d'être épaulables. Ces systèmes conviendraient mieux à l'attaque en secteur arrière d'avions pénétrants, aux opérations de commandos, aux guerrillas,...

3.6.2.2 Systèmes guidés en alignement sur faisceau laser

Les distances de passage obtenues avec ces systèmes sont en moyenne plus élevées qu'avec les systèmes autoguidés et un calibre de 90 mm semble être un minimum pour pouvoir être efficace face à des avions.

L'utilisation d'un pointage automatique du faisceau permet de réduire sensiblement les distances de passage vers les limites longues du domaine, la distance courte restant de toutes façons assez élevée puisqu'elle dépend surtout de la cinématique de la loi de guidage.

Le système de guidage ne limite la portée du système que quand la visibilité météorologique est mauvaise et, par beau temps, un système équipé d'un autopointeur et pourvu d'une désignation d'objectif très précise possède un domaine de tir théorique très étendu.

Malheureusement, rien n'indique que dans la pratique le tireur sera en mesure d'évaluer ces distances de tir, ce qui pourra conduire soit à un gâchis de missiles, soit à une utilisation opérationnelle en deçà des performances intrinsèques du système.

3.6.2.3 Systèmes télécommandés manuellement

Les systèmes à télécommande manuelle possédant un mode de pilotage sur deux axes en twist and steer apparaissent performants à longue portée dans la mesure où l'on envisage l'utilisation de propergols discrets.

En revanche, leur intérêt opérationnel est assez limité à courte portée et leurs performances cinématiques sont ainsi nettement inférieures à celles des systèmes autoguidés infrarouges de même calibre.

Les inconvénients de cette catégorie de systèmes semblent être liés au procédé de guidage mis en oeuvre dont la précision peut être limitée dans certains cas de tir par les difficultés de poursuite de l'objectif et du missile par l'opérateur.

3.6.2.4 Systèmes à autoguidage laser semi-actif

Les systèmes à autoguidage laser semi-actif ont semblé beaucoup moins séduisants qu'il ne pouvait paraître a priori.

Cependant leurs capacités d'amélioration étant grandes ils constituaient éventuellement une solution intéressante à un horizon plus lointain car il est certain, et les domaines de tir opérationnels le prouvent, que les distances d'accrochage sur avion venant de face sont importantes quand le système est doté d'un autopointeur électro-optique et quand l'acquisition visuelle est effectuée à l'aide d'une lunette grossissante. Ce système beaucoup plus prospectif pouvait donc avoir un intérêt opérationnel à condition que :

- les propulsions envisagées soient disponibles,
- les émetteurs laser légers puissent disposer de puissances crêtes supérieures à quelques MW à des cadences supérieures à ce qui était réalisable. La cadence d'illumination a en effet une influence assez importante sur la limite courte,
- la pointe avant du missile puisse être hémiconique ou encore mieux pyramidale,
- le système d'illumination soit équipé d'un autopointeur T.V.

Quoi qu'il en soit ce système restait à la limite de la portabilité et aurait sans doute dû être implanté sur un véhicule léger, avec si possible un affût multiple, un des intérêts de ce système étant qu'il permet le tir en salve de plusieurs missiles.

3.6.2.5 Systèmes à autoguidage T.V.

Malgré la miniaturisation des autodirecteurs T.V. pouvant être procurée par l'adoption des techniques CCD, certaines contraintes limitent encore l'utilisation opérationnelle de tels systèmes et en particulier le débattement maximum de l'autodirecteur qui réduit sérieusement le domaine de tir par le travers sur des cibles rapides.

La nécessité de contrôler le missile en roulis n'est pas à proprement parler une limite, mais cette contrainte a cependant une incidence sur la conception du système. Enfin, la miniaturisation, bien que déjà très avancée, ne permet guère de concevoir des missiles de calibres inférieurs à 100 mm, ce qui conduit, compte tenu de la nécessité d'avoir une pointe avant sphérique, à un vecteur possédant de mauvaises performances cinématiques.

Ce type de guidage présente cependant l'avantage, par rapport à tous les autres envisagés jusqu'ici, de fournir une image à l'opérateur ce qui permet de diminuer les fausses alarmes et éventuellement de s'affranchir de systèmes d'acquisition visuelle avec grossissement, les performances en distance de l'autodirecteur étant très bonnes. En outre, ce système est très précis et pourrait même permettre, si le procédé de corrélation d'image est bien étudié, de guider le missile vers un point plus ou moins choisi de la cible (utilisation d'un traqueur centroïde au lieu d'un traqueur d'angles par exemple).

3.6.2.6 Systèmes à autoguidage électromagnétique semi-actif

Le missile SATCP se situe à l'extrême limite des possibilités offertes par les techniques électromagnétiques. Encore convient-il que le missile ait un diamètre au moins égal à 100 mm et qu'il soit équipé d'un autodirecteur d'un type nouveau ayant fait l'objet d'études et de réalisations de principe : l'autodirecteur à antenne synthétique.

Il s'agissait donc d'un système prospectif dont la faisabilité paraissait pouvoir être assurée bien qu'elle n'ait pas été démontrée à cette époque par un modèle probatoire permettant de mesurer le niveau de performances réelles, de juger de l'aptitude à résister aux conditions d'utilisation, et d'apprécier les coûts.

L'intérêt de cette formule réside essentiellement, dans le cas du SATCP, du fait que cette antenne plaquée sur la structure permet :

- 1) d'obtenir des performances (gain, ouverture de lobe ...) bien supérieures à celles d'une antenne classique de petites dimensions.
- 2) d'adopter n'importe quel profil frontal pour le nez du missile, en particulier une forme conique, intéressante du point de vue traînée.

Du point de vue système, bien entendu, cette solution s'avère plus complexe puisqu'elle nécessite :

- un radar de veille ou un dispositif de désignation d'objectif précis,
- un système de poursuite préféablement de type radar si l'on veut rester tout temps (un autotraqueur optronique pourrait également convenir pour un système "temps clair"),
- un illuminateur asservi, le radar de poursuite pouvant jouer ce rôle s'il réunit les conditions nécessaires (onde continue notamment).

Dans sa structure, le système s'apparente donc déjà à un mini SACP surtout si, tenant compte des masses et des volumes, on considère qu'il doit être installé sur une plateforme ou un véhicule.

3.6.3 RECOMMANDATIONS

Cette étude comparative de systèmes d'armes Sol-Air à Très Courte Portée a permis de mettre en évidence un certain nombre de domaines où il semblait nécessaire d'entreprendre ou de poursuivre des recherches afin de pouvoir d'abord choisir le système SATCP le plus intéressant puis le réaliser de façon optimale à l'horizon considéré ; de telles recherches en effet, si elles aboutissent rapidement permettent de lever les incertitudes qui subsistent encore et donc de s'assurer lorsque le programme est lancé qu'il pourra être conduit dans les délais prévus.

Cette étude a donc permis d'identifier une liste d'actions qui apparaissaient indispensables, nécessaires, souhaitables ou utiles au vu des diverses études de faisabilité, des évaluations et des comparaisons effectuées au cours de cette étude. Ces recommandations ont été classées en quatre niveaux :

- les études indispensables pour aborder la définition d'un avant-projet de système SATCP,
- les études nécessaires sans lesquelles les systèmes les plus intéressants de cette étude pourraient difficilement être lancés,
- les études souhaitables qui pourraient permettre de diminuer le volume des études de recherche et de développement d'un système SATCP lorsqu'il sera lancé,
- les études utiles qui amélioreraient les connaissances dans les domaines des systèmes d'armes et en particulier des systèmes SATCP.

Au total une quarantaine d'études ont ainsi été recommandées concernant :

- le système (moyens de préalerte, d'identification, d'évaluation des cibles, ...)
- les objectifs et leur environnement (mesures de signatures, de bruits de paysage, ...)
- l'ergonomie (déttection visuelle, poursuite manuelle, systèmes de visée, poste de tir, ...)
- le missile (autodirecteurs I.R., irdômes pyramidaux, comparaison fine du pilotage un axe en autorotation et du pilotage deux axes en twist and steer, fusée de proximité laser, optimisation de charges à éciats, poudres à grande vitesse de combustion, etc...).

4 CONCLUSIONS

Cette étude illustre à notre avis le type de démarche qu'il est nécessaire d'entreprendre avant de lancer un programme et si, de plus, il reste un intervalle de temps de l'ordre de deux ans ou plus entre la fin d'une telle étude comparative et le lancement du programme, les principales études complémentaires mises en évidence pourront être effectuées et une seconde itération effectuée sur les systèmes les plus prometteurs en tenant compte des résultats de ces études complémentaires de recherche pourra être effectuée ; ainsi le décideur disposera de tous les éléments lui permettant de faire un choix optimal compte tenu de ses contraintes.

Dans le cas des systèmes SATCP, l'étude décrite dans cet exposé a permis d'orienter certains grands choix retenus pour le système MISTRAL dont le développement a débuté peu de temps après, en particulier :

- le type de guidage (IR) et la sensibilité nécessaire de l'autodirecteur,
- le sacrifice de l'épaulabilité (du moins pour la version de base) au profit de l'efficacité ce qui a dicté le choix du calibre,
- la forme de l'irdôme,
- la vitesse d'éjection nécessaire,
- les caractéristiques principales du système d'acquisition visuelle de la cible (choix d'une lunette grossissante),
- le type de charge et de système de détection pour l'initialisation de la mise à feu.

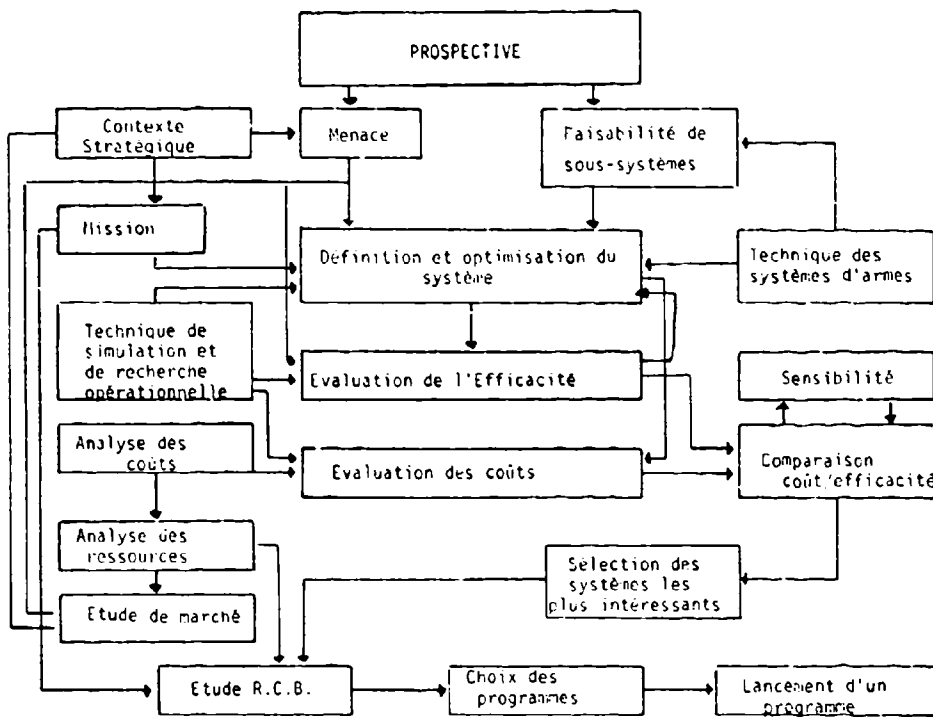


Figure 1 : Etudes d'Analyse de Systèmes préliminaires au lancement d'un programme

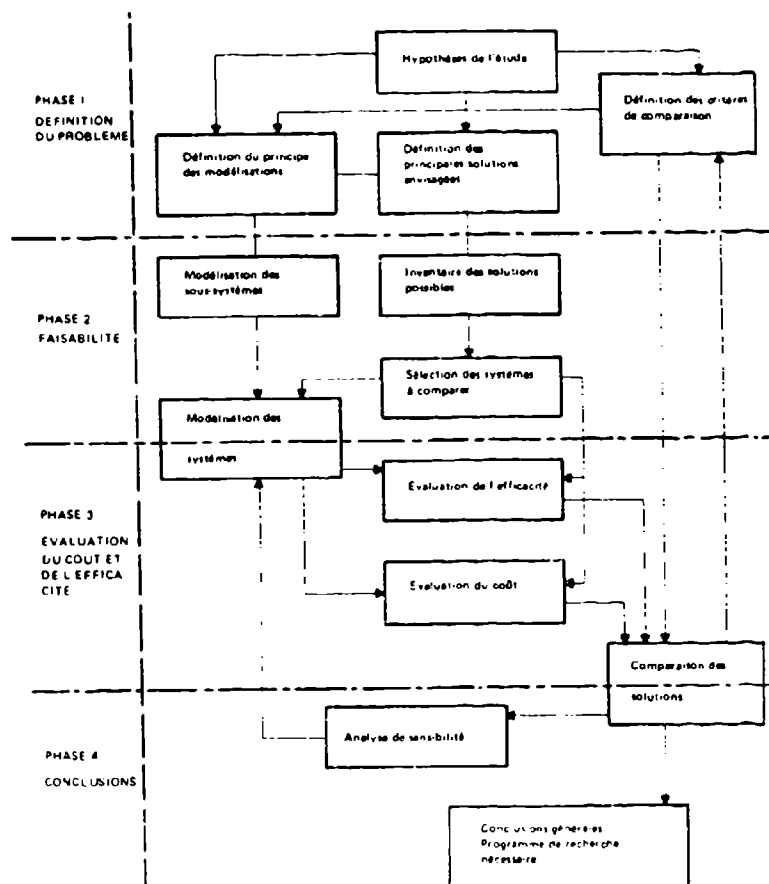


Figure 2 : Méthodologie de l'étude SATCP

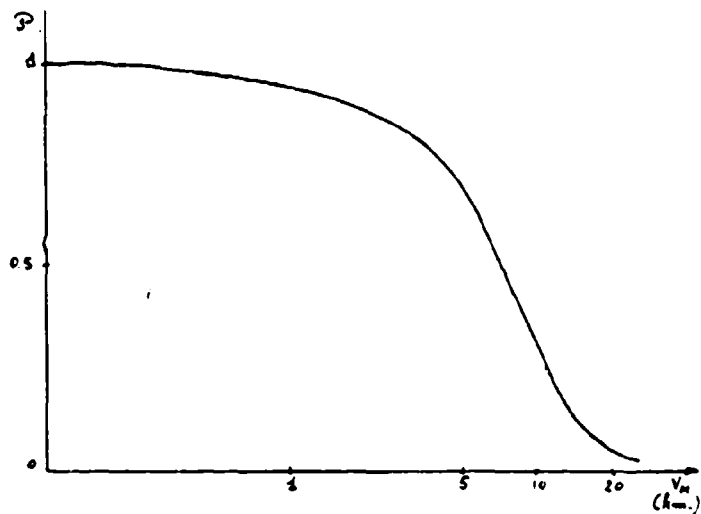


Figure 3 : Probabilité d'occurrence d'une visibilité météorologique supérieure à une valeur donnée - Région Centre-Europe

	FONCTIONS	LANCEMENT		ALERTE	ACQUISITION	IDENTIFICAT.	EVALUATION	POURSUITE	
		Implantation	Lanceur					Objectif	Misile
8 Y S T E M E S	SOLUTIONS ENVISAGEABLES	1 Épaulement fantassin 2 Affut portable 3 Véhicules 1 léger 2 lourd	1 Tube chargeable 2 Tube chargé 1 consommable 2 réutilisable	1 Visuelle 2 Optique 3 radar 4 Acoustique	1 Visuelle 2 Optique 1 Manuelle 2 automatique	1 Visuelle 2 par procédur	1 Empirique 2 Vision calcu 3 Télémétrie 4 Calculateur	0 pas de poursuite 1 Poursuite manuelle 1 Visuelle 2 Assistée	0 pas de poursuite 1 Poursuite manuelle Visuelle Assistée 2 Poursuite automatique

	NATURE DU SIGNAL	ILLUMINAT	GUIDAGE			RALLIEMENT	NAVIGATION
			Mode	Émission des ordres	Transmission		
8 Y S T E M E S	1 Optique visible 2 Optique IR 3 S.M. 4 Laser	1 Radar 2 Laser	1 Téléguidage manuel 2 Téléguidage automatique Télécommande Beam riding 3 Autoguidage 4 Guidage mixte	1 Manuelle 2 Émission d'ordres au sol 3 Faisceau codé 4 Autodirecteur	1 Sans 2 Télécommande radio 3 Faisceau 4 Filoguidage	1 Sans 2 Manuel 3 Automatique	1 Alignement 2 Poursuite 3 Navigation proportionnelle sans avance 4 Navigation proportionnelle avec avance

	FONCTIONS	CONFIGURA AÉRODYNAMIQUE	PILOTAGE		PROPELLAGE		ARMEMENT	
			Principe	Action	Ejection	Propulsion principale	Charge	Mise à feu
M I S I L E	SOLUTIONS ENVISAGEABLES	1 Classique 2 Centrifuge 3 Corps empenné 4 Corps fusée	1 Pilotage 3 axes 2 Pilotage 2 axes L R T 3 Pilotage 1 axe	1 Gouverne aérodynamiques 2 Gouverne de jet 3 Déviation de jet 4 Moteur "Clouté" 5 Effet canon	1 Pas d'éjecteur 2 Ejecteur intégré au lanceur 3 Ejecteur largable intégré au missile 4 Ejecteur intégré au missile 5 Effet canon	1 Pas de propuls 2 Propulsion 1 étage 3 Propulsion 2 étages	1 Aérais légers 2 à souffle 3 à barreau 4 à l'échelle 5 Creuse multiple 6 à effet directionnel 7 F.A.E	Fusée d'impact Fusée de proximité IR Laser EM Electrostatique

Figure 4 : Fonctions principales des systèmes SATCP et sous-systèmes envisageables

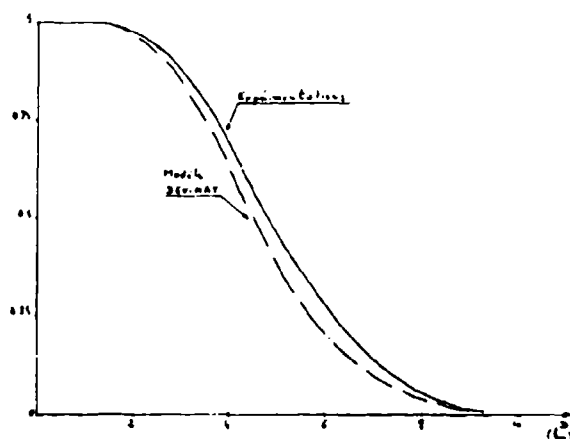


Figure 5 : Comparaison des probabilités de détection obtenues par le modèle de simulation avec les expérimentations - Cible chasseur bombardier

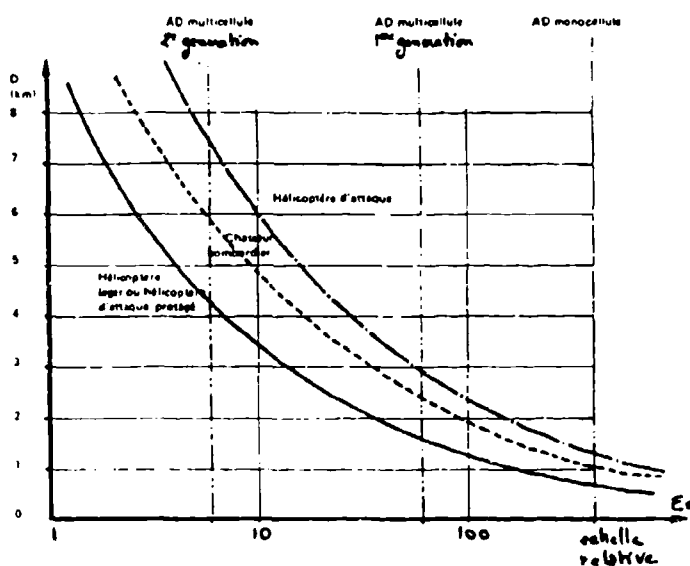


Figure 6 : Distances d'accrochage des autodirecteurs I.R. sur cibles en présentation frontale - Bande 3,8 - 4,7 μ

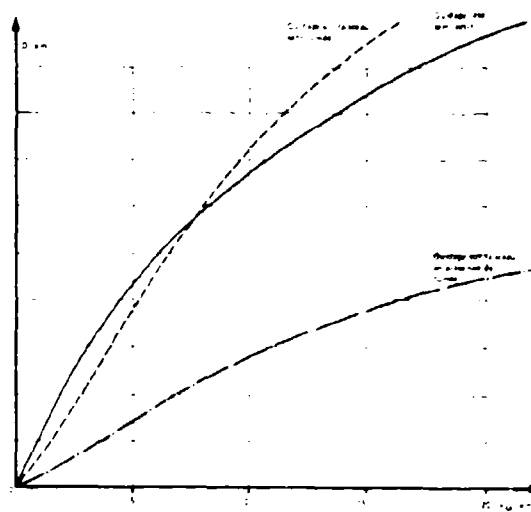
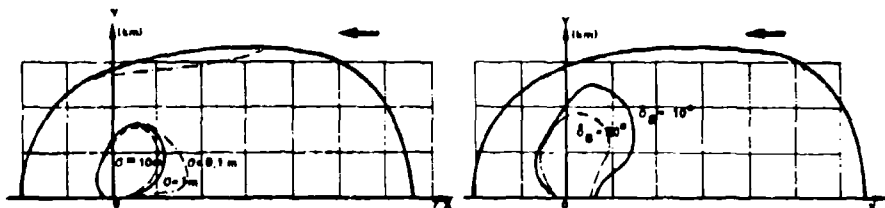
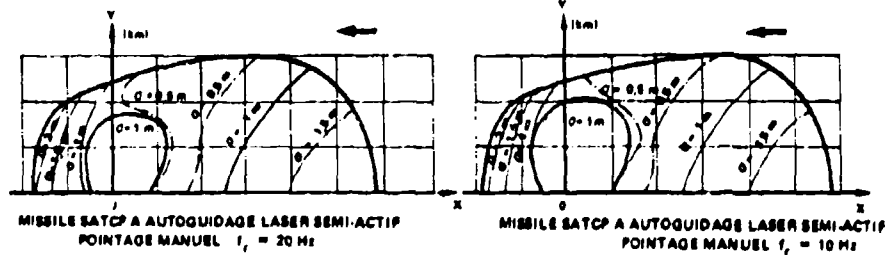
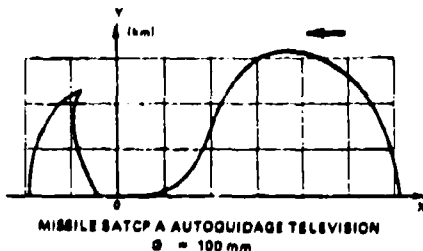
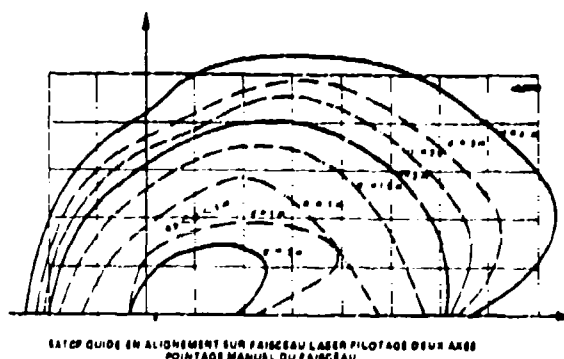
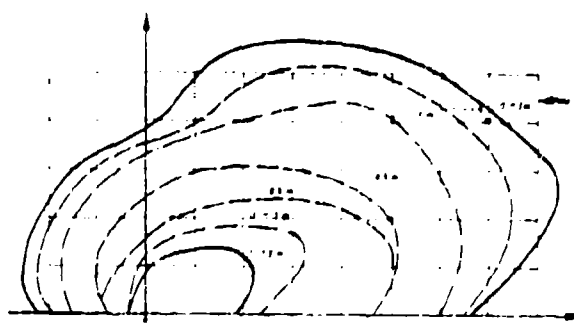


Figure 7 : Portées des systèmes laser

Syst.	Guidage	θ (mm)	Pointe Avant	Aérodynamique-Pilotage	Profil de vitesse	Implantation	Loi de Navigation
A.1	Autoguidage I.R.	70	Sphérique	Canard - autorotation	épaulable	N.P.	
A.2	Autoguidage I.R.	70	Sphérique	Canard - twist and steer	épaulable	N.P.	
A.3	Autoguidage I.R.	90	Hémisphérique	Canard - twist and steer	Effet canon possible	trépied	N.P.
B.1	Faisceau laser	90	Pointue	Canard - twist and steer	trépied	Alignment	
B.2	Faisceau laser	90	Pointue	Classique avec aile longue et pilotage trois axes	trépied	Alignment	
C	Faisceau laser + T.V.	90	Pointue		véhicule	Alignment	
D.1	Téléguidage	70	Pointue	Canard - twist and steer	épaulable	Alignment	
D.2	Téléguidage	70	Pointue	Autorotation + déviation du jet	épaulable	Alignment	
E	A.D. Laser	100	Sphérique	Canard - twist and steer	trépied ou véhicule	N.P.	
F	A.D. T.V.	100	Sphérique	Canard classique Pilotage trois axes	véhicule	N.P.	
G	A.D. E.M.	100	Conique	Canard classique Pilotage trois axes	véhicule	N.P.	

Figure 8 : Systèmes SACTP de base retenus pour l'évaluation

MISSILE SATCP A AUTOGUIDAGE I.R. $\Theta = 70$ mm
PILOTAGE DEUX AXES (MISSILE A₂)MISSILE SATCP A AUTOGUIDAGE I.R. $\Theta = 70$ mm
PILOTAGE UN AXE (MISSILE A₁)MISSILE SATCP A AUTOGUIDAGE LASER SEMI-ACTIF
POINTAGE MANUEL $f_r = 20$ HzMISSILE SATCP A AUTOGUIDAGE LASER SEMI-ACTIF
POINTAGE MANUEL $f_r = 10$ HzMISSILE SATCP A AUTOGUIDAGE TELEVISION
 $\Theta = 100$ mmSATCP GUIDE EN ALIGNEMENT SUR FAISCEAU LASER PILOTAGE DEUX AXES
POINTAGE MANUEL DU FAISCEAUSATCP GUIDE EN ALIGNEMENT SUR FAISCEAU LASER PILOTAGE DEUX AXES
POINTAGE AUTOMATIQUE TV DU FAISCEAUFigure 9 : Domaines de tir dynamiques des missiles et distances de passage
face à un avion volant à Mach 0,7

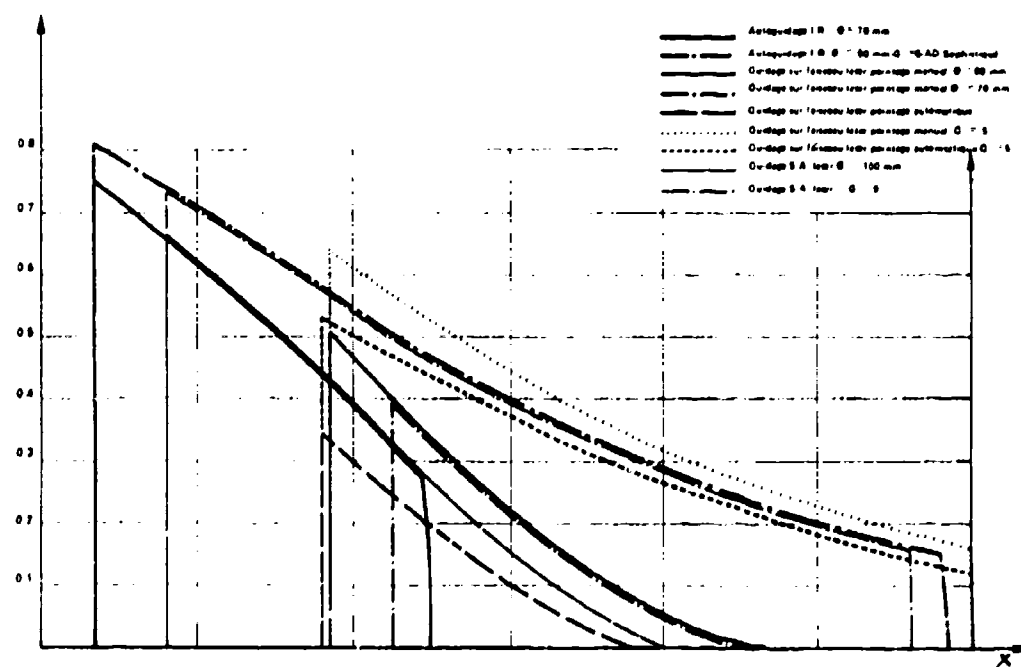


Figure 10 : Pourcentage du temps d'utilisation des systèmes en fonction de la distance de tir face à un avion volant à Mach 0,7

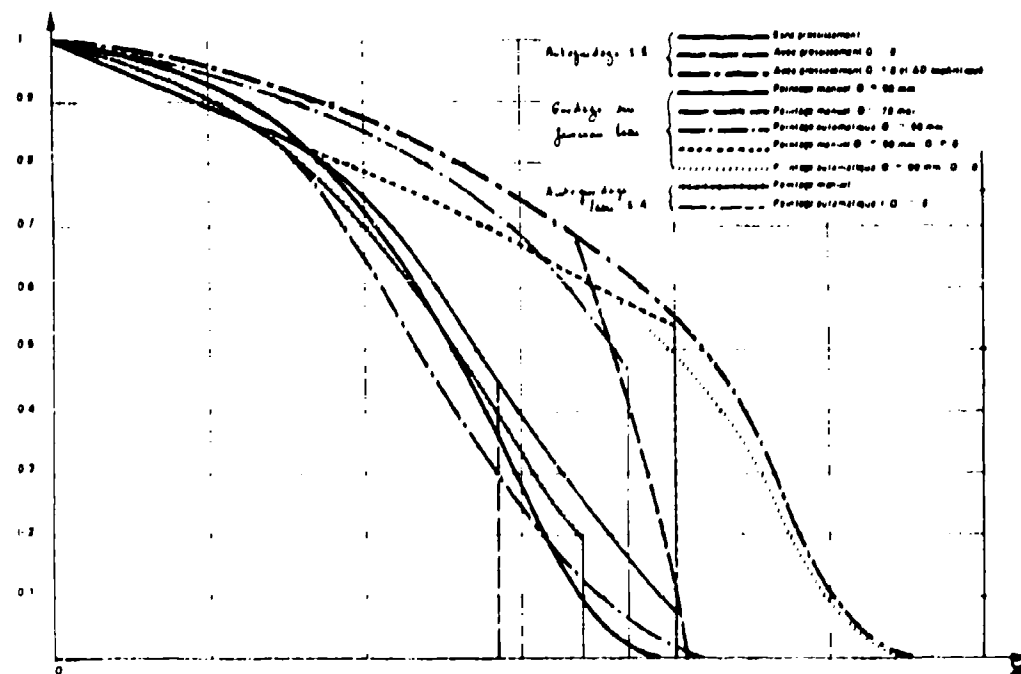


Figure 11 : Pourcentage du temps d'utilisation des systèmes face à un hélicoptère se déplaçant 20 secondes à la distance X

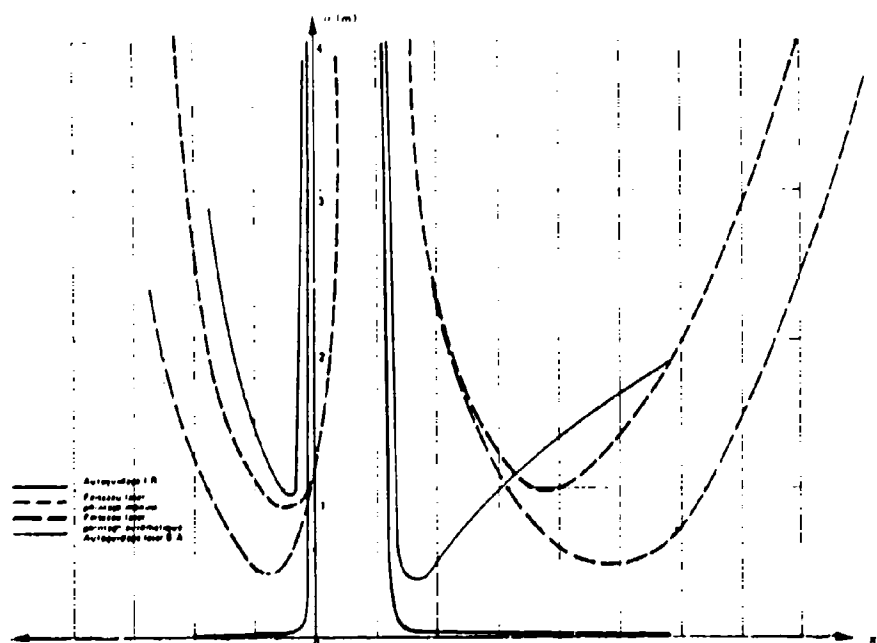


Figure 12 : Distances de passage en fonction du point de tir contre un avion volant à Mach 0,7

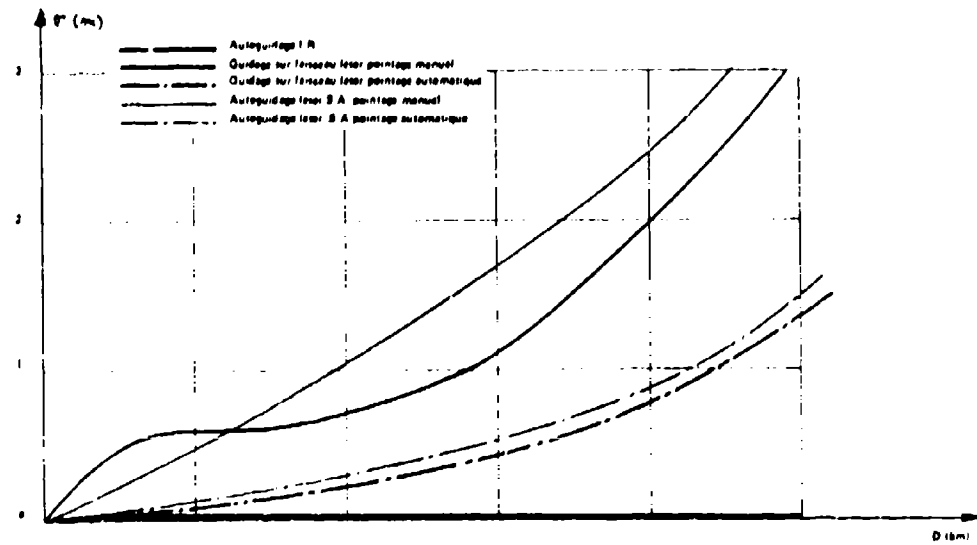


Figure 13 : Distances de passage en fonction du point de tir d'un hélicoptère stationnaire

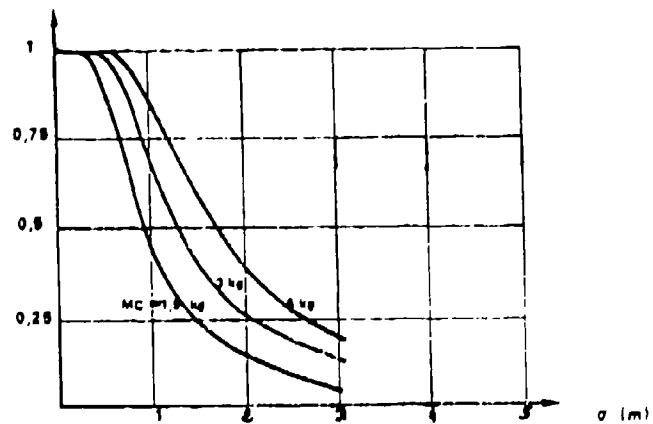


Figure 14 : Probabilité de destruction en fonction de la distance de passage

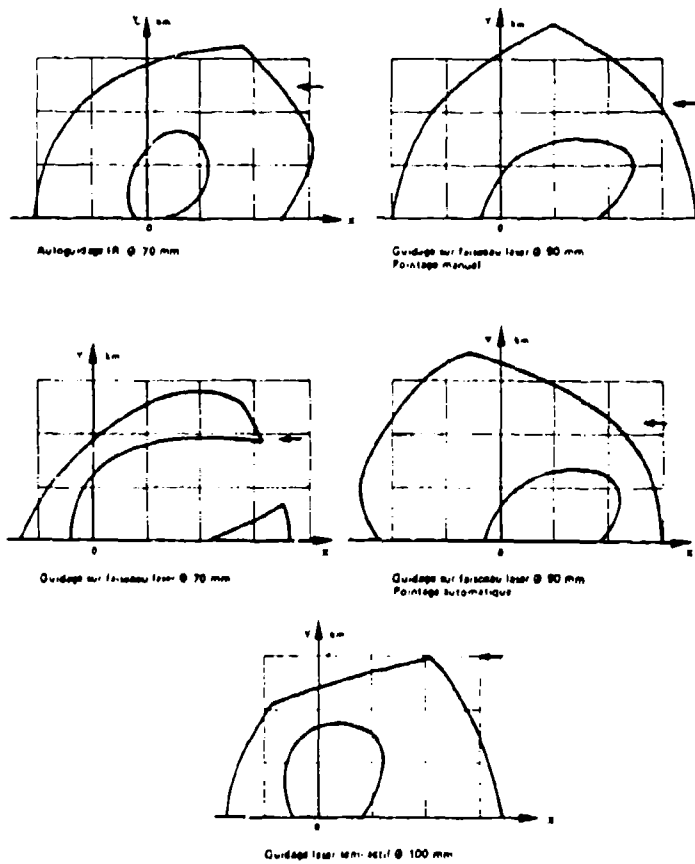


Figure 15 : Domaines de tir opérationnels pour une visibilité météorologique de 17 km

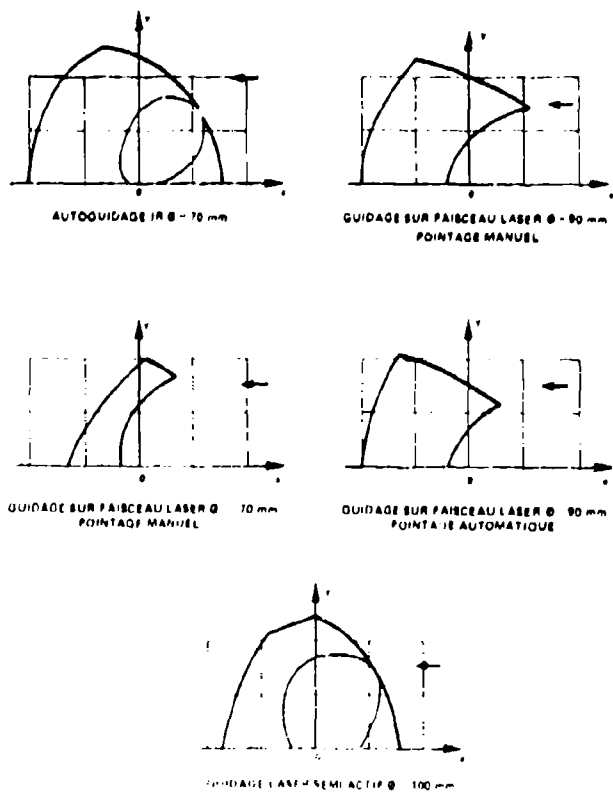


Figure 16 : Domaines de tir opérationnels pour une visibilité météorologique de 7 km

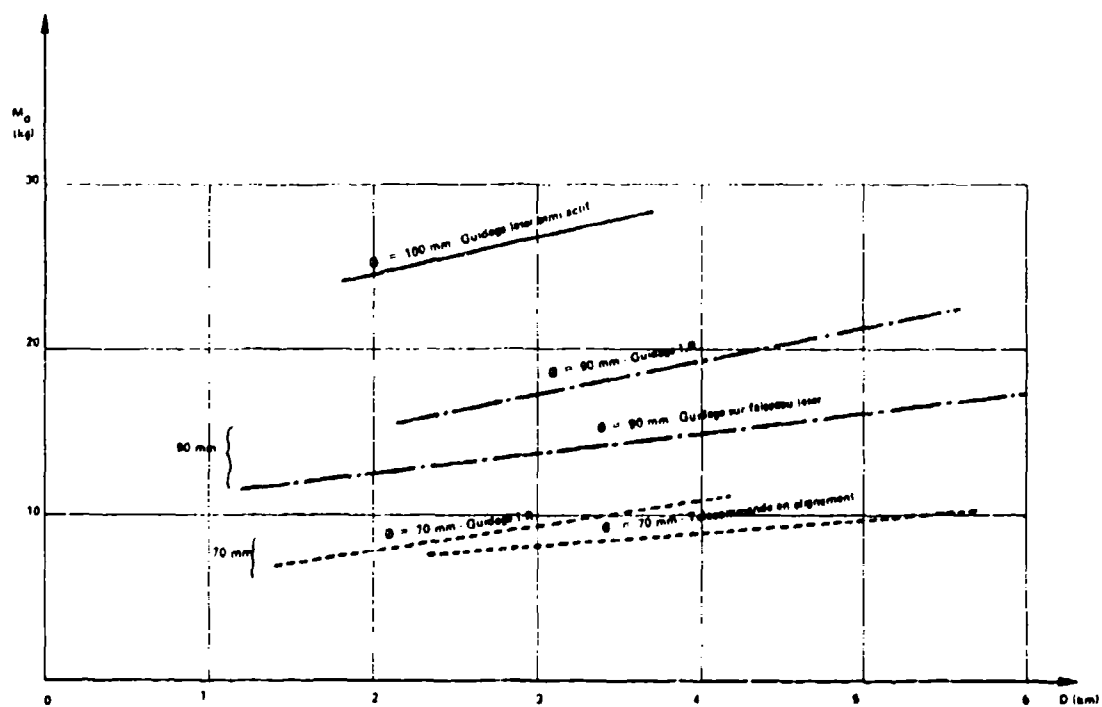


Figure 17 : Masse des missiles en fonction de la portée

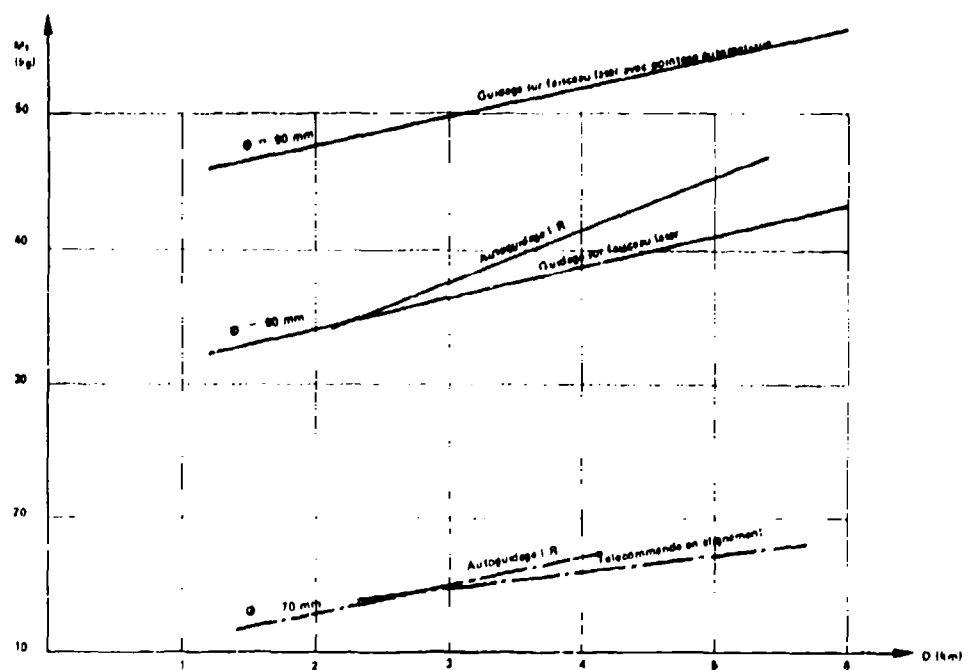


Figure 18 : Masse des systèmes en fonction de la portée

SOME ASPECTS OF GUIDANCE LOOP DESIGN FOR SAM SYSTEMS

by

D. J. East
 Royal Military College of Science
 Shrivenham, Swindon, Wilts
 United Kingdom

SUMMARY

The paper deals with the basic structure of guidance loops for SAM systems and discusses two important practical problems associated with their design and implementation if optimum performance is to be achieved. Firstly, the nature of the switching transients that occur when loop parameters are changed is examined and the fundamental requirements for transient free operation presented. Secondly, a computer aided design procedure for synthesising a minimum bandwidth system which satisfies a stringent sensitivity specification despite large uncertainty in the plant being controlled is illustrated by means of a significant autopilot design example.

NOTATION

f_M missile lateral acceleration (latax)
 v_M missile velocity
 v_T target velocity
 R_M missile range from tracker
 R_T target range from tracker
 σ_M angle of missile flight path to line of sight
 σ_T angle of target flight path to line of sight
 ψ_f angle of missile flight path to earth reference
 θ angle of line of sight to earth reference
 f_{MD} demanded missile latax
 θ_M angle subtended by missile to earth reference
 θ_T angle subtended by target to earth reference
 R_M' pre-programmed gain variation corresponding to assumed missile range
 K loop DC gain (beam stiffness)
 ϕ angle of target flight path to earth reference
 k proportional navigation constant
 v_r relative closing velocity between missile and target
 T time to go to interception

1. INTRODUCTION

The basic principles of guidance loop design for SAM systems are well established and future systems are unlikely to differ conceptually in any significant way from previous systems. That is, the fundamental limitations of command to line of sight (CLOS) or beam riding guidance systems and homing guidance systems remain the same although the implementation of such systems will, of course, be crucially dependent on the current state of hardware development. However, increased demands on system performance have highlighted deficiencies in the ability of the guidance loop design and synthesis techniques to achieve optimum performance within these fundamental limitations, where optimum can be interpreted in a number of very practical and intuitively meaningful ways and need not necessarily relate to the minimisation or maximisation of some mathematically defined performance index.

Two examples of deficiencies in design techniques concern the requirement to change parameters within a guidance loop without generating undesirable transients and the need to achieve minimum bandwidth sub-systems e.g. autopilots, whilst satisfying overall guidance loop objectives. Both of these problem areas have previously been tackled in a rather *ad hoc* manner and it is the intention of this paper to clarify the nature of the problems and then to indicate how steps may be taken to overcome them.

However, in order that the two design problems may be seen in context and to provide an overview of the basic guidance loop principles available to SAM designers, the first part of this paper will be largely tutorial in nature and will compare CLOS, beam riding and homing guidance loops and, in particular, the kinematic transfer functions of the respective systems will be discussed and the necessary guidance loop compensation functions established.

2. TWO AND THREE POINT GUIDANCE

Although CLOS and beam riding systems cannot be implemented in exactly the same manner, since the CLOS missile is generally regarded as one that receives its commands from a remote ground station whereas the beam riding missile generates its own commands internally, they are nevertheless essentially the same type of system with regard to the generation of latax (lateral acceleration) commands. In particular, the behaviour of the system is governed by the relative positions of three points, viz the target tracker (which defines the beam or line of sight), the missile and the target. Accordingly, CLOS or beam riding systems may be designated as three point guidance systems.

Such systems should be contrasted with homing systems which are essentially two point guidance systems, with characteristics determined by the positions of the missile and target only. This distinction applies not just to active or passive homing systems but equally to semi-active systems since, although the illuminating radiation must necessarily be directed at the target, the exact position of the illuminating source does not influence the desired trajectory and hence the latax demands on the missile. It should be noted that considerable variations can and do exist within these two broad classifications of two and three point guidance (e.g. CQLOS or command off the line of sight systems can exhibit characteristics similar to a two point guidance system) but, for our purposes, these two classifications will suffice.

The full derivation of the latax requirements for the two types of guidance system have, for most relevant conditions of missile and target velocity and type of guidance law, been presented elsewhere [1,2,3]. However, these derivations can soon become overwhelmingly complex if entirely realistic conditions are imposed and so here we will concentrate on the two-dimensional case with the missile and target respectively travelling at constant velocities. The justification for this simplification is that our objective is primarily to establish the form only of the required guidance loop and in so doing to appreciate some of the problems that are likely to arise in implementing such a guidance loop.

2.1 3-point guidance loops

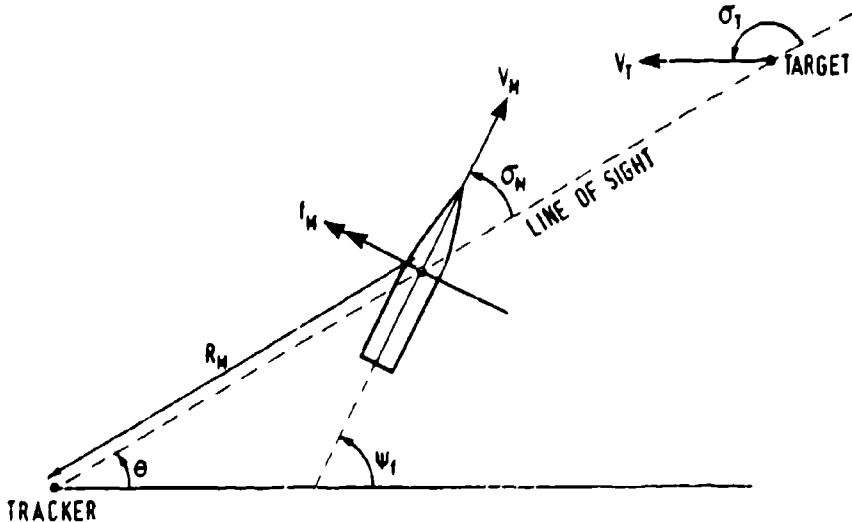


Figure 1: Notation for 3-point guidance

Using the notation of Fig 1, and assuming zero incidence, we have

$$f_m = V_m \dot{\psi}_f$$

i.e. lateral acceleration = missile velocity x flight path rate

$$\text{also } \dot{\psi}_f = \dot{\theta} + \dot{\sigma}_m$$

$$\text{therefore } f_m = V_m (\dot{\theta} + \dot{\sigma}_m) \quad (1)$$

However, in order to interpret this last equation more easily we must express $\dot{\sigma}_m$ in terms of variables that can be measured or inferred from tracker based observations. Thus, we have

$$\dot{\theta} = \frac{V_m \sin \sigma_m}{R_m} \cdot \frac{V_T \sin \sigma_T}{R_T} \quad (2)$$

from which

$$\sin \sigma_m = \frac{R_m \dot{\theta}}{V_m}$$

and differentiating this gives

$$\cos \sigma_m \dot{\sigma}_m = \dot{\theta} \frac{R_m}{V_m} + \dot{\theta} \frac{\dot{R}_m}{V_m} + R_m \ddot{\theta} \left(-\frac{\dot{V}_m}{V_m^2} \right) \quad (3)$$

also

$$\dot{R}_m = V_m \cos \sigma_m \quad (4)$$

Hence, substituting for $\dot{\sigma}_M$ and \dot{R}_M from (3) and (4) into (1), we get

$$f_M = 2\dot{\theta}V_M + \frac{R_M \dot{\theta}}{\cos \sigma_M} - \dot{V}_M \tan \sigma_M \quad (5)$$

which represents the latax needed by the missile to stay on the line of sight.

This equation, although so readily derived, is highly informative and enables many useful qualitative observations to be made with regard to the coverage of a CLOS or beam riding missile. Firstly, if the missile is neither accelerating nor decelerating ($\dot{V}_M = 0$) then the latax required will be highly dependent on both the sightline rate ($\dot{\theta}$) and the sightline acceleration ($\ddot{\theta}$). Although $\dot{\theta}$ will clearly be a maximum when $\theta = 90^\circ$ (assuming a constant speed straight flying target), $\dot{\theta}$ is readily shown to be a maximum at $\theta = 60^\circ$, to decay to zero at $\theta = 90^\circ$, and to be a minimum (i.e. most negative) at $\theta = 120^\circ$. Thus, ignoring the variations in R_M and $\cos \sigma_M$, it is clear that for any given maximum latax that may be achieved by the missile then the coverage will be most restricted for high speed targets (implying high $\dot{\theta}$ and $\dot{\theta}$) in the sector $\theta \in [60^\circ, 90^\circ]$.

Another observation that can be made from equation (5) related to the case when V_M varies. If \dot{V}_M is negative, such as during the coast phase for a boost-coast propelled missile, then this too will set limits on the missile latax, thus further restricting the coverage.

Further limitations on the coverage of a CLOS or beam riding missile can result from excessive body to beam angle (σ_M), causing the missile tracker to lose lock on the beacon or flare or other source of identification used by the missile. The region in which σ_M will be largest will generally be where the latax demands are greatest and so there are likely to be further "bites" taken out of the coverage diagram near minimum crossing distance. Another possible limitation is at the tracker itself where, if $\dot{\theta}$ is too large, it may have insufficient bandwidth to follow the target. Obviously, for a straight flying target, $\dot{\theta}$ will be a maximum at $\theta = 90^\circ$ but it would be unrealistic to suppose that the target could be subsequently re-acquired when $\dot{\theta}$ decreases for $\theta > 90^\circ$ and so there will be a further restriction in coverage, as indicated in Fig 2 in the sector $\theta \in [90^\circ, 180^\circ]$. In general, therefore, the coverage diagram of a CLOS or beam riding system will have the form shown in Fig 2 and it must be accepted that the very kinematics of this type of 3-point guidance must inevitably result in limitations on coverage.

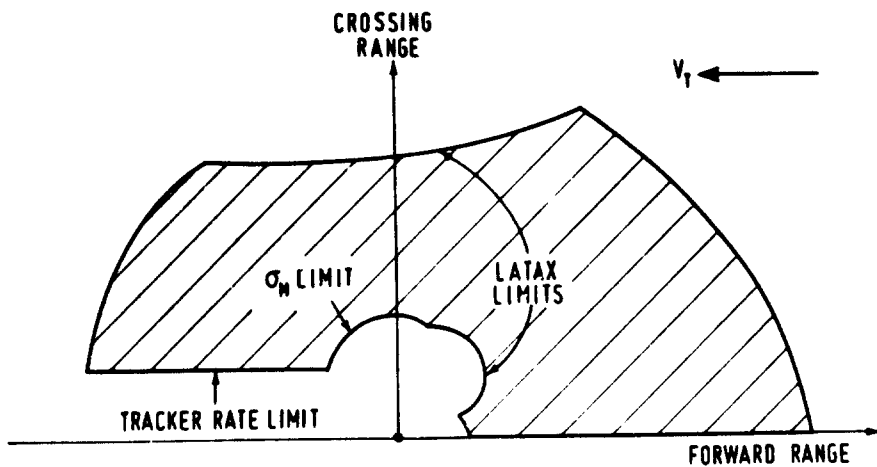


Figure 2: Typical Coverage Diagram for CLOS or beam riding system

As well as providing a qualitative indication of the nature of the coverage diagram, equation (5) can also be used to immediately derive a kinematic transfer function as a basis for a guidance loop block diagram. Thus, from equations (2) and (4) we have

$$\sin \sigma_M = \frac{R_M \dot{\theta}}{V_M}, \cos \sigma_M = \frac{\dot{R}_M}{V_M}$$

which may be substituted into (5) to yield the transfer function

$$\frac{\theta_M}{f_M} = \frac{1}{((2V_M - \dot{V}_M R_M / \dot{R}_M) + (R_M V_M / \dot{R}_M) S)} \quad (6)$$

where θ_M replaces θ to emphasise that this is the angle subtended by the missile (which will only be exactly the same as the angle subtended by the target, from henceforth denoted θ_T , if the missile is precisely on the beam). The missile kinematics are thus represented by a first order lag and an integrator in cascade.

For accurate stability analysis and loop design the transfer function (6) would have to be used with appropriate values for V_M , \dot{V}_M , R_M and \dot{R}_M substituted for a sufficient number of flight conditions within the missile coverage. However, in order to appreciate the general nature of the loop design problem

We can approximate this transfer function for the case where V_M is reasonably constant ($\dot{V}_M \approx 0$), σ_M is small so that $V_M \approx R_M$, and R_M can be considered sufficiently large so that for all but the lowest frequencies $|R_M| \gg |2V_M|$ and the kinematic transfer function reduces to

$$\frac{\theta_M}{f_M} = \frac{1}{R_M^2}$$

The CLOS guidance loop is thus essentially a classic two integrator system and must be stabilised by some form of phase advance stabilisation as shown in Fig 3.

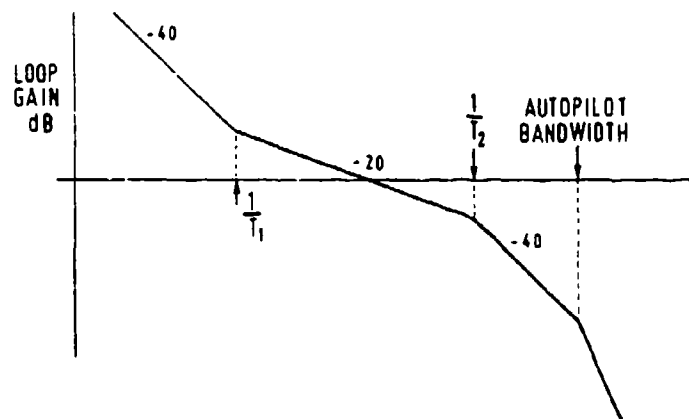
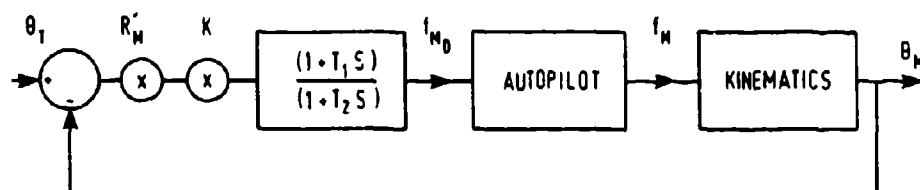


Figure 3: Stabilisation of a CLOS guidance loop by appropriate shaping of the open loop Bode plot

It should be noted that even with this simplified version of the kinematics, there is still an inherent range variation term R_M and this must be accommodated by means of a pre-programmed gain variation R'_M within the guidance computer since otherwise the stability characteristics of the loop will change during the flight of the missile. Even so, it may still be desirable to alter K (the so-called "beam stiffness"), and hence T_1 and T_2 , during different phases of the flight since the need for high gain K , and hence high loop bandwidth, for good tracking of a moving target sightline may compromise the overall accuracy (and even stability) that can be achieved when high frequency noise is allowed to enter the system.

This conflict of requirements on the loop bandwidth is common to most high performance control systems and various methods have been proposed for alleviating the need to extend bandwidth more than absolutely necessary. One such method is the use of "feed-forward" as shown in Fig

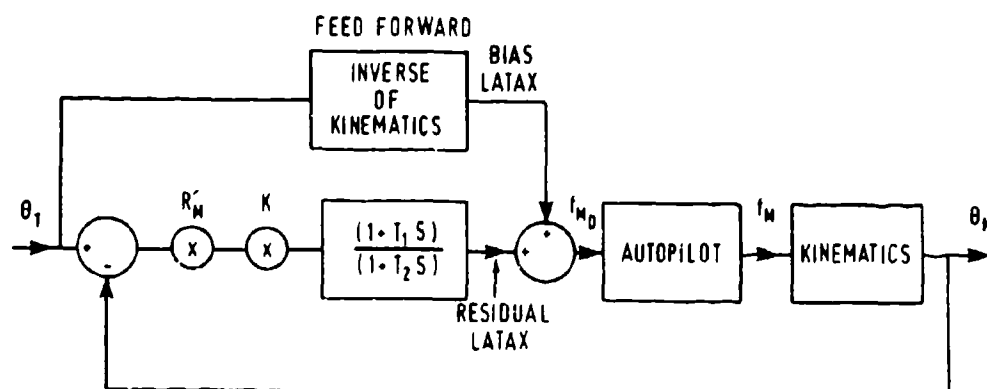


Figure 4: The use of feed-forward in a CLOS system

This is essentially an open-loop computation based on equation (5) and is fundamentally an inverse transfer function to the kinematics.

Clearly, if we ignore the latax autopilot of the missile, the closed guidance loop would not be required to provide any additional commands to the missile if the feedforward and kinematic blocks cancel exactly and so its bandwidth can be made arbitrarily small. In practice, of course, such perfect cancellation will not occur and also the missile autopilot will have a finite bandwidth but feedforward will, nevertheless, allow for a significant reduction in loop bandwidth. However, it should be stressed that feedforward introduces its own problems, most notably a high gain to high frequencies, and this will tend to negate the advantage gained by reducing the loop bandwidth.

The main point to be emphasised here is that maximum performance can only be obtained from CLOS guidance loops if loop bandwidths are reduced as much as possible, commensurate with tracking requirements and noise levels, and this can be done by employing an optimum, i.e. minimum bandwidth, synthesis technique and/or an adaptive scheme that switches the loop gain K , together with T_1 and T_2 , on a pre-programmed or even autonomous basis. Sections 3 and 4 will deal more fully with these techniques but meanwhile, in order to complete the tutorial objectives of this paper, the next sub-section will briefly deal with 2-point or homing guidance loops.

2.2 2-point guidance loops

The analytical derivation of the latax requirements for homing systems is generally not possible and consequently the corresponding kinematic transfer functions can only be derived in special circumstances [4,5,6]. However, if we assume that proportional navigation is being employed, wherein the missile flight path rate is made proportional to the sightline rate between missile and target, and that the missile has become established on an interception course from which it is subjected only to comparatively small perturbations then it is readily shown [3] that the corresponding homing guidance loop block diagram has the form shown in Fig 5.

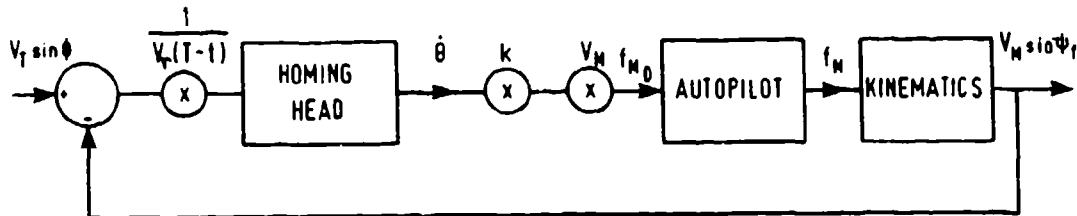


Figure 5: A homing guidance loop

In this case, the kinematic transfer function has the form $\cos \theta / S$ and so the loop frequency response is clearly dominated by a single integrator if the autopilot and homing head bandwidths are sufficiently large. It is seen, therefore, that loop stability is not likely to be a problem, at least until near interception when $1/V_t(T-t) \rightarrow \infty$, and so it is not necessary to use phase advance compensation with the concomitant increase in bandwidth and associated noise amplification problems. However, it is still highly desirable to keep the homing guidance loop bandwidth as small as possible and so optimum synthesis techniques are again called for. It is also possible that the control parameters of the loop, such as the navigation constant, will need to be changed during different phases of the flight and so adaptive switching techniques will be required. Accordingly, section 3 will consider some of the fundamental problems associated with the switching of parameters within a closed loop system and section 4 will discuss an optimum or minimum loop bandwidth synthesis technique.

3. THE ELIMINATION OF SWITCHING TRANSIENTS IN ADAPTIVE GUIDANCE LOOPS

We saw in section 2.1 that the simplest representation of a CLOS guidance loop consists of two integrators, representing the kinematics, and a compensation network of the form $K(\frac{1+T_1s}{1+T_2s})$. It is easy to envisage circumstances in which it might be desirable to change the loop bandwidth by altering K . For example, during the gathering phase, or whilst engaging a high speed crossing target, a high beam stiffness K would be required but once the missile is established on a low rate line of sight, particularly if the guidance loop is subject to high levels of noise, it would be preferable to reduce K as much as possible.

Typically, we might wish to switch K between two fixed values of, say, 1 and 10; of course, in order to maintain the desired degree of stability the time constants T_1 , T_2 must also be altered in sympathy with K and it is readily confirmed that the following compensation networks give satisfactory stability margins:

$$1 \times \left(\frac{1 + 2s}{1 + 0.2s} \right)$$

low gain
compensation network

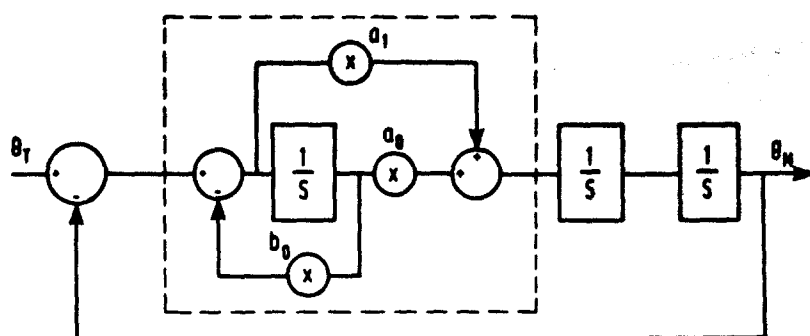
$$10 \times \left(\frac{1 + 0.625s}{1 + 0.0625s} \right)$$

high gain
compensation network

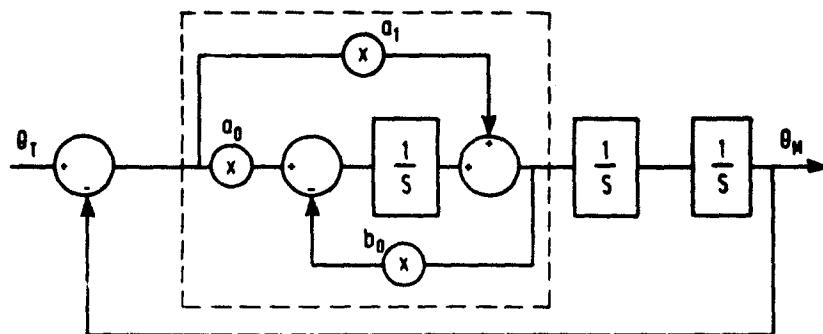
In order to facilitate the extension of the results from this particular example to more complex cases it is convenient to adopt the following representation for the compensation network, namely:

$$\frac{a_0 + a_1 s}{b_0 + s} \text{ where } K = a_0/b_0, T_1 = a_1/a_0, T_2 = 1/b_0$$

This network, together with the two integrators representing the remainder of the simplified CLOS guidance loop, can be decomposed into a form suitable for simulation, as shown in Fig 6(a). It should be noted that, at this stage, no particular consideration has been given to the structure of the compensation network and another possibility is that shown in Fig 6(b). Indeed, for a linear system with constant coefficients (a_0, a_1, b_0) , there are many possible structures and all are equally valid.



(a) STRUCTURE 1



(b) STRUCTURE 2

Figure 6: Alternative representations of the CLOS system mathematical model

Both of the structures shown in Fig 6 were simulated, taking θ_T as a step input ($\theta_T = 1, t > 0$) and with the low gain compensating network initially in the loop. After 2.5 seconds the coefficients of the compensation network were instantaneously switched to those corresponding to the high gain compensation network with the results shown in Fig 7.

Clearly, the transient produced when the network coefficients of structure 1 are switched (henceforth referred to as the "switching transient") is not at all consistent with the desired objective in changing to a high bandwidth system; namely to make θ_M approach θ_T even more rapidly than was being achieved with the low bandwidth system. Furthermore, a transient occurring near interception could have a most deleterious effect on miss-distance and if no guarantee could be made that such transients could be minimised or suppressed completely then there would be no possibility of employing adaptive networks in a missile guidance loop.

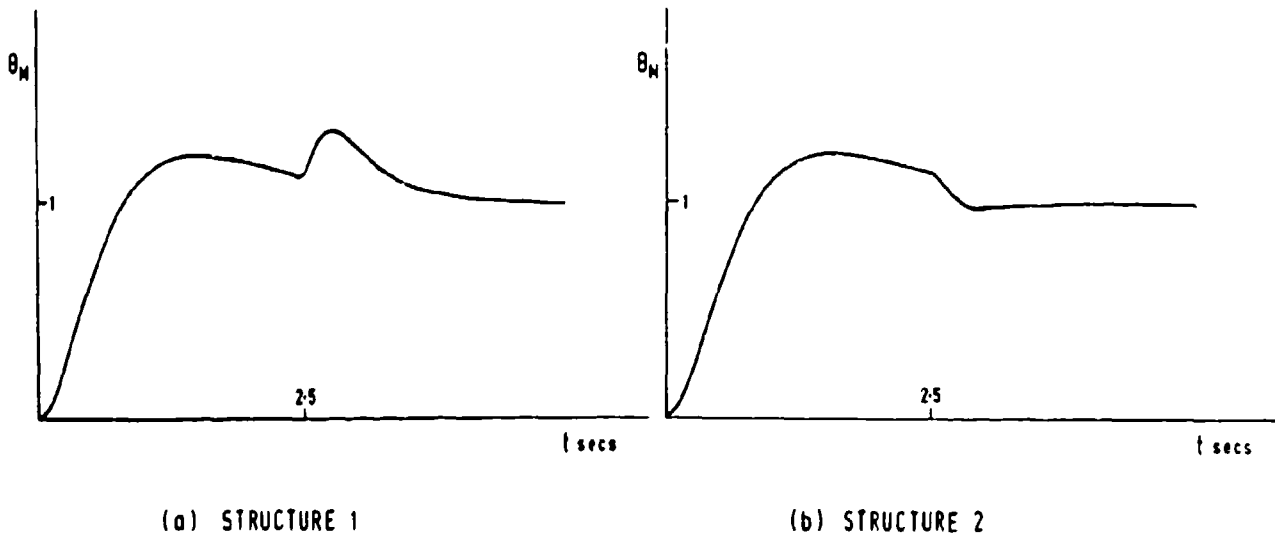


Figure 7: Results obtained when switching network coefficients

On the other hand, the behaviour of structure 2 is quite acceptable and should, therefore, provide some insight into the mechanism of the switching transient when compared with structure 1. Such indeed is the case and the development and motivation behind the results which follow can be found in [7], in which it is shown that a transient free structure for the compensation network used above must take the form shown in Fig 8.

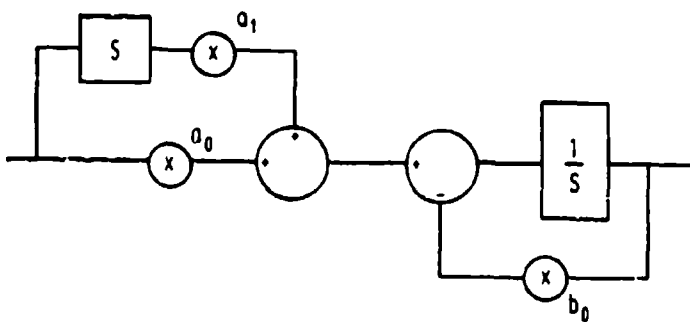


Figure 8: A transient free structure for the network $(a_0 + a_1 s) / (b_0 + s)$

The two fundamental principles behind this structure are that:

- i. Switched parameters should occur after differentiators in order to avoid transients of the form $\theta_1 a_1$ (see Fig 10).
- ii. Switched parameters should occur before integrators in order to avoid transients of the form $\theta_0 b_0 / b_0$.

Unfortunately, the structure shown in Fig 8 is not readily implemented in practice since it involves an explicit differentiator. Nevertheless, the term in s can be eliminated if it can be replaced by a feedforward path bypassing the integrator, an equivalent way of achieving differentiation and indeed the method used in all practical implementations of rational transfer functions. However, if this method is applied directly to the network structure in Fig 8 it is seen that the s term is not eliminated since the coefficient a_1 interposes between the differentiator and the integrator in the feedforward path and prevents cancellation (Fig 9).

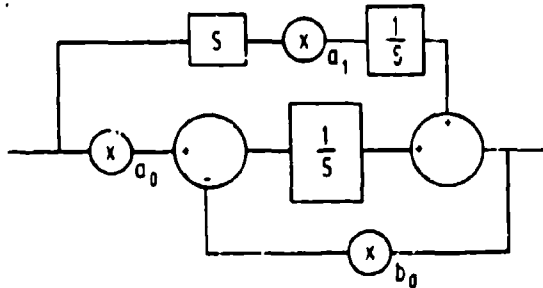


Figure 9: Re-arrangement of Figure 8

Clearly, some method for transferring coefficients from one side of a differentiator (or integrator) to the other is required if flexibility in the implementation of the desired network structure is to be obtained. This can be done only if due allowance is made for the extraneous transient terms that can arise when dealing with time varying coefficients. For example, the network shown in Fig 10(a) is not equivalent to that shown in Fig 10(b) (if the coefficient a is time varying) but it is equivalent to that shown in Fig 10(c).

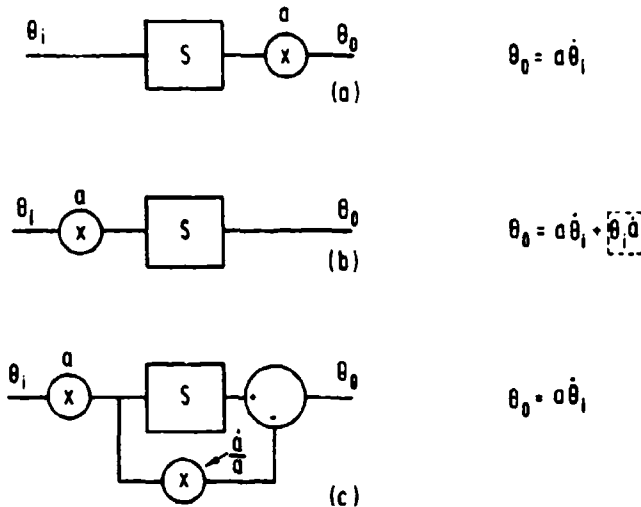


Figure 10: A differentiator with time varying coefficient a

Thus, the coefficient a can be moved from the output of the differentiator to the input provided an extra path, bypassing the differentiator and operative only when the coefficient a is changing, is included. Hence the structure of Fig 9 can be simplified as shown in Fig 11, the differentiator and integrator in the feedforward path now being allowed to cancel.

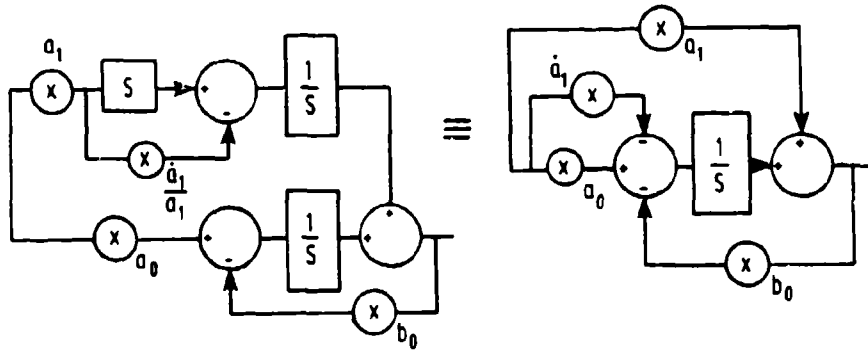


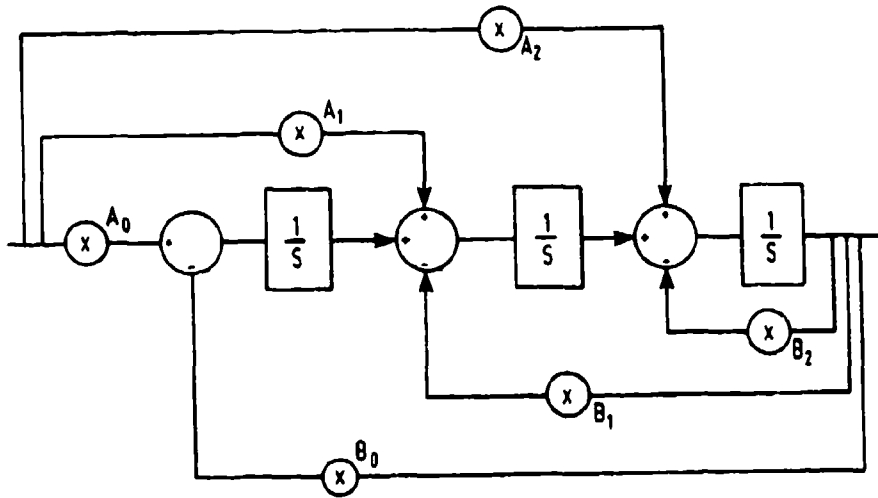
Figure 11: A practical implementation of the transient free structure for the network $(a_0 + a_1 s) / (b_0 + s)$

Now it is possible, by adhering to the principles developed above, to construct any network with time varying coefficients in such a way that extraneous transient terms are eliminated. However, such an ad-hoc approach would be very tedious with high order networks and a more general procedure can be followed that allows the necessary network structure to be deduced directly from the given time-varying coefficient transfer function [7]. For example, the practical transient free structure for a third order network is shown in Fig 12 and it is of interest to note that the coefficients of the practical network are related to the coefficients and their derivatives of the original network by means of a Pascal triangle with alternating signs.

Having shown how the guidance loop bandwidth may be adjusted by switching parameters, it is now appropriate to consider how an optimum bandwidth can be achieved using a fixed set of compensation network parameters.

4. OPTIMUM SYNTHESIS OF AUTOPILOTS AND GUIDANCE LOOPS

It is important to stress that feedback, whether applied to the implementation of guidance loops, autopilots or the multitude of other closed loop systems that occur within a guided weapon system, is used essentially to combat uncertainty. This uncertainty may be due to a lack of knowledge about the plant being controlled, e.g. the missile airframe dynamics will be dependent on speed and air density, or about the disturbances affecting the plant, e.g. atmospheric turbulence. Although this aspect of feedback is universally recognised, surprisingly little work has been done in developing synthesis techniques that attempt to quantify the amount of uncertainty and then to design just sufficient feedback into the system to counter the uncertainty and achieve specified levels of insensitivity in the closed



$$A_2 = a_2$$

$$A_1 = a_1 - 2a_2$$

$$A_0 = a_0 - \dot{a}_1 + \ddot{a}_2$$

$$B_0 = b_0 - b_1 + b_2$$

$$B_1 = b_1 = 2b_0$$

B-3-1

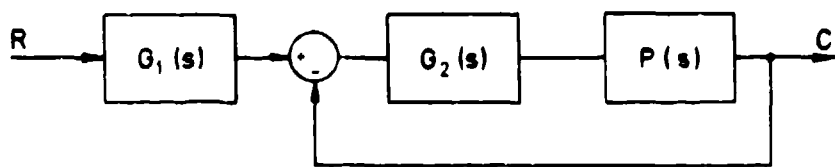
Figure 12: A practical implementation of the transient free structure for the network $(a_0 + a_1s + a_2s^2)/(b_0 + b_1s + b_2s^2 + s^2)$

loop response. The reason for this concern with applying a minimum amount of feedback is that it is very easy to overdesign feedback systems by including too much loop gain, which in turn implies high loop bandwidth and excessive amplification of high frequency noise. The problem has been emphasised repeatedly by Horowitz and others [8,9,10] and Horowitz first demonstrated his synthesis approach in 1959 [9]; unfortunately, the original Horowitz technique relied heavily on designer involvement at a fairly routine level and by its nature was not easily adapted to Computer Aided Design (CAD) procedures when the digital computer became widely available as a design tool in the 1960s. Since then, the technique has been modified, both by Horowitz and his colleagues [11] and others [12,13] and the remainder of this paper will illustrate the application of one of these modified techniques by means of a CAD autopilot design. It should be noted, however, that since the technique is quite applicable to the design of any feedback control device within the guided weapon of the innermost actuator servo loops or the outermost guidance loop itself.

The theoretical basis of the synthesis procedure is now briefly explained although further details can be obtained from the references [13,14]. Using the notation of the general two-degree-of-freedom feedback system shown in Fig 13, it is readily verified that

$$\frac{S_N}{S} - 1 = \frac{P_N}{P} - 1 \quad (7)$$

where the suffix N denotes the closed loop transfer function S , the plant transfer function P and the loop transfer function L when the plant parameters take on their nominal values, which for the present time can be assumed to be arbitrarily fixed within the range of possible parameter values. In fact, equation (7) is a sensitivity measure that relates variations in the closed loop system S , about its nominal condition S_N , to variations in the plant P , about its nominal condition P_N . Thus, at each frequency of interest, $S_N/S(j\omega)$ and $P_N/P(j\omega)$ map out regions or plots in the complex plane which represent the total amount of the variation in the closed loop system S and the plant P respectively about the point $1 + j0$ as the parameters of P vary.



$$\frac{C}{R} = S = \frac{G_1 L}{1 + L} , \quad L = G_2 P$$

Figure 13: A two-degree-of-freedom feedback system

By taking the maximum value (with respect to the variable parameters of P) of the modulus of (7) we have

$$\max \left| \frac{S_N}{S}(j\omega) - 1 \right| = \frac{\max |P_N(j\omega) - 1|}{|1 + L_N(j\omega)|}$$

and it can be shown [13] that an optimum loop design (defined as the one that satisfies the closed loop sensitivity specification with the minimum h.f. loop gain for a given excess of poles to zeros in the loop transfer function, i.e. essentially a minimum bandwidth loop) results when S_N and P_N are chosen to lie within the centre of their respective plots at each frequency. In this case $\max |S_N/S - 1|$ can be expressed analytically in terms of the Fourier transforms of the bounds $a(t)$ and $b(t)$ placed on the desired system time response (Fig 14), as

$$\max \left| \frac{S_N}{S}(j\omega) - 1 \right| \leq \left| \frac{v(j\omega)}{A(j\omega)} \right|$$

This will ensure that, on average, variations in $c(t)$ about the mean $m(t)$ will be less than $v(t)$.

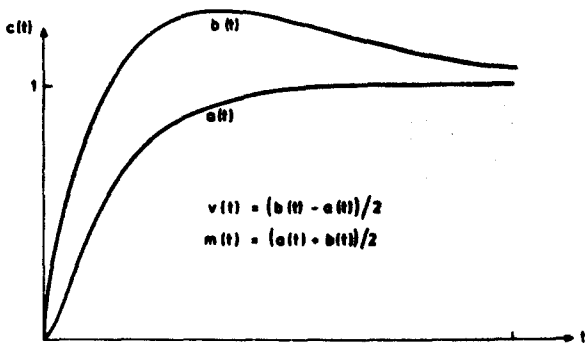


Figure 14: Specifying system time response bounds

In general it is not possible to deduce $\max |P_N/P - 1|$ analytically and normally it will be necessary to construct a separate P_N/P plot at each frequency. This indeed, is the approach adopted in the design example.

Finally, having defined $\max |S_N/S - 1|$ and $\max |P_N/P - 1|$ at each frequency of interest, $L_N(j\omega)$ must be chosen to satisfy $|1 + L_N| = \max |P_N/P - 1| / \max |S_N/S - 1|$. This effectively defines a circular bound on $L_N(j\omega)$, centred on the $1 + j0$ point, and allows a particularly straightforward iterative application of the Bode integrals relating the gain and phase of a minimum phase shift system [14].

We can now proceed with an application of this CAD synthesis technique. The data used for the design example actually relates to a high performance aircraft but the ranges of parameter variation and the sensitivity specification placed on the autopilot closed loop response are equally typical of a SAM missile being boosted from launch up to supersonic speeds. The airframe transfer function is represented as

$$P(s) = K_p \frac{(1 + T_p s)}{(1 + 2 \frac{\zeta_p s}{\omega_p} + \frac{s^2}{\omega_p^2})}$$

where, due to altitude and speed changes, the parameters can vary as shown in the table below:

K_p	0.1066	0.312	0.262	0.0583	0.0223	0.0198	0.0199	0.362	1.950	3.42	2.03	2.97
T_p	8.13	3.55	4.85	11.36	27.32	54.35	38.68	3.08	0.48	0.51	1.05	0.86
ω_p	1.988	2.972	2.769	2.631	1.919	1.203	1.859	4.327	7.492	4.915	2.571	2.550
ζ_p	0.131	0.150	0.135	0.040	0.021	0.016	0.015	0.075	0.332	0.470	0.367	0.436

(derived from Ostgaard, et al 1962 [15])

It is clear from inspection of the table that the plant undergoes considerable parameter variations. In particular, the h.f. gain (proportional to $K_p T_p \omega_p^2$) varies by 31 dB and, for most conditions, the response is dominated by a very underdamped pole pair.

Determination of $\max|S_N/S - 1|$

In terms of bounds on its time response (Fig 14), the assumed system specification may be interpreted as requiring

$$A(j\omega) = \frac{1}{j\omega(1 + \tau j\omega)}, \quad B(j\omega) = \frac{1 + C_1(\frac{j\omega}{\omega_0})}{j\omega(1 + C_2(\frac{j\omega}{\omega_0}) + (\frac{j\omega}{\omega_0})^2)}$$

where $\tau = 1.3$, $C_1 = 2.5$, $C_2 = 2$, $\omega_0 = 0.5$.

From these expressions

$$\max|\frac{S_N}{S} - 1| = \frac{V(j\omega)}{A(j\omega)} = \frac{|B(j\omega) - A(j\omega)|}{|A(j\omega)|}$$

is readily determined as a function of frequency.

Determination of $\max|P_N/P - 1|$

Because the coefficients of $P(s)$ are highly correlated there is no simple method of establishing $\max|P_N/P - 1|$. The approach adopted here is to find, by computer search, the conditions corresponding to $\max|1/P|$ and $\min|1/P|$ for a few frequencies in the range of interest (in practice 12 discrete frequencies in the range 0.01 rad s⁻¹ to 100 rad s⁻¹ were used), to assign the nominal P_N such that $1/P_N$ lies midway between the two extreme points at each frequency (i.e. the optimum central nominal condition), and then to fit a model to these points which can be used to determine $\max|P_N/P - 1|$ at any frequency. The approach saves considerable time compared with determining the central nominal at each frequency (which for irregular P_N/P plot shapes would usually need to be done by manual inspection) and provides a good approximation to the true central nominal. The nominal values found by this method were $K_{P_N} = 0.04$, $T_{P_N} = 29.4$, $\omega_{P_N} = 1.6$, $\zeta_{P_N} = 0.4$.

Determination of the optimum L_N

Before proceeding with the determination of the overall nominal loop response L_N , another part of the system design specification must be considered, namely the response of the missile airframe to disturbances. This is because the optimum L_N design must fall off as rapidly as possible at h.f. and this will necessarily erode stability margin. Such erosion will not affect the response of the system to input demands since these will pass through the pre-filter G_1 , but inputs entering the loop directly (e.g. gust disturbances) could excite unacceptable transients. For this reason minimum stability margins must be specified. In the present example we will assume a specification which requires that "gust disturbances will be damped to less than one-fourth amplitude in one cycle". On a Nichols chart this is equivalent to ensuring that $L_N(j\omega)$ lies outside the dotted region surrounding the 0dB, -180° point (Fig 15). The length of the vertical section of this "disturbance boundary" is equal to the maximum increase in h.f. gain of $P(j\omega)$ from its nominal value (25dB).

The synthesis of $L_N(j\omega)$ may now proceed and is conveniently split into two parts. Firstly, the choice of $L_N(j\omega)$ at low and mid frequencies where the resulting optimum $L_N(j\omega)$ must sit on the L_N boundaries (defined by $|1 + L_N| = \max|P_N/P - 1|/\max|B_N/S - 1|$) at each frequency and also satisfy the disturbance boundary (Fig 15 - upper). Secondly, the h.f. design must ensure that $|L_N(j\omega)|$ falls off as rapidly as possible for a given excess of poles to zeros (taken as 4 in this example) whilst also satisfying the disturbance boundary (Fig 15 - lower).

The 1f-mf design is carried out using iteration on numerical representations of the Bode integrals [14,16] and is seen to be optimum since $L_N(j\omega)$ just sits on its respective boundaries at each frequency [11] (the L_N boundaries are shown in Fig 15 merely to illustrate this; their construction is not mandatory as it is with other optimum loop synthesis methods).

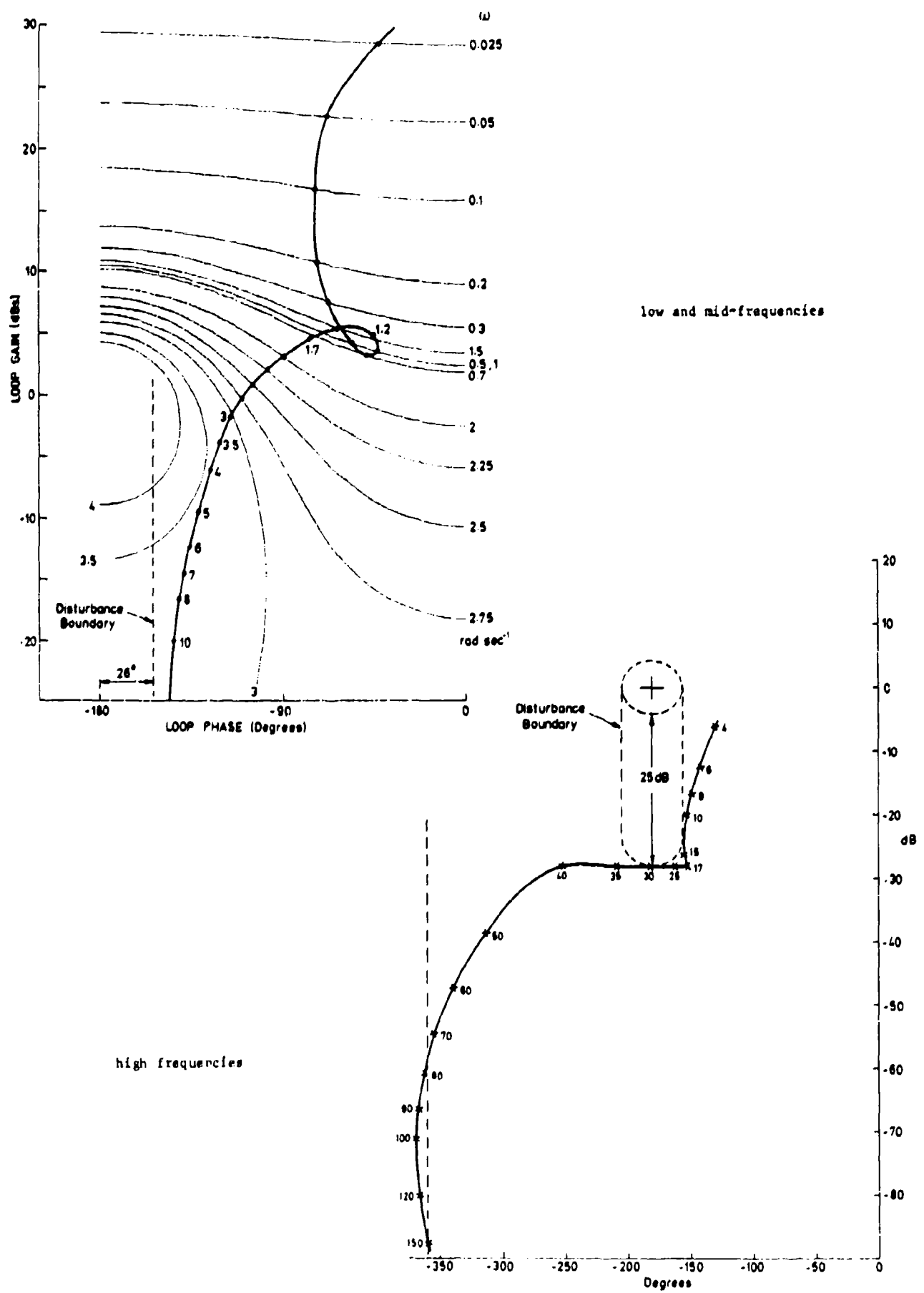
At high frequencies the $L_N(j\omega)$ is fitted by trial and error methods (Fig 15 - lower) but this is straightforward since the only requirement is to avoid the disturbance boundary with the minimum of over-design. The overall $L_N(j\omega)$ is checked using the Bode integral program to ensure that no change has occurred in the low and middle frequency region.

Implementing $G_1(j\omega)$ and $G_2(j\omega)$

The optimum $G_2 = L_N/P_N$ must, of course, be implemented by a rational transfer function and the result of fitting

$$G_2 = \frac{80(1 + s)^2}{s(1 + \frac{s}{0.007})(1 + \frac{s}{8})(1 + \frac{s}{400})(1 + \frac{0.2s}{40} + \frac{s^2}{40^2})}$$

to the true optimum G_2 is shown in Fig 16.

Figure 15: Nichols chart of $L_N(j\omega)$

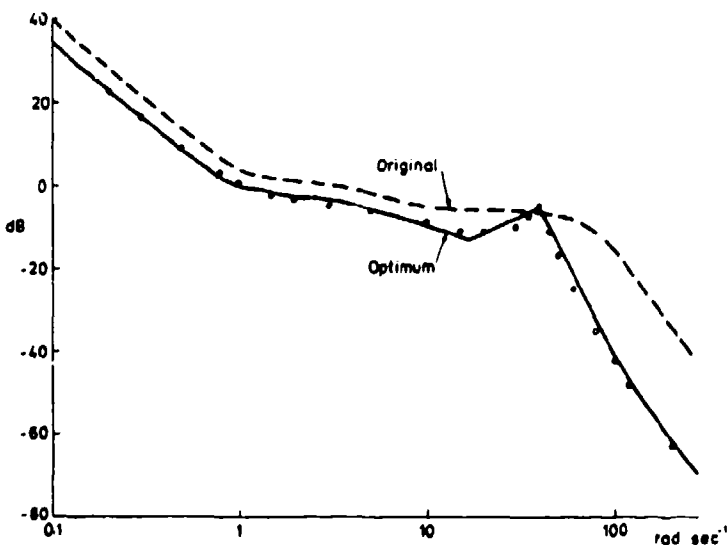


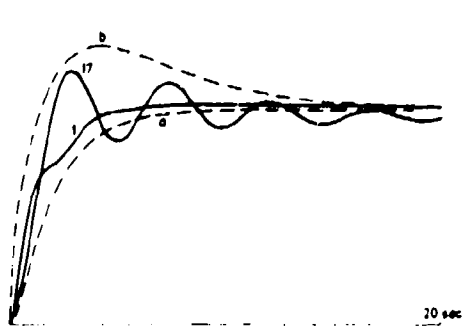
Figure 16: Comparison of $|G_2|$ for the current (optimum) design and the original design (Horowitz [17])

Also shown is the original G_2 (Horowitz [17]), which represents the first attempt at an optimal autopilot design for the same plant variation data and system design specification used above. It should be stressed that in [17] Horowitz was concerned primarily with drawing attention to the effectiveness of passive (i.e. fixed compensation network) adaption in extreme cases of plant variation and the original G_2 was, perhaps, designed largely using trial and error techniques.

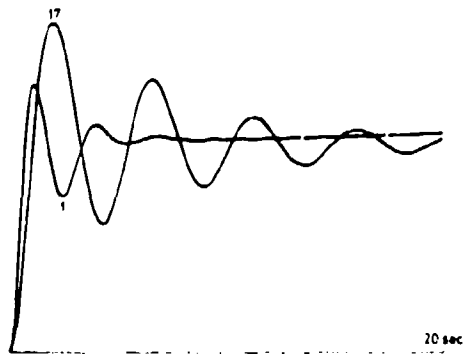
Finally, $G_1 = S_N (1 + L_N) / L_N$ is obtained. In this case G_1 has an excess of zeros to poles and so its exact practical implementation using the structure shown in Fig 13 is not possible. However, it is possible to construct a realisable approximation to G_1 which is valid for all but the highest frequencies and this is given by

$$G_1 = \frac{(1 + \frac{s}{0.35})}{(1 + \frac{1.4s}{0.65} + \frac{s^2}{2})(1 + \frac{s}{30})}$$

A simulation using the above G_1 and G_2 was carried out for all sets of the plant parameters and in all cases the responses satisfied the specification, albeit only marginally in some cases, but this is to be expected from an optimum design. For example, two typical sets of responses are shown in Fig 17 and it is seen that the step response specification (requiring that on average the variations in $c(t)$ about the mean should be less than $V(t) = (b(t) - a(t))/2$) has been met, as too has the disturbance response.



System step responses



Loop disturbance responses

Figure 17: Two typical sets of responses of the optimum design

The synthesis procedure outlined in this section represents one approach to the problem of "robust" system design, an area of control engineering that has only comparatively recently received much attention from the control fraternity. Its chief advantage lies in its use of frequency response ideas and is therefore accessible to the engineer with a classical control background. Furthermore, it is highly transparent in revealing where tradeoffs may be made between bandwidth (and what that implies in terms of the size and power requirements of actuators etc) and sensitivity specifications and is thus an ideal tool for use in parametric studies on SAM systems.

5. CONCLUDING REMARKS

We have discussed the general structure of guidance loops for SAM systems and have considered two important design problems associated with their implementation.

Firstly, the importance of structure and the necessity to include additional signal paths when implementing networks with switchable parameters has been emphasised if transients are to be eliminated from the guidance loop itself.

Secondly, a CAD technique for synthesising optimum or minimum bandwidth closed loop systems has been illustrated by means of a significant design example.

Both topics are essentially concerned with optimising performance in a very practical sense and the solutions proposed are applicable to a wide range of situations that are encountered in SAM system design.

6. REFERENCES

- [1] Heap, E., "Methodology of Research into Command-line-of-sight and Homing Guidance", AGARD Lecture Series No 52 on Guidance and Control of Tactical Missiles, 1972.
- [2] Hofmann, W., and D. Joos, "Missile Guidance Techniques", AGARD Lecture Series No 101 on Guidance and Control for Tactical Guided Weapons with emphasis on Simulation and Testing.
- [3] Garnell, P., and D.J. East, "Guided Weapon Control Systems", Pergamon Press, Oxford, 1977.
- [4] Cornford, E.C. and R.W. Bain, "The kinematics of proportional navigation courses for a missile with a time lag", Royal Aircraft Establishment Tech Note No GW 85, 1950.
- [5] Bain, R.W. and F.E. Trebble, "Proportional navigation for a missile with a quadratic time lag", Royal Aircraft Establishment Tech Note No GW 307, 1954.
- [6] Bain, R.W., "The analysis of linear homing navigation systems", Royal Aircraft Establishment Tech Note No GW 427, 1956.
- [7] East, D.J., "The elimination of transients in adaptive networks", Royal Military College of Science Tech Note E/76/1, 1976.
- [8] Horowitz, I.M., "Synthesis of Feedback Systems", Academic Press, 1963.
- [9] Horowitz, I.M., "Fundamental theory of automatic linear feedback control systems", Trans IRE Automatic Control, 3, 5-19, 1959.
- [10] Horowitz, I.M. and U. Shaked, "Superiority of transfer function over state variable methods in linear time-invariant feedback system design", IEEE Trans Automatic Control, 20, 84-97, 1975.
- [11] Horowitz, I.M., and M. Sidi, "Synthesis of feedback systems with large plant ignorance for prescribed time domain tolerances", Int. J. Control., 16, 287-309, 1972.
- [12] Ashworth, M.J., and D.R. Towill, "Realisation of plant sensitivity specifications via multi-loop feedback compensation", IFAC Symposium on Computer Aided Design of Control Systems, Zurich, 1979.
- [13] East, D.J., "A new approach to optimum loop synthesis", Int. J. Control., 34, 731-748, 1981.
- [14] East, D.J., "A CAD procedure for optimum loop synthesis", Royal Military College of Science Tech Report No RT 146/83, 1983.
- [15] Ostgaard, M.A., et al, "The case for adaptive controls", AGARD Flight Mechanics Panel, Paris, 1962.
- [16] Gera, A., and I.M. Horowitz, "Optimisation of the loop transfer function", Int. J. Control., 31, 389-398, 1980.
- [17] Horowitz, I.M., "Linear-adaptive flight control for re-entry vehicles", IEEE Trans. Automatic Control, 9, 90-97, 1964.

TERMINAL CONTROL FOR
COMMAND TO LINE OF SIGHT GUIDED MISSILE

by
Jean-Loup DURIEUX
CETA
28 rue de Bélat
16000 ANGOULEME
France

SUMMARY

This paper deals with the implementation of terminal control guidance laws on line-of-sight, radio-commanded missiles. Specific problems examined include : range-finding accuracy, effects of tracker filtering, and switching from stationary to terminal controller. Performance is compared with active homing guidance for the case of medium-range, surface-to-air missiles. The parameters compared are : missile path curvature, agility, and effects of sensor noise. Both conventional and optimal control laws are considered.

INTRODUCTION

The main differences between radio-commanded missiles, referred to hereafter simply as "command missiles", and homing guidance types are well known. First, assuming continuous tracker-missile-target alignment, command systems are generally considered to have a less favorable path in the case of long-range applications against high-altitude targets. Moreover, the fact that the seeker of a homing missile is on the missile itself means reduced influence of range dependent noise hence improved accuracy against long-range targets. However, various other considerations must be taken into account including protection against jamming, low-altitude efficiency, and ease of operation. The agility of the respective systems is also frequently compared. It is often claimed, for instance, that homing missiles are more accurate against maneuvering targets because the response time of homing guidance terminal control is better than that of the command guidance stationary control. However — and this is the central theme of this paper — if missile-to-target range is measured, terminal control can be used for command systems so that this difference disappears.

The paper is organized as follows. First, the basic statements of optimal terminal control are reviewed. Then section two looks at the ways in which terminal control can be used in command guidance systems, and specific constraints. In the third section, the accuracy of homing and command systems, using both conventional and optimal control laws in the two cases are compared in the case where sensor noise is limited to thermal noise.

Note that the flight paths considered here for command systems are all characterized by alignment, irrespective of whether the control law is stationary or terminal. This requirement is imposed by the fact that a common tracker beam is used for both target and missile. A terminal guidance law is termed "conventional" if it corresponds to classical proportional navigation ; it is further termed "absolute" if guidance is by homing, or "relative" if guidance is by command.

1. OPTIMAL TERMINAL CONTROL : BASIC STATEMENTS

The optimal control law for the terminal guidance of a missile includes an estimator of the instantaneous state variables of both the missile and the target. This is connected to an optimal deterministic controller. The law yields the minimal missile-target miss distance.

If the model of the missile and target is linearized and if the performance index is a linear quadratic gaussian (LQG), then the certainty equivalence principle is valid and the estimator and controller can be dealt with separately.

The statistical definition of sensor noise and target maneuvers is then required solely for the computation of the maximum likelihood estimates (Kalman filters).

The optimal controller, which drives a commanded acceleration via an autopilot, is computed to minimize a performance index, J , of the form :

$$J = E \left(y(t_f)^2 + \rho \int_{t_0}^{t_f} a_c^2(t) dt \right) \quad (1)$$

where : t_f intercept time, $y(t_f)$ miss distance, a_c commanded acceleration, ρ weighting factor (penalty on commanded acceleration).

or

$$J = \int_{t_0}^{t_f} a_c^2(t) dt \quad (2)$$

with $y(t_f)$ assigned the value of exactly zero, rather than being approximated to zero.

Bryson and Ho (5) have shown that the solution to Eq.2 is :

$$a_c = -a(t) z(t) \quad (3)$$

where $z(t)$ is the miss distance, called the zero effort miss (ZEM). This is obtained by setting $a_c = 0$ at time t . The variable gain, $a(t)$, then tends to infinity as t approaches t_f . When $\rho = 0$ the solutions to Eq.1 and Eq.2 are the same.

An interesting point concerning the law defined by Eq.3 is that the miss distance value and the miss distance estimate are the same for stationary noise and an asymptotic filter. This, in turn, clearly demonstrates the practical importance of the estimator.

It should be noted that there are an infinity of linear controller laws for which the miss distance is zero in the absence of noise, and that these laws differs as regards their acceleration histories. It should be further noted that these laws yield zero miss distances irrespective of the missile response time and of target maneuvers. However, the situation is radically changed if constraints are placed on the missile's lateral acceleration. One must, in fact, resort to laws that anticipate missile motion if one is to avoid or reduce the impact of saturation phenomena and minimize the resulting miss distance. From the accuracy standpoint, bang-bang control ensures the best use of the missile. A special and particularly interesting case of such a law is provided by differential games with bounded command. Shinar (1) has shown that, for a zero-sum game with cost function $|y(t_f)|$, and assuming that both the target and missile correspond to first-order transfer functions, then the optimal law has the structure illustrated in Fig.1.

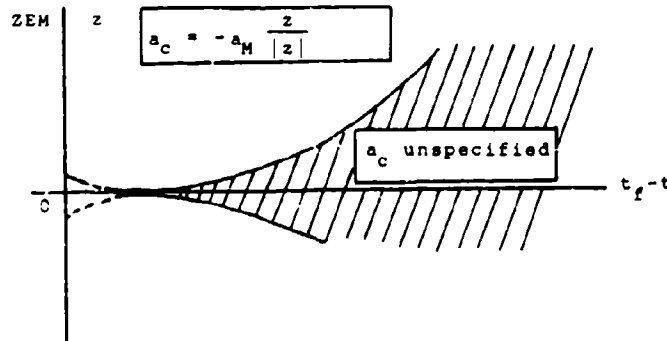


Fig.1 Terminal controller with bounded command

The cross-hatched area is bounded by the minimal isocost curves giving the value of the minimax miss distance as a function of the maximum lateral acceleration of the missile, a_M that of the target, a_T , and of the missile and target time lags, τ_M and τ_T . Without noise, the miss distance can be zero only if

$$a_M > a_T \quad \text{and if} \quad (5)$$

$$\frac{a_M}{\tau_M} > \frac{a_T}{\tau_T} \quad (6)$$

An upper bound for the miss distance is obtained by assigning $\tau_T = 0$. For given a_M and a_T , this bound is proportional to τ_M^2 which clearly indicates the practical importance of missile response time. Note that in this non-linear case, the separation theorem does not hold.

2.

TERMINAL CONTROL OF COMMAND MISSILES

Generally speaking, command missiles are represented as being controlled by a PID (proportional, integral and derivative) type stationary controller operating on the missile position coordinate normal to the launcher-to-target line and here termed the "metric misalignment" (which contrasts with the "angular misalignment" commonly encountered in angle tracking). The metric misalignment is thus the product of the missile-to-target angular misalignment, as measured by the launcher-mounted tracker, and the range, R_M , from launcher to missile. This range may be that measured by a range finder or it may be an estimated range obtained by calculation. See Fig.2 and Fig.3.

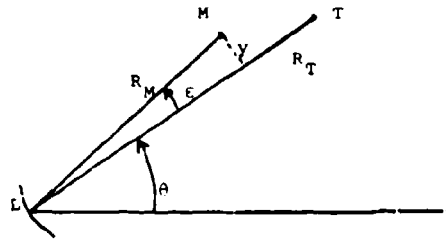


Fig.2 Geometry of command guidance

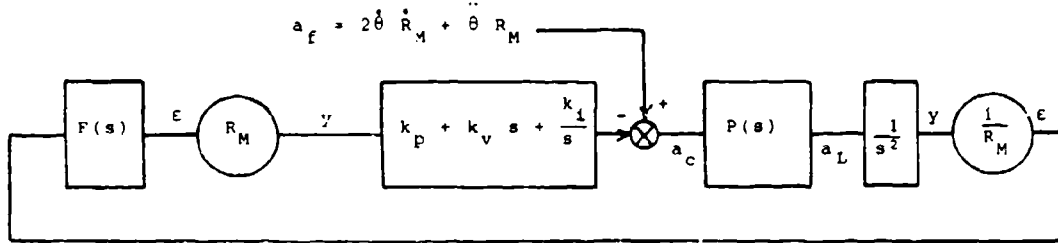


Fig.3 Block diagram representing stationary controller for command guidance

R_M launcher-to-missile range, R_T launcher-to-target range, θ absolute target direction, ϵ angular misalignment between missile and target, y metric misalignment between missile and target (missile position coordinate normal to LT), k_i , k_p , k_v controller gains. a_f acceleration feed-forward, a_L achieved acceleration, $F(s)$ tracker transfer function, $P(s)$ autopilot transfer function.

Closed-loop command is helped by a feed-forward term resulting from an estimation of the acceleration component perpendicular to the velocity vector and induced by the alignment constraint. This estimator is computed by processing the output signals from the tracker gyros and the tracker itself. The estimate is exact if the target velocity vector is constant.

The tracker transfer function, $F(s)$, in fact corresponds to the tracker output filter applied to the angular misalignment, ϵ . Another filter, not represented in Fig.3, is generally applied to the metric misalignment, y .

The loop gains are adjusted so that y is minimized at each instant in time. This is necessary both to keep the missile within the beam and to ensure interception with a target an unknown range.

If the target range is known, a terminal law can be used instead of a stationary law.

2.1 CONVENTIONAL TERMINAL LAW. RELATIVE PROPORTIONAL NAVIGATION

This law is the transposition of the classical proportional navigation law into the coordinate system of the tracker.

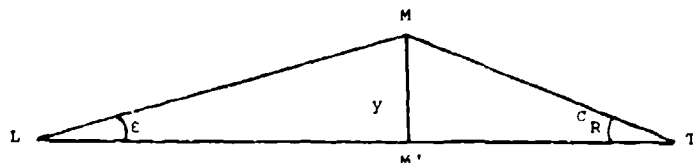


Fig.4 Geometry of relative proportional navigation

If θ_R is the relative bearing and R_{MT} the missile-target range, then :

$$a_c = -N \dot{R}_{MT} \dot{\sigma}_R \quad (\dot{R}_{MT} > 0) \quad (7)$$

$$\sigma_R = \frac{y}{R_{MT}} = \epsilon \frac{R_M}{R_{MT}} \quad (8)$$

Using Eq.8 to compute $\dot{\sigma}_R$, then substituting this into Eq.7, we obtain :

$$a_c = -N \left(\frac{y}{(t_f - t)^2} + \frac{\dot{y}}{t_f - t} \right) \quad (9)$$

This RPN law is identical to the PID law if we assign the variable gains as follows :

$$k_p = \frac{N}{(t_f - t)^2}, \quad k_v = \frac{N}{t_f - t}, \quad k_i = 0 \quad (10)$$

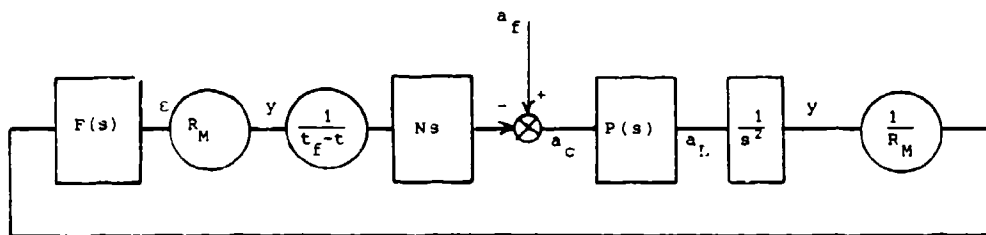


Fig.5 Block diagram representing relative proportional navigation (RPN)

Fig.5 represents RPN if it is assumed that $R_{MT} = \dot{R}_{MT}(t_f - t)$

2.1.1. SWITCHING FROM STATIONARY TO TERMINAL CONTROLLER

The RPN gains given by Eq.10 are not sufficient to keep the missile within the tracker beam when $(t_f - t)$ is large. It is thus necessary to reserve RPN for the intercept phase and to use a stationary law during the initial phase

In the absence of noise, it is possible to exactly null the miss distance induced by the state variables (i.e. by y and its derivatives) on switching from stationary to terminal law. However, this method is not robust. It is thus better to wait for the extinction of the natural response, i.e. to switch from the stationary law to RPN at a time-to-go that is at least equal to the response time of the RPN loop. This time is, in turn, strongly dependent on the available lateral acceleration. Practical values range between 0.5 s and 3 s. Eq.10 tells us that continuity between the stationary and RPN gains at switchover time only exists under the following conditions :

$$N = \frac{k_v^2}{k_p} \quad \text{and} \quad t_f - t = \frac{k_v}{k_p}$$

Now, assuming that $k_i = 0$ and that k_p and k_v are adjusted so that the damping ratio of the stationary loop is 0.7, we then have, roughly at least, $k_v = \sqrt{2k_p}$ and $N = 2$. However, such value for N being scarcely used, one frequently observes a discontinuity which in fact expresses the difference between the dynamic behavior of a stationary loop and that of an RPN loop.

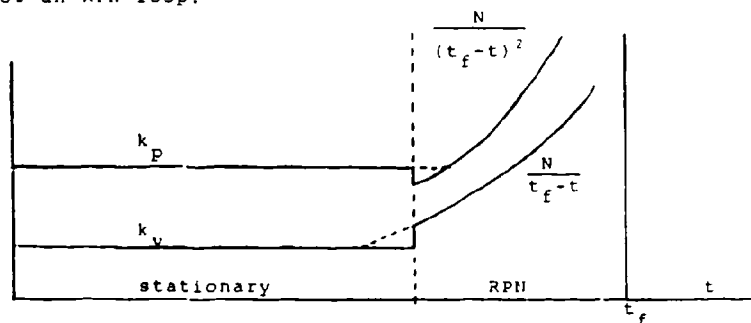


Fig.6 Stationary and terminal gains as a function of time

2.1.2 EFFECTS OF RANGE FINDING ACCURACY

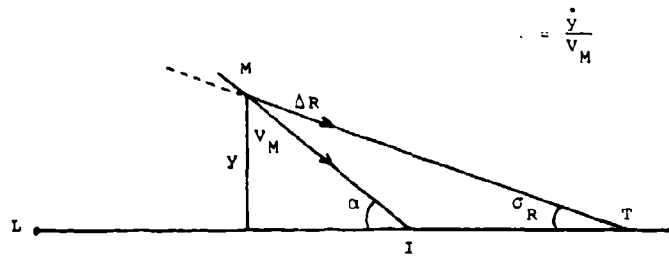


Fig.7 Effects of range finding accuracy

1 point of intercept, V_M missile relative velocity vector, ΔR range measurement error, α inclination of V_M relative to tracker beam.

The range measurement error, ΔR , includes a constant or slowly varying term, ΔR_c , induced by calibration bias or filter lag and a stochastic component, ΔR_f , with zero mean. For most range finders, ΔR_c is much greater than ΔR_f . The stochastic component, ΔR_f , induces a new metric noise $\sigma_R \Delta R_f$. However, given that ΔR_f and σ_R are both small, the effect is generally negligible in comparison with those of glint and angular noise.

The constant or slowly varying components, ΔR_c , induces an equivalent displacement of the point of intercept, I , which, in turn, results in a parasitic miss distance equal to $\alpha \Delta R_c$.

Note that, in the presence of range measurement errors, σ_R must be minimized, and hence α too. This means that alignment should, at all times, be as nearly perfect as possible.

2.1.3 EFFECTS OF METRIC AND ANGULAR FILTERING

The noisefilter associated with the guidance law can be applied either to \dot{c}_R (Eq.7) or to y (Eq.9). The first case corresponds to the insertion of an angular filter after the variable gain $\frac{1}{t_f - t}$ in Fig.5, the second to that of a metric filter before the variable gain. In conventional homing guidance, the filter is angular. In contrast, the Kalman filter used in optimal terminal guidance corresponds to what is here termed a "metric filter". During the RPN phase, the tracker filter, $F(s)$, is equivalent to a metric filter, in spite of the fact that it is applied to an angle. One can indeed assume that, during the final RPN phase, R_M is constant ; which means that R_M and $1/R_M$ both vanish by compensation in Fig.5.

The dynamic properties of the conventional terminal loop (be it homing or RPN) are profoundly modified according to whether the filtering is angular or metric. From a theoretical standpoint, this can be seen in the response $x(t)$ (with Laplace transform $X(s)$) to a position impulse of the adjoint system to the basic linear system depicted in Fig.8.

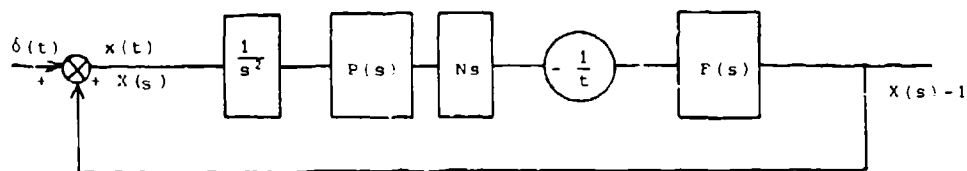


Fig.8 Adjoint model of RPN

It is well known that (6) $X(s)$ can be used to compute the miss distances induced respectively by a stochastic target maneuver $\Phi_{TT}(s)$, stationary metric noise $\Phi_{nn}(s)$

$$\sigma_T^2 = \frac{1}{2\pi j} \int_{-j\infty}^{j\infty} \frac{X(-s)}{s^2} \frac{X(s)}{s^2} \phi_{TT}(s) ds \quad (11)$$

$$\sigma_n^2 = \frac{1}{2\pi j} \int_{-j\infty}^{j\infty} (X(s) - 1)(X(-s) - 1) \phi_{nn}(s) ds \quad (12)$$

or by an evasive deterministic target maneuver such as an acceleration step :

$$E(s) = \frac{X(s)}{s^3} \quad (\text{Inverse Laplace } e(t)) \quad (13)$$

Without metric filtering ($F(s) = 1$), the open-loop transfer function of the adjoint system can be expanded as follows :

$$\frac{NP(s)}{s} = \frac{a_1}{s} + \sum_i \frac{b_i}{s - p_i} \quad (14)$$

and one has :

$$X(s) = s^{a_1} \prod_i (s - p_i)^{b_i} \quad (15)$$

With metric filtering, $X(s)$ does not exist and the response, $e(t)$, is generally unstable [2]. In the simple case where $F(s) = \frac{1}{1+Ts}$ and $P(s) = 1$, the response, $e(t)$ can be depicted as in Fig.9.

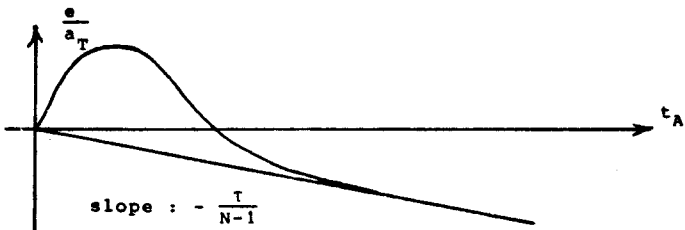


Fig.9 Position response of adjoint system to an acceleration step

Thus, when using RPN, it is important that the filtering applied to the tracker output signals be reduced.

2.1.4. OPTIMIZATION OF ANGULAR FILTERING

Using Eq.11 and Eq.12 we can compute the form of $X(s)$ required to minimize the total miss distance $d^2 = \sigma_T^2 + \sigma_n^2$. The result can then be used to compute the corresponding overall missile transfer function, $P(s)$, using Eq.14 and Eq.15.

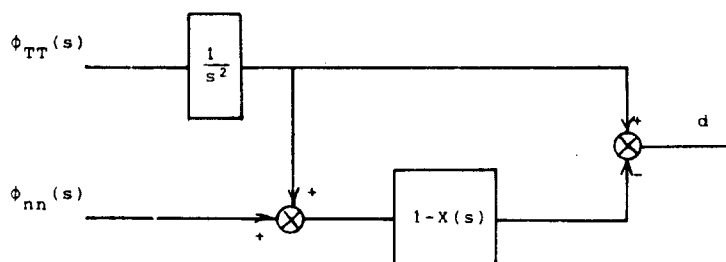


Fig.10 Minimization of d^2

The diagram in Fig.10, representing Eq.11 and Eq.12 shows that d is also the error estimation \hat{y} of the metric deviation y at each time by a Kalman filter (more precisely a Wiener filter) $K(s) = 1-X(s)$. Hence this important theoretical conclusion : when

both noise and target maneuvers are stationary, the miss distance given by an optimal angular filter is equal to that given by an optimal terminal law using the performance index of Eq.2.

Some simple case studies.

a) $\phi_{TT}(s) = \phi_{TT}$, $\phi_{nn}(s) = \phi_{nn}$ (ϕ_{TT} and ϕ_{nn} constant)

$$\hat{X}(s) = \frac{s^2}{s^2 + m\sqrt{2}s + m^2} \quad \text{with } m = \left(\frac{\phi_{TT}}{\phi_{nn}}\right)^{\frac{1}{4}} \quad (16)$$

$$\hat{d}^2 = \sqrt{2} \phi_{TT}^{\frac{1}{4}} \phi_{nn}^{\frac{3}{4}} \quad (17)$$

$$N = 2 \quad \hat{P}(s) = \frac{m\sqrt{2}s + m^2}{s^2 + m\sqrt{2}s + m^2} \quad (18)$$

b) $\phi_{TT}(s) = \frac{1}{s^2} \phi_{JJ}$, $\phi_{nn}(s) = \phi_{nn}$ (ϕ_{JJ} constant)

$$\hat{X}(s) = \frac{s^3}{s^3 + 2ps^2 + 2p^2s + p^3} \quad \text{with } p = \left(\frac{\phi_{JJ}}{\phi_{nn}}\right)^{\frac{1}{6}} \quad (19)$$

$$\hat{d}^2 = 2 \phi_{JJ}^{\frac{1}{6}} \phi_{nn}^{\frac{5}{6}} \quad (20)$$

$$N = 3 \quad \hat{P}(s) = \frac{\frac{2}{3}ps^2 + \frac{4}{3}p^2s + p^3}{s^3 + 2ps^2 + 2p^2s + p^3} \quad (21)$$

c) $\phi_{TT}(s) = \frac{1}{s^{2n}} \phi$, $\phi_{nn}(s) = \phi_{nn}$

The poles of $X(s)$ and $P(s)$ follow a Butterworth configuration of degree $(n+2)$ and $N = n+2$

In most cases, neither the poles of the autopilot nor those (if there are any) of the seeker coincide with the poles of $P(s)$. This, in turn, means that it is generally impossible to implement an optimal angular filter. In contrast, and as is well known, it is generally possible to implement the metric Kalman filter used in the optimal terminal law.

2.2 OPTIMAL TERMINAL LAW

The implementation of the optimal terminal law in the case of a command guidance system is illustrated, for the simplified case of a Kalman estimator of degree 2, in Fig.11. It is assumed that no signals generated by missile accelerometers are available to the computer, which implies the need to model the missile autopilot. Note, the higher the degree of the estimator, the higher the loop sensitivity to the accuracy of the model. Nesline and Zarchan give examples of such sensitivity for homing guidance with an estimator of deg: 6 3 (3).

The feedforward term is used as shown in Fig.11. This term is generated through the separate estimation of $\dot{\theta}$ and $\ddot{\theta}$ as functions of target noise. The reason for resorting to separate estimation, rather than common estimation by the Kalman filter, is that the assumptions made concerning the target's mean trajectory are not the same as those concerning its evasive maneuvers.

Metric Kalman filtering does not result in the instability mentioned above in response to an acceleration step by the target. But, in the case of a degree-2 filter, it does result in a bias of $1/m^2$. In the case of a degree-3 filter, this bias is zero.

The effects of range measurement errors are the same as for RPN. The timing of the switchover between stationary and optimal terminal law depends, as with RPN, on the available lateral acceleration and the estimator response time.

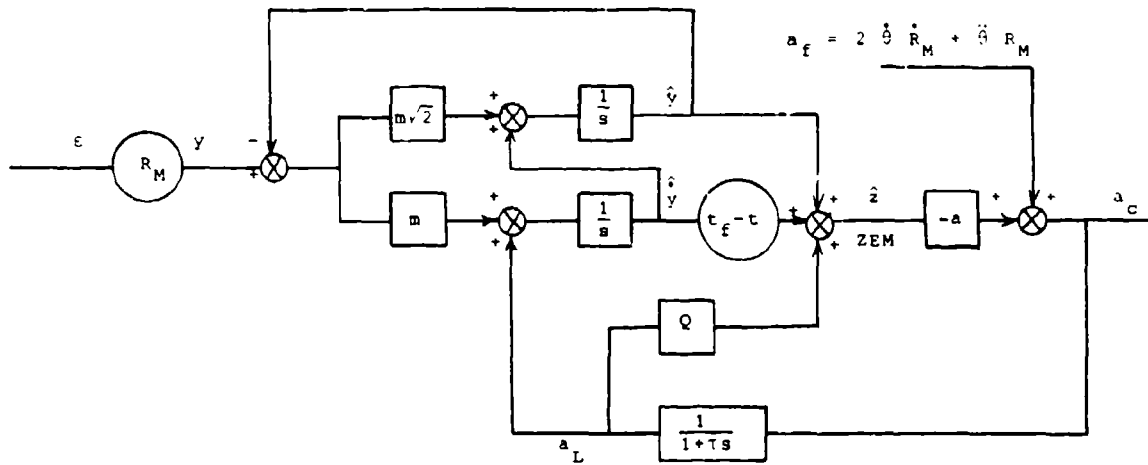


Fig.11 Command guidance. Optimal terminal law

$$a = \frac{3(t_r - (1-e_r)\tau)}{3\rho + 3/2 \tau^3 (1-e_r^2) + 3 \tau^2 t_r (1-2e_r) + t_r^2 (t_r - 3\tau)} \quad (22)$$

$$q = \tau^2 (e_r - 1) + t_r \tau \quad (23)$$

$$t_r = t_f - \tau \quad e_r = e^{\frac{t_r}{\tau}}$$

2.3 STATIONARY LAW ADJUSTEMENT. COMPARISON OF STATIONARY AND TERMINAL LAWS

It is good policy to minimize y at each instant in time so that the system is able to cope with a fortuitous loss of range measurement, as in the case of jamming. This is of course the only policy if target range is not available. Recall also that, whatever the circumstances, good alignment always minimizes the impact of range measurement errors on miss distance.

In a LQG sense, the optimal stationary law includes a Kalman estimator identical to that used in the terminal law, and a controller minimizing the following performance index :

$$J = \int_{t_0}^{t_f} (y^2(t) + \mu a_c^2(t)) dt \quad (24)$$

The miss distance induced by such a law is always greater than that induced by a terminal law with a performance index such as that given by Eq.2. In practical terms, this means that the advantages of terminal control are greatest in the case of targets characterized by weak noise and energetic maneuvering. This is due to the fact that the gain levels used during the terminal phase are in a range that would be unacceptable during the mid-course phase (see Fig.6).

3 COMPARISON OF COMMAND AND HOMING GUIDANCE

Consider the case of a medium-range (say 12 km) surface-to-air missile. We wish to compare the performance of one type, featuring a stabilized active seeker, with that of another type featuring a launcher-mounted, narrow-beam tracker. It is assumed that the target range is available in both cases. Let us now compare the following quantities :

- missile path curvature,
- missile agility or response to evasive target maneuvers, and
- effects of sensor noise.

3.1. MISSILE PATH CURVATURE

If the target cross-range is non-zero, then the lateral acceleration required by a command guidance (CG) missile is always much greater than that required by a homing guidance (HG) missile, even taking into account homing head gimbal angle constraints. Neglecting the missile's deceleration and angle of attack, the lateral acceleration required to intercept a constant-speed target on a straight trajectory is, according to reference (4) :

$$a_L = \frac{2 V_M V_T}{c} \frac{\sin \theta \sin(\theta + \phi)}{\cos \phi} \quad (25)$$

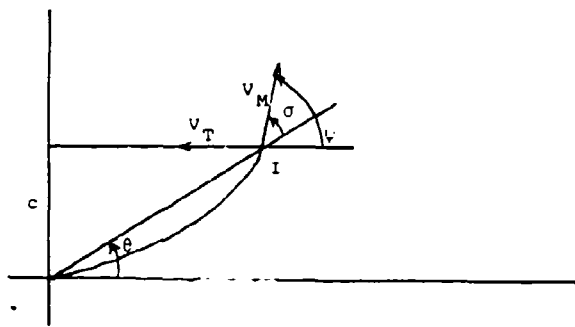


Fig.12 Command missile flight path. Interception phase

If we consider the case where $C = 2000 \text{ m}$, $V_T = V_M = 500 \text{ ms}^{-1}$ and $\theta = \pi/2$, then $a_L = 250 \text{ ms}^{-1}$ for a CG missile and $a_L = 0$ for HG missile.

However, if the target cross-range is zero, the situation is reversed. Simulation studies show that, for the target paths sketched in Fig.13, the lateral acceleration required by a homing missile is generally greater than that required by a command missile irrespective of the range at which the seeker locks on to the target. In both cases the missile is assumed to coast after initial acceleration (i.e. to be decelerated during the intercept phase). The homing missile is also assumed to have been launched in the general direction of the intercept point.

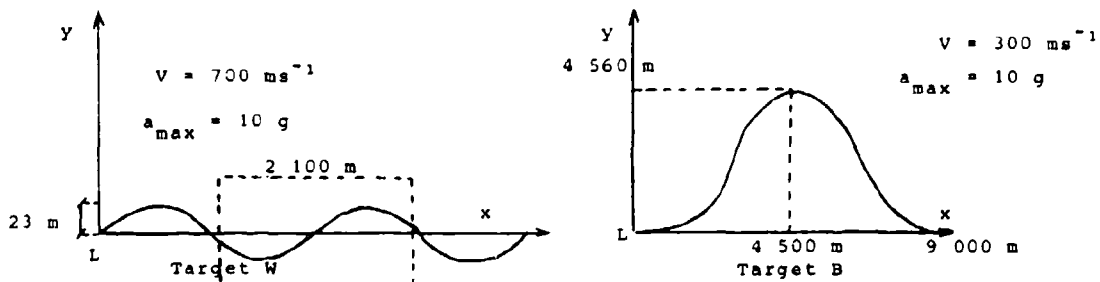


Fig.13a Sinusoidal target path

Horizontal intercept ranges (km)

1	2	3	4	5	6
21	15	10	7	8	12
>25	13	7	10	25	25

Command

Homing

Fig.13b Maximum missile lateral acceleration on target B (g)

Horizontal intercept ranges (km)

1.25	1.5	1.75	2	2.25	2.5
12	7	6	8	10	9
21	23	16	15	20	24

Command

Homing

Fig.13c Maximum missile lateral acceleration on target W(g)

The kinematic advantage of command guidance over homing guidance in this case can be attributed to the fact the maneuvers the missile has to develop to follow those of the target are attenuated by a factor of approximately R_M/R_T .

3.2 RESPONSE TO TARGET EVASIVE MANEUVERS

Here we assume no noise in each case. In the linear case, i.e. with no bounds on

lateral acceleration, the terminal law with a performance index of the form given in Eq.2 yields a zero miss distance irrespective of the nature of the maneuvers executed by the target. Hence, in this case, there is no difference between CG and HG.

If we now assume that lateral acceleration is bounded by a_M , the useful component against target lateral acceleration is $\frac{a_M}{\cos\psi}$, where ψ is the angle between the missile and target velocity vectors. Here, CG suffers a penalty if the target cross-range is non-zero because the corresponding value of ψ is greater than for HG. If the cross-range is zero then, as we have already seen, CG is better than HG.

Returning to the case of conventional linear proportional navigation with constant gain (N) and without filtering (no noise), the overall missile transfer function strongly differentiates between CG and HG. What we are in fact comparing are the loops of Fig.14 where $P(s)$ is the autopilot transfer function and $A(s)$ the seeker transfer function.

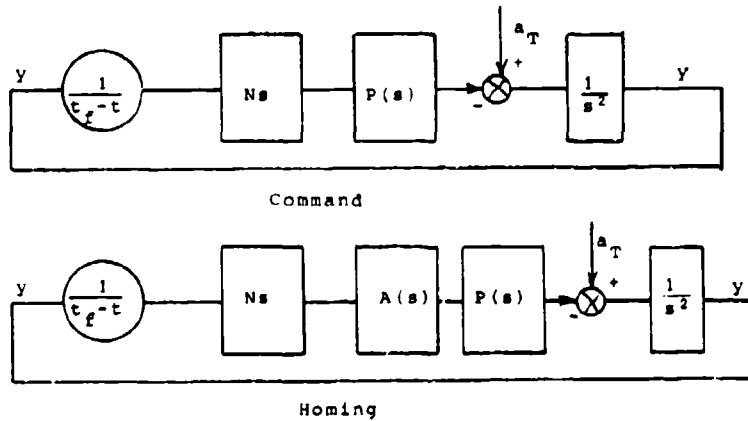


Fig.14 Linear guidance loops

If P and A are assumed to correspond to first-order lags of $\tau_m = \frac{1}{\omega_m}$ and $\tau_A = \frac{1}{\omega_A}$, then the adjoint impulse response is found, using Eq.14 and Eq.15, to be :

$$X(s) = s^N \frac{\frac{N \omega_A}{\omega_m - \omega_A}}{(s + \omega_m)} \frac{\frac{N \omega_m}{\omega_A - \omega_m}}{(s + \omega_A)} \quad (26)$$

which reduces to

$$X(s) = s^N (s + \omega_m)^{-N} \quad \text{if } \tau_A = 0 \quad (27)$$

and

$$X(s) = s^N (s + \omega_m)^{-N} e^{\frac{N \omega_m}{s + \omega_m}} \quad \text{if } \omega_A = \omega_m \quad (28)$$

Curves for $\left| \frac{X(s)}{\omega^2} \right|$ are shown in Fig.15. These give the maximum miss distance observed for a missile fired at a target with sinusoidal acceleration characterized by angular frequency ω , amplitude 10 g, and random phase (uniform distribution between 0 and 2π).

As can be seen, the lag of the seeker heavily penalizes HG. This finding is confirmed by simulation. Moreover, the difference is even larger if parasitic coupling (due to, say, random aberration) is introduced and if more realistic representations of transfer functions A and P are used.

3.3 EFFECTS OF SENSOR NOISE

3.3.1 CHARACTERIZATION OF SENSOR NOISE

Assuming zero range measurement error, then clearly this quantity can have no effect on conventional or optimal command guidance, nor on optimal homing guidance. Assuming also that the glint noise is the same in both cases, the comparison is reduced to that of the effects of thermal noise only in both cases. Thermal noise can be conveniently characterized by its spectral density, $\frac{N}{\omega}$, and its bandwidth. The thermal noise bandwidth always being much greater than that of the guidance loop, it can be assumed that $\frac{N}{\omega}$ is uniform.

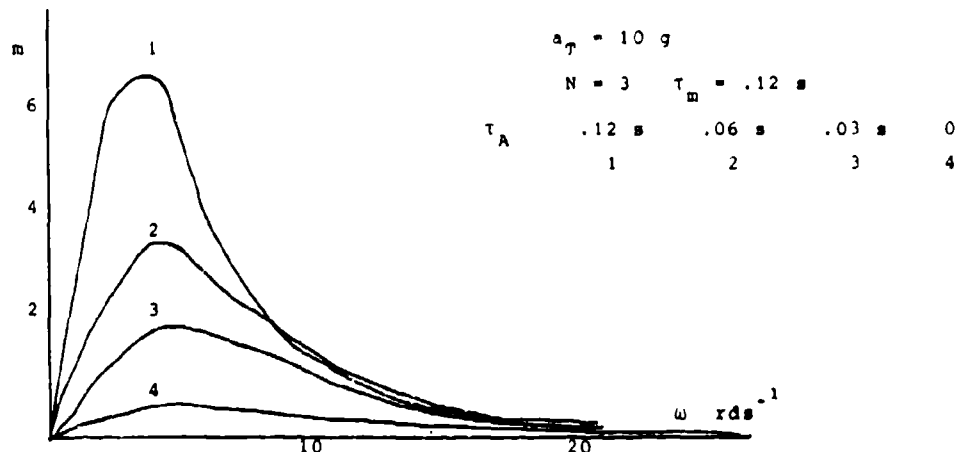


Fig.15 Maximum miss distance induced by sinusoidal target path

$$\phi_{tt} = \beta \frac{k^4}{\sigma} \quad (29)$$

where R is the range from tracker or seeker to target and C is the target's radar cross-section.

$$\beta = \frac{(4\pi)^3 \theta_B^2 K T L F}{m^2 P_a G^2 \lambda^2} \quad (30)$$

where θ_B is the antenna 3-dB bandwidth, K Boltzmann's constant, T the temperature, L the overall loss factor, F the receiver noise figure, m the system error detection slope angle, P_a the average transmitted power, G the antenna power gain, and λ the wavelength. Of course the main difference between CG and HG is the fact that in one case R is the tracker-to-target range and in the other the missile-to-target range.

3.3.2. COMPARISON BETWEEN CG AND HG FOR CONVENTIONAL GUIDANCE

Referring to Fig.14, it is assumed that the only noise filtering is that naturally attributable to $A(s)$ and $P(s)$.

In the case of CG, it can be assumed that the thermal noise level is constant in the vicinity of the point of interception, and that its mean metric spectral density, i.e. the mean spectral density expressed in terms of distance instead of angle, is given by :

$$\phi_{ttm} = \beta_R \frac{R_I^6}{\sigma} \quad (31)$$

where β_R is the tracker β factor and R_I the tracker-to-intercept range. Now, assuming that $P(s)$ is a first-order lag, T_m , and that $N = 3$, Eq.12 yields the corresponding miss distance :

$$\sigma_{nc}^2 = \frac{33}{16} \frac{\phi_{ttm}}{T_m} = \frac{33}{16} \frac{R_I^6 \beta_R}{\sigma T_m} \quad (32)$$

In the case of HG, thermal noise is radically non-stationary. The mean metric spectral density of this noise is given by :

$$\phi_{ttm} = \beta_S \frac{\frac{R}{MT}^6 (t_f - t)^6}{\sigma} = \phi_{ttm0} (t_f - t)^6 \quad (33)$$

where β_S is the seeker β factor. However, Eq.12 is no longer applicable. In the adjoint system shown in Fig.8 the impulse $\delta(t)$ inducing $X(s)$ must be replaced by $\delta(t) t^6$. Hence in Eq.12 one must also replace $X(s) - 1$ by $Y(s)$ where $Y(s)$ is defined by :

$$Y(s) = \mathcal{L}((x(t) - \delta(t))t^6) \quad \text{or} \quad (34)$$

$$Y(s) = \frac{d^6}{ds^6} (X(s) - 1) = \frac{d^6}{ds^6} X(s)$$

If we now assume that the overall $A(s) \cdot P(s)$ transfer function is a first-order lag, τ_{Am} , and that $N = 3$, then the corresponding miss distance can be expressed as :

$$\sigma_{nH}^2 = \frac{675}{32} \tau_{Am}^5 \phi_{ttm}, \quad \text{or as} \quad (35)$$

$$\sigma_{nH}^2 = \frac{675}{32} \frac{\dot{R}_{MT}^6 B_S \tau_{Am}^5}{\sigma}$$

The range, R_{I_0} , can then be computed for the case where the miss distance induced by thermal is the same for both CG and HG. This is done by combining Eq.32 and 35 :

$$R_{I_0} = \sqrt{(\tau_{Am}^5 \tau_m)^{\frac{1}{6}} \dot{R}_{MT}} \quad (36)$$

Now consider a numerical example with the following plausible values : $B_R = 4 \cdot 10^{-25}$, $B_S = 2 \cdot 10^{-19}$ (rad².s.m⁻²), $\tau_m = 0.12$ s, and $\tau_{Am} = 0.24$ s. This yields $R_{I_0} = 1.8 \dot{R}_{MT}$ which demonstrates that the range beyond which CG is penalized relative to HG is short, about 3 km.

However, a valid comparison must focus on the overall miss distance resulting from both thermal noise and target maneuvers. As stated above, the component induced by glint noise is assumed to be same in both cases. Using the simplified transfer functions previously assigned to P and A.P, the maximum miss distance is given, in rms form, for a target executing a sinusoidal trajectory, by Eq.27 as :

$$\sigma_T = \frac{1}{\sqrt{2}} a_T \tau^2 \frac{2}{N-2} \left(1 - \frac{2}{N}\right)^{\frac{N}{2}} \quad (37)$$

Therefore, with $N = 3$, we have :

$$\sigma_{TC} = .29 a_T \tau_m^2 \quad \text{for CG} \quad (38)$$

$$\sigma_{TH} = .29 a_T \tau_{Am}^2 \quad \text{for HG} \quad (39)$$

The range, R_I , for which the overall miss distances, $(\sigma_{nC}^2 + \sigma_{TC}^2)^{\frac{1}{2}}$ and $(\sigma_{nH}^2 + \sigma_{TH}^2)^{\frac{1}{2}}$ are equal is given by :

$$R_I^6 = R_{I_0}^6 + .29^2 a_T^2 (\tau_{Am}^4 - \tau_m^4) \frac{\sigma_T \tau_m}{B_R} \frac{16}{33} \quad (40)$$

The effects of the term involving a_T^2 are indicated in the table below (Fig.16) for the same numerical example as stated above and for $\dot{R}_{MT} = 1 \text{ 000 ms}^{-1}$.

$a_T(g)$	$\sigma (\text{m}^2)$		
	0.1	1	10
0	2 800	2 800	2 800
5	4 640	6 760	9 920
10	5 810	8 510	12 500

Fig.16 Intercept ranges giving the same miss distances for both CG and HG

For each range given in the table, CG is more accurate than HG at shorter ranges and less accurate at longer ranges. Thus, broadly speaking, we can state that CG is better than HG for large targets capable of high-power maneuvers. In each case, the ranges indicated in Fig.16 are greater the more realistic the seeker and autopilot models.

3.3.3 COMPARISON BETWEEN CG AND HG FOR OPTIMAL TERMINAL GUIDANCE

It was found in § 2.1.4 that optimal terminal CG can only be implemented using a metric model. The corresponding implementation for optimal terminal HG has also been

presented by Nesline (3) using a third-order estimator. The block diagram shown in Fig.17 is essentially the same except that the estimator has been simplified to the second order. This implementation should be compared with that for CG (Fig.11).

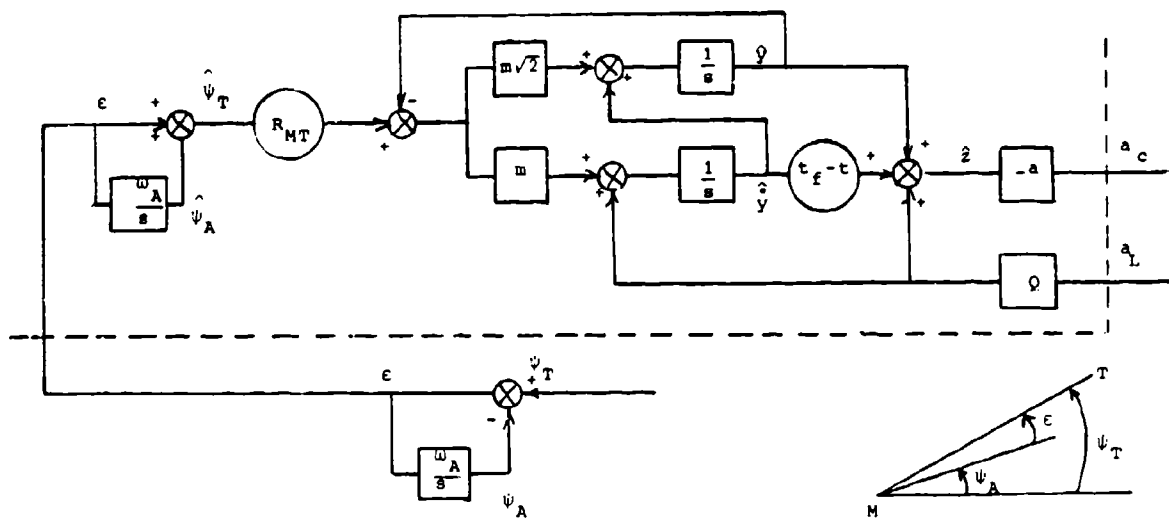


Fig.17 Optimal terminal HG

ψ_T absolute direction of missile-to-target line

ψ_A absolute direction of seeker boresight axis

ϵ seeker boresight or tracking error.

The important point here is that the seeker lag, $1/\omega_A$, is compensated by the estimator, so that the reason for the difference in agility between CG and HG in the case of conventional guidance vanishes. Note that the same result can be achieved by measuring ψ_A using an IMU.

If the seeker lag were perfectly compensated, the overall transfer functions of the missiles would be identical and the range, R_I , up to which CG out performs HG would be reduced. In practice, however, such phenomena as radome aberration and parasitic coupling effects limit the potential for effectively reducing R_I .

4

CONCLUSIONS

An interesting theoretical result, concerning both CG and HG, is that optimization, in an LQG sense, of the terminal law results in the same statistical accuracy, irrespective of whether this is done using angular or metric filtering, if target maneuvers and noise are stationary. But, only the metric optimal law can be implemented.

With regard to pure kinematics, the line-of-sight (or alignment) trajectory of a CG missile tracking a target with non-zero cross-range results in missile lateral accelerations greater than those required in the case of a HG missile on a proportional navigation trajectory. Even if these accelerations do not exceed the missile's maximum acceleration capability, they reduce the efficiency of its response to target evasive maneuvers requiring further increasing of curvature of the missile path. The situation is reversed when it comes to a radial target (zero cross-range), i.e. the curvature of the alignment trajectory of a CG missile is less than that of a HG missile, irrespective of any maneuvers when closing on the launcher. In the case of conventional terminal guidance, i.e. for an HG missile using absolute proportional navigation or a CG missile using relative proportional navigation, the limited bandwidth of the seeker tracking loop heavily penalizes the HG missile when homing on a maneuvering target. This, in turn, effectively reduces the advantage of HG associated with the fact that its thermal noise vanishes in the vicinity of the point of interception. It is thus possible to define a range that is a function of target size and target maneuvering capability and below which CG is more accurate than HG.

In the case of optimal terminal guidance, this disadvantage of HG vanishes to the extent that the response time (or lag) of the seeker loop can be compensated. However HG must take account of certain specific sources of disturbance which cannot be compensated because they are unknown. These disturbances include radome aberration, parasitic coupling between seeker and missile, and noise introduced by inertial sensors. Thus we once again find a zone of short ranges, where CG out performs HG.

REFERENCES

- (1) Shinar in Leondes - Control an dynamic systems - Tome 17- Academic Press 1981 pp 64-120.
- (2) Durieux - On the location of filtering in a linear terminal control systems - Trans IEEE - Automatic Control Vol-AC-28-N°5-May 1983 pp 611.
- (3) Nesline and Zarchan - A new look at classical versus modern homing missile guidance - Proc AIAA guidance cont. Conf. Boulder Colorado-230 (1979).
- (4) Garnell - Guided weapon control systems - Pergamon Press 1980. pp 154.
- (5) Bryson and Ho - Applied optimal control - Hemisphere publishing corp. 1975. pp 158-164.
- (6) J. Lanning and R. Battin - Random Processeses in Automatic Control - New York : Mc Graw Hill. 1956.

UN NOUVEAU CONCEPT DE PILOTAGE DES MISSILES
APPLICATION AUX SOL-AIR

G. SELINCE

AEROSPATIALE - DIVISION DES ENGINS TACTIQUES
 2 à 18 rue Béranger - 92320 CHATILLON - FRANCE

RESUME

Le pilotage d'un missile à l'aide d'un dispositif pyrotechnique créant directement la force normale nécessaire au pilotage au voisinage immédiat de son centre de gravité, possède des propriétés dynamiques remarquables, pratiquement indépendantes de l'altitude et de la vitesse de vol.

Du fait de sa consommation élevée en poudre, les applications aux missiles tactiques ont, semble-t-il, été jusqu'ici restreintes à des missiles antichars à temps de vol court et à faible capacité de manœuvre.

L'application aux missiles sol-air devient possible à condition d'associer le pilotage pyrotechnique à un pilotage aérodynamique classique. L'association ainsi réalisée possède les avantages de ses deux constituants, en particulier un temps de réponse très faible et une capacité de manœuvre intéressante à haute altitude et/ou basse vitesse.

Ce type de pilotage permet de réduire la distance de passage d'un missile guidé en présence, par exemple, d'une cible manœuvrante ou volant à grande vitesse à haute altitude.

Cette communication présente les principes généraux d'un tel pilotage et des exemples d'applications possibles à des missiles sol-air à capacité antimissile.

1. INTRODUCTION

La défense contre les missiles tactiques de la génération actuelle est un problème dont la difficulté et l'importance vitale ont été récemment illustrées par l'EXOCET lors du conflit des Iles Malouines. La menace future, à terre comme en mer, sera encore plus contraignante du fait de l'accroissement prévisible de la vitesse et de la manœuvrabilité des missiles assaillants, d'un niveau élevé de brouillage et du caractère saturant des attaques.

Face à cette menace, de nouveaux systèmes de défense, actifs, à base de missiles autoguidés, seront nécessaires.

Un des problèmes posés à ces missiles est de réaliser la destruction structurale de l'hostile - voire la destruction de sa charge militaire - pour assurer une protection rapprochée efficace des objectifs défendus.

La destruction structurale d'un missile à l'aide d'une charge classique exige une très faible distance de passage sous peine de devoir accroître dans des proportions inadmissibles la masse de cette charge et celle de l'antimissile. En présence d'une cible supersonique très manœuvrante cette faible distance de passage implique une dynamique de l'interception finale très supérieure à celle des missiles sol-air actuels. Les paramètres qui régissent cette dynamique peuvent être résumés en termes de : senseur (la vue), guidage (l'intelligence), capacité de manœuvre (la force) et de pilotage (le réflexe). Des progrès, parfois majeurs, ont été réalisés ou se dessinent, dans ces différents domaines et sont susceptibles d'apporter une réponse partielle aux problèmes posés. Citons, sans souci d'être exhaustifs, les capacités nouvelles de traitement de l'information, les techniques de filtrage ou de guidage optimal, une maîtrise accrue de l'aérodynamique des hautes incidences...

Il existe cependant une butée dans le domaine du "réflexe". Elle est liée au principe même du pilotage aérodynamique classique dans lequel le dispositif de commande (gouverne, déviateur de jet ...) crée un couple qui provoque un mouvement d'assiette lui-même générateur de l'incidence propre à créer la force utile. Il en résulte :

- une limitation de rapidité du pilote automatique du fait de la multiplicité des "intermédiaires" à contrôler et des couplages tridimensionnels qui prennent naissance aux incidences élevées,

- une limitation du temps de réponse global admissible d'un missile autoguidé, sous peine de le destabiliser, par exemple sous l'action conjuguée d'une prise d'incidence et des aberrations de radôme.

En présence d'une cible rapide et agile, cette insuffisance de réflexe conduit à une distance de passage importante. En effet, la plupart des composantes élémentaires de cette dernière croissent avec le temps de réponse du missile guidé - par exemple comme son carré en présence de manœuvres.

Le pilotage des futurs missiles à vocation antimissile devra posséder des caractéristiques significativement améliorées, c'est-à-dire à la fois une grande capacité de manœuvre et un temps de réponse très diminué, même en altitude, sans qu'il en résulte une sensibilité accrue aux effets néfastes liés à la prise d'incidence du pilotage classique.

Le pilotage par ailes mobiles présente des limitations (capacité des vérins, effet de l'altitude ...) qui ne permettent pas d'atteindre l'ensemble de ces objectifs. Un pilotage pyrotechnique agissant au voisinage immédiat du centre de gravité possède pour sa part de très bonnes performances dynamiques, mais est pénalisé par une consommation de poudre excessive qui limite son domaine d'application à des temps courts et/ou des manœuvres modestes.

Ses avantages (rapidité, prise d'incidence très faible, efficacité quasi indépendante de l'altitude et de la vitesse...) sont cependant tels qu'il a paru intéressant de le valoriser en l'associant à un pilotage aérodynamique classique. Cette association dénommée dans la suite PIF-PAF (Pilotage en Force - Pilotage Aérodynamique Fort), constitue un dispositif homogène profitant des avantages propres de ses deux constituants et minimisant leurs inconvénients respectifs.

La présente communication présente, après un rappel sur le pilotage en force classique, les principes généraux et les applications possibles de ce concept qui fait l'objet d'un programme de recherche et de développement à l'AEROSPATIALE avec le soutien des Services Officiels Français.

2. LE PILOTAGE "EN FORCE" (PIF)

On s'intéresse dans ce qui suit à un pilotage dans lequel la force transversale nécessaire à l'évolution du missile est directement créée au voisinage de son centre de gravité par des jets de gaz propulsifs. Par abréviation on appellera ce mode de pilotage PIF pour Pilotage en Force.

2.1. Principes possibles

- Une première possibilité (figure 1) consiste à équiper le missile d'une batterie d'impulseurs organisée en couronne au voisinage de son centre de gravité.



Figure 1 : Pilotage en force par impulseurs

L'axe de chacun des impulseurs est incliné de manière telle que la force élémentaire passe au centre de gravité du missile ou légèrement en avant. La mise à feu d'un impulsor crée un incrément de force dont la composante normale $F \sin\alpha$ sert au pilotage et la composante axiale $F \cos\alpha$ contribue à l'entretien de la vitesse.

Un tel dispositif est bien adapté au pilotage d'un missile en autorotation. Le temps d'apparition de l'impulsion élémentaire peut être faible (5 ms par exemple). Le temps de réponse équivalent du pilotage est un peu plus grand du fait de la rotation, surtout en fin de vol lorsque le nombre d'impulseurs non brûlés devient faible.

Comme il est difficile, dans la pratique, d'augmenter considérablement le nombre d'impulseurs, ce mode de pilotage est utilisé lorsque la durée de vol et le besoin en maniabilité sont faibles (ex Missile Antichar DRAGON).

- Une autre possibilité autorisant un niveau de manœuvre plus élevé consiste à utiliser un système de distribution associé à un générateur de gaz débitant en permanence. La fixité du centre de gravité peut être obtenue, dans ce cas, en utilisant deux demi-générateurs de gaz organisés de part et d'autre du centre de gravité. Les gaz sont dirigés par l'intermédiaire d'un commutateur vers l'une ou l'autre d'un ensemble de tuyères, en maintenant la section de sortie globale sensiblement constante.

La figure 2 ci-après illustre ce type de réalisation :

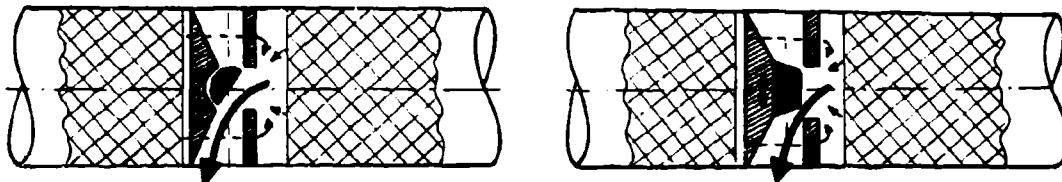


Figure 2 : Générateur de gaz et obturateur

a) rotatif

b) linéaire

Le nombre de tuyères nécessaires peut aller de 2 pour un missile en autorotation de roulis, à 3 ou 4 pour un missile stabilisé en roulis.

Le dispositif de commutation (ou d'orientation) peut avantageusement être commandé par un système pneumatique travaillant en + et - par emprunt de gaz au générateur principal. Le temps d'établissement des forces peut alors être très bref, typiquement de l'ordre d'une dizaine de millisecondes pour un dispositif de taille moyenne.

Par ailleurs, de même que dans le pilotage par impulsions, on peut incliner les tuyères vers l'arrière pour entretenir la vitesse du missile. L'angle d'inclinaison nécessaire étant en général faible, la force normale, $F \cos \alpha$, est très peu modifiée.

2.2. Dynamique du pilotage PIF

La réponse du missile à la force PIF peut-être caractérisée par les fonctions de transfert décrivant les petits mouvements par rapport à un point d'équilibre :

$$\frac{NT}{F_p} = K \frac{1 + A_1 S + A_2 S^2}{1 + B_1 S + B_2 S^2} \quad (\text{tangage ou lacet})$$

$$\frac{\dot{\theta}}{F_p} = K \frac{1 + A_3 S}{V_m T + B_1 S + B_2 S^2}$$

avec

NT accélération normale au cdg

$$K = -\frac{1}{m} \cdot \frac{(\ell_m V_m - M \alpha \Lambda)}{(M \alpha \Lambda + M q)}$$

F_p Force PIF

$$A_1 = -M q \cdot \Lambda / (\ell_m V_m - M \alpha \cdot \Lambda)$$

$\dot{\theta}$ vitesse d'assiette

$$A_2 = I \cdot \Lambda / (\ell_m V_m - M \alpha \cdot \Lambda)$$

α incidence

$$A_3 = \Lambda \frac{\ell_m V_m}{\ell_m V_m - M \alpha \cdot \Lambda}$$

V_m vitesse du missile

$$B_1 = (M q \Lambda - I) / (M \alpha \Lambda + M q)$$

m masse du missile

$$B_2 = -I \cdot \Lambda / (M \alpha \Lambda + M q)$$

s marge statique (> 0 si engin stable)

$$\Lambda = m V_m / (\phi - R_x + F_d)$$

ℓ bras de levier de la force PIF (> 0 si canard)

I inertie de tangage (lacet)

$$F_d = \bar{q} \cdot S_r \cdot \frac{\delta C_N}{\delta \alpha}$$

δ poussée

$$M q = \bar{q} \cdot S_r \cdot \frac{\delta \alpha}{V_m} \cdot \frac{\delta C_M}{\delta q}$$

R_x trainée

$$M \alpha = \bar{q} \cdot S_r \cdot \frac{\delta C_m}{\delta \alpha}$$

S_r , l_r longueur et surface de référence

\bar{q} pression dynamique.

Dans le cas d'un pilotage en force vrai ($\beta_s = 0$ ou $\ll 1$) on vérifie que :

$$K \rightarrow \frac{1}{m} \cdot \frac{M \alpha \cdot \Lambda}{M \alpha \cdot \Lambda + M q} \approx \frac{1}{m}$$

$$A_1 / B_2 \rightarrow \frac{M \alpha \cdot \Lambda}{M \alpha \cdot \Lambda + M q} \approx 1$$

$$A_3 \rightarrow 0$$

Il en résulte que la F.T. en accélération normale :

- a un gain quasi indépendant de la vitesse et l'altitude,
- possède deux zéros au numérateur proches des pôles du dénominateur.

La réponse naturelle du missile à un ordre de pilotage est de ce fait fidèle, rapide et peu affectée par l'oscillation d'incidence. La figure 3 montre de façon comparée la réponse temporelle, hors stabilisation, d'un missile piloté en force et celle de ce même missile piloté par des gouvernes aérodynamiques arrière. La figure 4 présente les incidences correspondantes en fonction du temps.

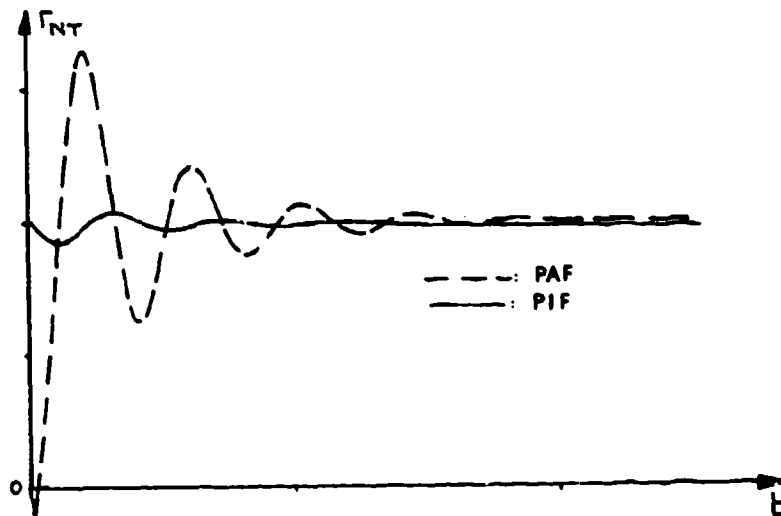


Figure 3 : Réponses en accélération normale (missiles non stabilisés)

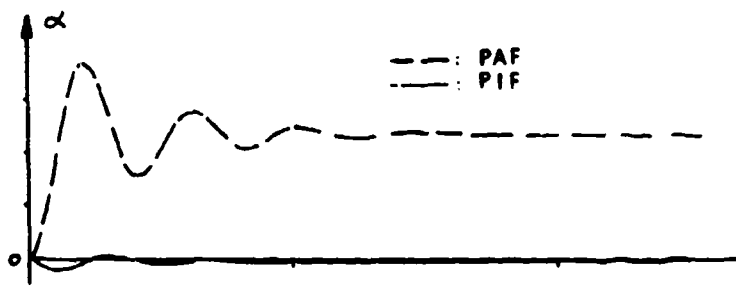


Figure 4 : Réponses en incidence (missiles non stabilisés)

Le comportement naturel du missile piloté en force est suffisamment pur pour qu'on puisse réduire le pilote automatique à un simple gain. Le retard total d'exécution de l'accélération normale se limite alors à celui, très faible, du dispositif de déviation de jet.

A titre d'exemple la figure 5 présente la réponse à un échelon d'accélération commandée du même missile que précédemment tant en pilotage PIF qu'en pilotage aérodynamique classique en boucle fermée pour ce dernier.

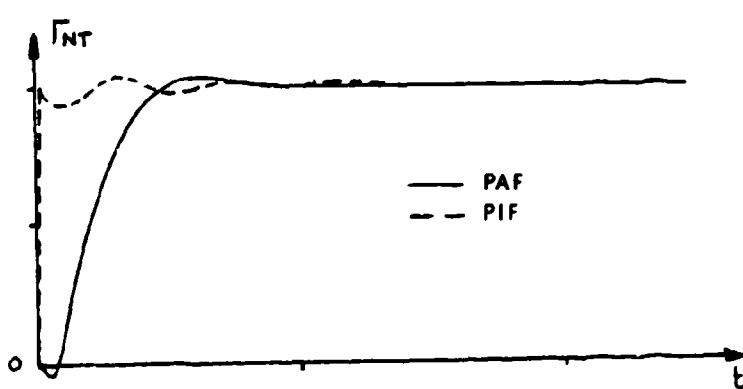


Figure 5 : Réponses PIF (non stabilisée) et PAF (stabilisée)

Le gain en temps de réponse atteint un facteur 10 environ. Ceci est particulièrement intéressant pour un missile guidé :

- s'il est guidé en alignement, parce que cela autorise une dynamique d'asservissement à la ligne de visée de hautes performances,

- s'il est autoguidé parce que la distance de passage diminue avec les retards de la chaîne et l'ordre de la fonction de transfert globale. Un autre avantage du PIF est, pour ce type de guidage, l'absence de constante de temps de mise en virage ($A_3 = 0$), ce qui améliore sa robustesse vis-à-vis des aberrations de radôme.

2.3. Aspects spécifiques

2.3.1. Intéractions entre le jet et l'écoulement extérieur

Le (ou les) jet(s) latéral(s) de pilotage constitue un obstacle (spoiler gazeux) pour l'écoulement principal ce qui induit un champ d'interactions avec l'aérodynamique externe (réf. 1 et 2). L'allure des phénomènes est représentée par la figure 6.

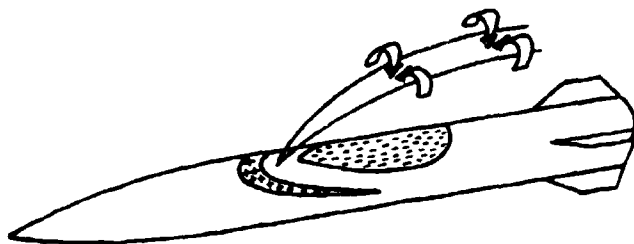


Figure 6

On distingue schématiquement deux zones d'interactions :

- une zone rapprochée au voisinage de la section de sortie du jet ou un choc détaché apparaît en amont de la tuyère séparant une zone de surpression amont et de dépression aval.

- une zone lointaine résultant du sillage du jet qui s'organise en deux tourbillons contrarotatifs susceptibles d'affecter les surfaces arrières du missile.

L'ensemble, complexe, de ces phénomènes fait qu'on recueille, au lieu de la force F_0 mesurable au banc statique, un torseur \mathbf{G} caractérisé par

$$\left. \begin{array}{l} \text{- une force } F = K(M, \alpha, \dots) F_0 \\ \text{- un couple } C(M, \alpha, \dots) \neq 0 \end{array} \right\} \mathbf{G}$$

Le rendement K sur la force dépend d'un grand nombre de paramètres (géométrie, Mach, incidence, ρ_i/ρ_0 ...). Il peut être inférieur ou supérieur à l'unité.

L'allure de son évolution avec le mach et l'incidence est, typiquement, la suivante.

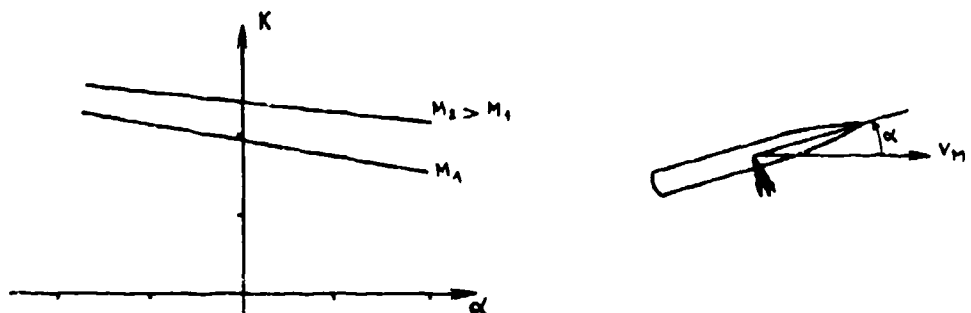


Figure 7 : Evolution du rendement avec l'incidence et le Mach

L'évolution du couple d'interactions est plus complexe. Une tendance assez fréquente est que sa composante en lacet (ou tangage) ait tendance, lorsque le rendement K diminue, à créer une incidence du signe de la force due au jet, ce qui assure une certaine constance de l'effet global.

Pour un pilotage en force pur, ou pratiquement pur ($\beta_6 \ll 1$), l'incidence reste très faible et l'essentiel est de définir une cellule pour laquelle, à l'incidence nulle, le rendement est bon (supérieur à 1 si possible) et l'effet du couple faible (bonne stabilité) et en tout cas dans le sens favorable.

Cette recherche de définition est essentiellement du ressort de la soufflerie.

2.3.2. Restrictions dues à la consommation

Utilisé comme seul moyen de pilotage, le PIF voit son domaine d'utilisation limité par sa consommation en poudre. En particulier dans le cas d'un générateur de gaz associé à une distribution par tuyères, la consommation est la même que la manœuvre demandée soit nulle ou maximale.

La possibilité de recourir au pilotage PIF pour une mission dépend donc de la valeur souhaitée pour la quantité (n.tp) avec,

n = nombre de g nécessaires à la mission

tp = durée du vol piloté.

La valeur acceptable de ce critère dépend :

- du type de pilotage retenu : le pilotage d'un missile en autorotation à un plan de commande est environ 30 % plus économique qu'un pilotage sur deux plans,

- de la participation du PIF à la propulsion, la rentabilité globale étant alors d'autant meilleure que le missile est plus rapide.

Elle peut varier d'une dizaine de g x s (sans participation à la propulsion) à quelques dizaines de g x s.

Ces valeurs peuvent cependant être relevées si un pilotage en PIF pur n'est pas nécessaire pendant toutes les phases de la mission. Il reste, dans ce cas, possible de faire participer l'aérodynamique aux manœuvres en décalant légèrement le point d'application de la force PIF vers l'avant du missile (pilotage en PIF canard).

2.4. Intérêt, limitations et domaine d'application du pilotage PIF

L'intérêt du pilotage PIF réside d'abord dans la rapidité de sa réponse et sa faible dépendance des conditions de vol. On peut y ajouter la simplicité du pilote automatique et un bilan de trainée favorable (pas ou peu de trainée induite par les manœuvres, surfaces portantes réduites à de simples stabilisateurs).

La limitation essentielle du PIF réside dans sa capacité en "n.tp" limitée, et l'impossibilité d'utiliser le missile après sa phase propulsée. De plus la difficulté de contrôler simplement le roulis par les jets, restreint, de fait, l'usage du PIF à des missiles travaillant en autorotation de roulis. Enfin, il ne faut pas négliger les contraintes que la présence du PIF impose à la définition du missile, en particulier à cause :

a) de l'obligation d'une faible variation du centre de gravité

b) des effets d'interaction créés par le jet.

Il en résulte que le PIF est bien adapté à des missions antichar ou sol-air à très courte portée. Cette dernière application, qui représente la limite pratique d'utilisation du PIF pur, correspondrait typiquement à un missile (figure n° 8) d'une quinzaine de kilos, en autorotation de roulis, et guidé à l'aide d'un autodirecteur infrarouge.

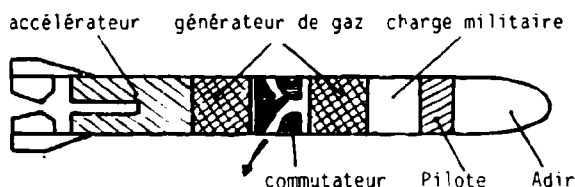


Figure 8 : SATCP piloté en force

Son pilotage est réalisé par un plan de tuyères commutables, la distribution dans l'espace étant effectuée par la rotation en roulis.

Le pilotage en croisière est du type PIF pur. Pendant la phase accélérée, il est du type PIF "canard" de manière à assurer le contrôle à très basse vitesse ce qui améliore le comportement à très courte portée par rapport à un missile à pilotage aérodynamique.

Le vitesse du missile est, après la phase d'accélération, maintenue supersonique grâce à l'inclinaison des tuyères PIF vers l'arrière d'un angle voisin de 20°.

3. LE PILOTAGE MIXTE PIF-PAF

On peut étendre le domaine d'application du pilotage PIF au-delà de ce qui a été dit précédemment à condition de le mettre en oeuvre seulement dans la phase finale du guidage et de l'associer à un pilotage aérodynamique. On dispose ainsi d'un pilote automatique ayant, en finale, une capacité de manœuvre accrue (somme de la manœuvrabilité aérodynamique et PIF) et bénéficiant du très faible temps de réaction du PIF.

3.1. Principe d'un pilote PIF-PAF

Le principe décrit est essentiellement adapté au pilotage d'un missile autoguidé. Dans ce type de guidage, l'effet défavorable du retard du pilote automatique provient du trainage qu'il induit entre la commande et l'exécution de l'ordre. La solution la plus naturelle pour réaliser une association PIF-PAF consiste donc à profiter de la rapidité d'exécution du PIF pour combler l'erreur dynamique de l'asservissement PAF. En d'autres termes le PIF doit travailler en verner sur l'erreur du PAF. Dans ce mode de fonctionnement le niveau de manœuvre PIF nécessaire peut être modéré, ce qui rend le système satisfaisant au plan des masses.

Le schéma théorique correspondant à un fonctionnement en verner est le suivant :

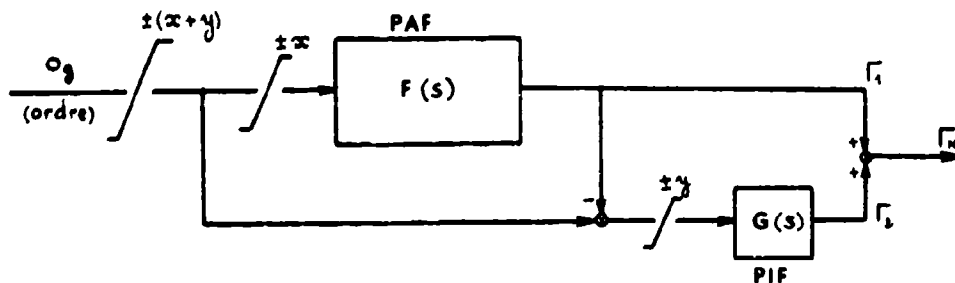


Figure 9

Dans le domaine linéaire la fonction de transfert du pilote mixte s'écrit

$$\frac{F_N}{\sigma_g} = F(s) + G(s) - F(s) \cdot G(s)$$

$$\text{Soit encore avec : } F(s) = \frac{1}{1 + a_1 s + a_2 s^2 + \dots} \quad G(s) = \frac{1}{1 + b_1 s + b_2 s^2 + \dots}$$

$$\frac{F_N}{\sigma_g} = \frac{1 + (a_1 + b_1)s + (a_2 + b_2)s^2 + \dots}{(1 + a_1 s + a_2 s^2 + \dots)(1 + b_1 s + b_2 s^2 + \dots)}$$

ce qui montre que le trainage en présence d'un échelon de vitesse est annulé en régime permanent et d'autant plus faible en régime transitoire que le terme $a_2 \cdot b_1$ est faible, c'est-à-dire que le retard du PIF est faible.

Il est clair par ailleurs que la capacité totale d'exécution du pilote est bien la somme de capacités individuelles de ses deux constituants.

Un schéma de principe du Pilote Automatique est donné par la figure 10. On y trouve, outre la structure d'un pilote aérodynamique adapté à l'autoguidage (réf. 3) :

- Un dispositif de commande du PIF
- Un "estimateur" imposé par l'incapacité des senseurs à distinguer la participation respective du PIF et du PAF dans le mouvement d'ensemble.

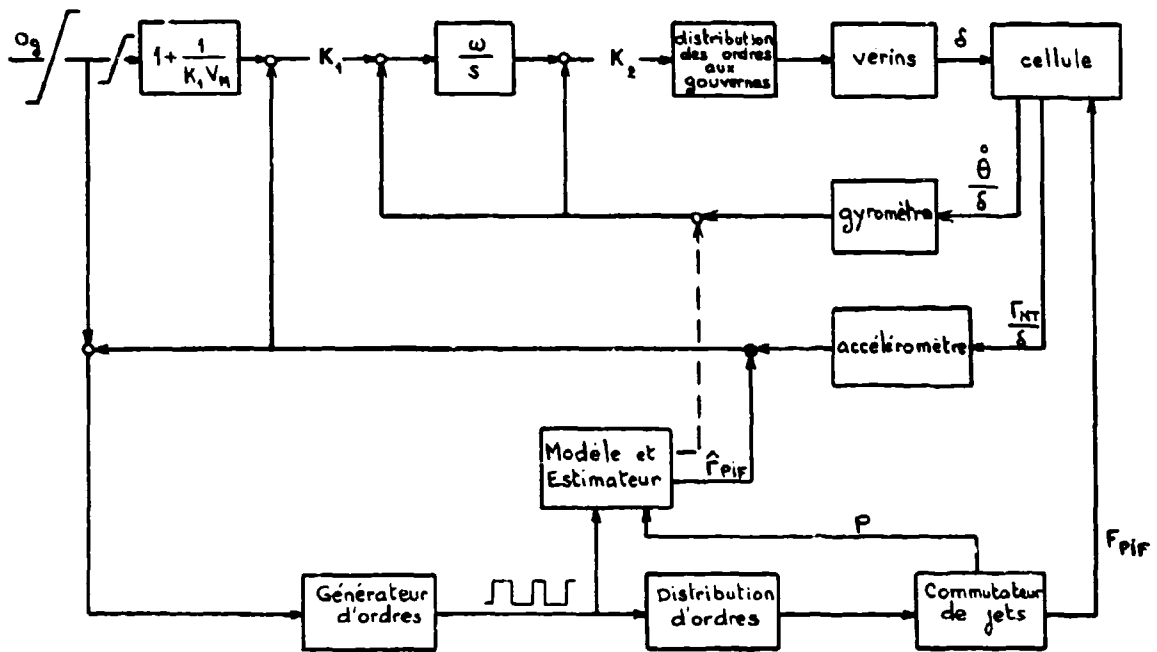


Figure 10 : Bloc diagramme d'un pilote PIF-PAF

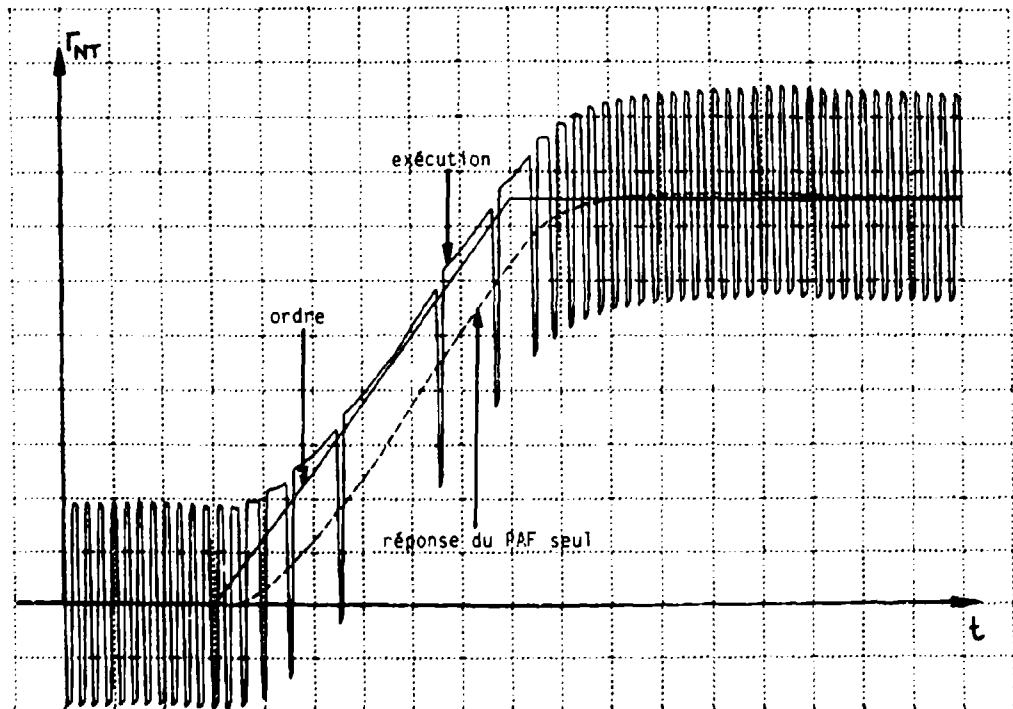


Figure 11 : Réponse d'un pilote PIF-PAF à un échelon de vitesse

Le dispositif de commande du PIF est constitué d'un générateur de signaux modulés en durée particulièrement bien adapté à une commande en + et - des commutateurs. Il peut comporter un effet d'intégration évitant, en particulier en présence de bruits, que des impulsions de commande trop brèves ne viennent solliciter la partie mécanique de la déviation de jet.

L'estimateur permet de restituer, à partir d'un modèle et de mesures, les accélérations $\hat{\Gamma}_{PIF}$ et $\hat{\Gamma}_{PAF}$ ainsi que l'erreur d'exécution ($Og - \hat{\Gamma}_{PAF}$) de la partie aérodynamique du pilote.

Les informations nécessaires sont la pression P du générateur de gaz et le signal accélérométrique S_a . La mesure de la position du commutateur (X_c) pourrait être envisagée mais peut être remplacée par la réponse d'un modèle aux signaux d'ordres.

La connaissance de ces éléments permet de calculer les termes souhaités, soit :

$$\hat{\Gamma}_{PIF} = \frac{\lambda P X_c}{m_0 - \mu \int_0^t P dt} \quad \hat{\Gamma}_{PAF} - Og = Sa - \hat{\Gamma}_{PIF} - Og$$

Remarques

- a) la présence du coefficient P , en facteur dans l'expression de $\hat{\Gamma}_{PIF}$ rend le système autoadaptatif aux variations éventuelles de débit du générateur de gaz,
- b) une estimation de $\hat{\Gamma}_{PIF}$ serait possible mais n'est pas indispensable dans la pratique.

Sollicité par une entrée en échelon de vitesse, un pilote, de la définition précédente, répond sans erreur de trainage. Son comportement est visualisé sur la figure 11 dans le cas d'un PIF commandé en + et -.

3.2. Influence du dimensionnement du PIF

Du fait de son mode de travail en vernier sur l'erreur du PAF, le niveau nécessaire du PIF reste modéré; de plus son action peut être limitée aux derniers instants du guidage ce qui rend son emploi satisfaisant au plan des masses.

Dans le cas de la navigation proportionnelle classique, une règle satisfaisante est que la capacité de manœuvre du défenseur soit d'environ 3 fois celle de l'attaquant. Dans le cas du PIF la règle correspondante est que son potentiel de manœuvre soit de l'ordre de grandeur de celui du but et son temps d'action d'environ 4 à 5 constantes de temps (T_g) du missile guidé et piloté en PAF seul. Cette règle, qui résulte de simulations complètes d'interceptions, peut s'interpréter comme suit : le PIF doit combler l'erreur de trainage du PAF lorsqu'une perturbation est susceptible de créer une distance de passage importante, c'est-à-dire lorsqu'elle survient peu avant la fin du guidage. Dans le cas d'une manœuvre du but et de la navigation proportionnelle ($N' = 3$), cette erreur de trainage prend la forme : $3 k \Gamma_B \cdot T_{PAF}^2 / (n T_g)$, T_{PAF} étant la constante de temps du pilote aérodynamique, et k un coefficient allant de 1 à 2 selon le type de manœuvre (permanente ou alternée) du but. La distance de passage qui en résulterait, en l'absence de PIF, serait maximale pour n compris entre 3 et 5. Il faut donc que : $\Gamma_{PIF} = 3 k \Gamma_B \cdot T_{PAF} / (3 T_g)$, ce qui, pour les valeurs courantes de T_{PAF}/T_g conduit à un niveau PIF un peu inférieur à Γ_B .

Dans ces conditions, l'impulsion totale nécessaire du dispositif de pilotage PIF est de l'ordre de grandeur de la dizaine de $g \times s$, c'est-à-dire physiquement réalisable.

Afin de préciser la validité de la règle $\Gamma_{PIF} \approx \Gamma_{But}$, les figures n° 12 et 13 présentent les distances de passages induites, en navigation proportionnelle classique ($N' = 4$), par une manœuvre en hélice du but de période T_B et pour quelques valeurs de $\Gamma_{PIF} / \Gamma_{But}$.

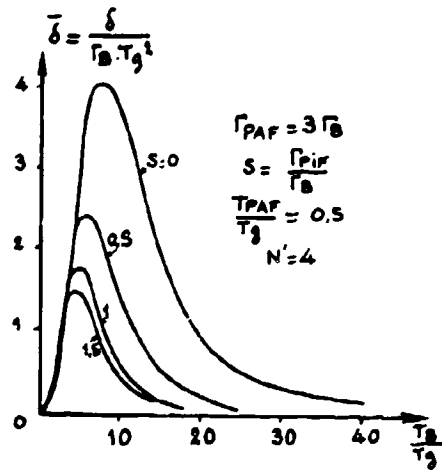


Figure 12

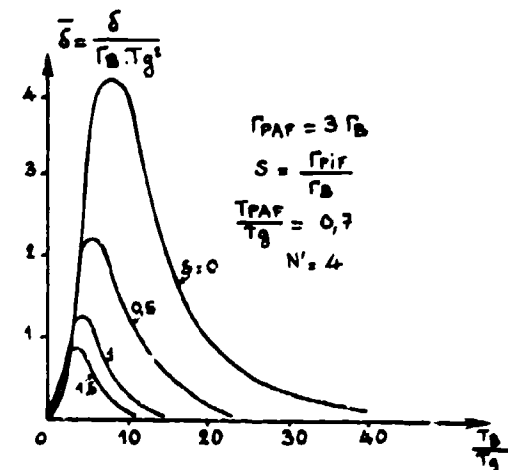


Figure 13

Ainsi, opposé à un hostile manœuvrant à $10g$ à la période $T_B = 2,5s$ environ, un missile PIF-PAF autorisera une distance de passage inférieure à $2m$ contre plus de $20m$ pour un missile guidé classiquement ($T_g = 0,25s$).

Dans le même esprit la figure 14 donne, en fonction de la durée de guidage t_g , normée par T_g , la distance de passage créée par une erreur angulaire de pointage initial $\Delta\beta$. La présence du PIF permet de réduire dans un rapport de 2 le temps nécessaire pour corriger ce type d'erreur.

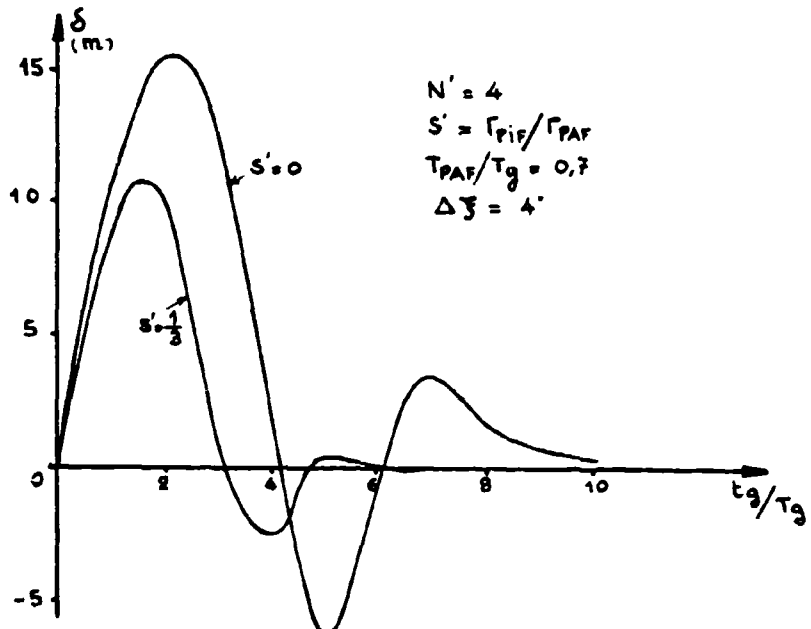


Figure 14 : Correction d'un dépointage initial

En présence de bruits les conclusions précédentes restent valables en moyenne. Pour ce qui concerne la composante de la distance de passage due aux bruits (thermique, glint ...) le PIF-PAF n'apporte par contre pas d'amélioration sensible, l'effet de certains d'eux ayant tendance à augmenter, d'autres à diminuer, pour un résultat d'ensemble peu changé.

3.3. Apport du pilote PIF-PAF

L'adaptation d'un pilote PIF-PAF à un missile autoguidé permet :

- Une réduction importante de la distance de passage en présence des cibles difficiles et en particulier très manœuvrantes.
- Une augmentation du domaine d'emploi d'un missile tant en portée qu'en altitude, le PIF permettant de compenser une perte de performances du pilote aérodynamique aux faibles pressions dynamiques.

La justification économique du PIF se trouve dans l'augmentation des performances de la menace, ce qui rend "rentable" un investissement dans le réflexe plutôt que dans la masse de la charge militaire.

3.4. Exemples de concepts de sol-air PIF-PAF

Le principe du pilotage PIF-PAF peut se concevoir dans le cadre d'un certain nombre de missions et, en particulier, dans les deux exemples type suivants :

- Missile sol-air courte portée (à booster largable, donc bi-étage) principalement destiné à intercepter des missiles assaillants à grande vitesse ($M > 2$) et à forte capacité de manœuvres ($> 10g$).
- Missile monoétage à plus grand rayon d'action (sol-air moyenne portée) dont l'objectif est l'interception des avions attaquant en formation serrée dans une ambiance ECM sévère et celle des missiles air-sol ou sol-sol tactiques.

3.4.1. Missile bi-étage

Ce missile, tiré à la verticale pour assurer avec un temps de réaction très court une couverture tout azimut, est accéléré pour atteindre une vitesse de l'ordre de Mach 2 à 3 avant séparation du booster.

Compte tenu des exigences de courtes portées, en particulier dans le cas de réengagements successifs, le vecteur vitesse est ramené à l'horizontale pendant la phase composite.

Peu après séparation de son accélérateur, le missile, stabilisé en roulis, est guidé vers la cible grâce à un autodirecteur actif.

En fin de guidage, le pilotage PIF vient assister un pilote aérodynamique à fort potentiel de manœuvrabilité, pour assurer une précision d'interception telle qu'une charge militaire de masse et dimensions modérées assure la destruction structurelle de la cible.

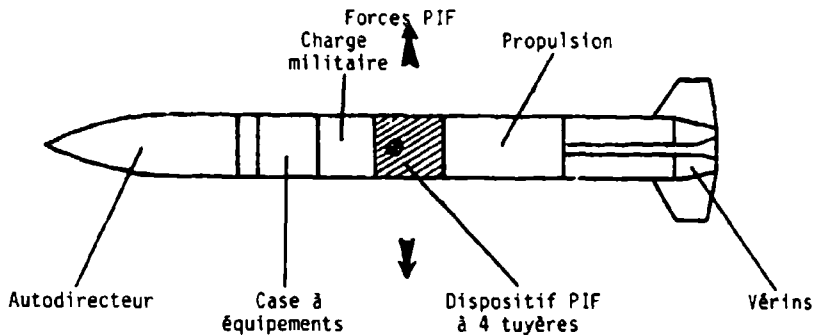


Figure 15 : SACP Antimissile

Avec la technologie actuellement disponible un tel missile répond aux exigences d'interception des assaillants les plus sévères prévisibles dans les décennies à venir.

3.4.2. Missile monoétage

Le principe de pilotage PIF-PAF est également applicable à un missile de plus longue portée (SAMP), propulsé par un statoréacteur dont la chambre de combustion est occupée, pendant les premières secondes de vol, par le bloc de poudre du propulseur d'accélération.

Ce missile monoétage (figure 16) est tiré soit à la verticale (couverture tout azimut), soit sur rampe inclinée (couverture sectorielle). Son booster l'amène au Mach de fonctionnement du statoréacteur.

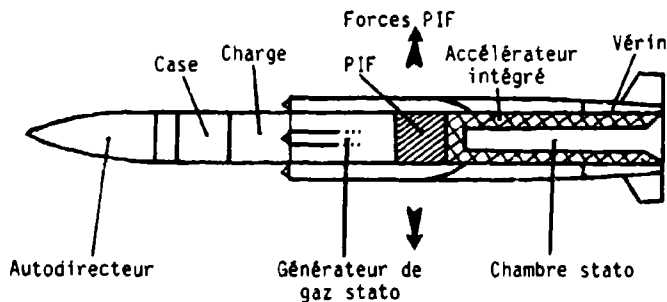


Figure 16 : SAMP - PIF-PAF

Le dispositif PIF est intercalé entre le générateur du statoréacteur et sa chambre de combustion pour être le plus voisin possible du centre de gravité. Ce dispositif apporte au SAMP un certain nombre d'avantages supplémentaires liés au domaine d'emploi et aux missions de ce type de missiles :

- A haute altitude, le facteur de charge aérodynamique diminue sensiblement alors que le facteur de charge PIF conserve la même valeur. Ce supplément de manœuvrabilité est acquis sans prise d'incidence, ce qui est favorable au fonctionnement des entrées d'air et n'accentue pas la sensibilité aux aberrations.
- Face à une attaque constituée d'avions en formation serrée et de brouilleurs puissants, la sortie de la sphère de brouillage s'effectue, dans bien des cas, au dernier moment : un dispositif agissant par forces directes, c'est-à-dire quasi instantanément, se révèle dans ce cas très intéressant pour corriger rapidement la trajectoire.

4. CONCLUSION

Nous avons décrit, au cours de cet exposé, un nouveau principe de pilotage et essayé de montrer son intérêt pour l'attaque des cibles aériennes.

La nécessité de prévoir une capacité antimissile pour les armes antiaériennes de demain donne à ce concept une importance accrue. Les cibles futures, supersoniques très manœuvrantes nécessitent au niveau du missile défenseur à la fois une forte manœuvrabilité et un temps de réponse très court.

Ces qualités peuvent être obtenues en alliant un pilotage aérodynamique classique et un pilotage par jets au centre de gravité. Elles permettent de conserver des dimensions raisonnables à la charge militaire, et donc au missile, en conduisant à de faibles distances de passage, quelle que soit l'esquive de l'objectif.

L'application de ces idées a entraîné la nécessité d'études poussées tant de la technologie des dispositifs de commande par jets, que de l'interaction de ces jets avec l'aérodynamique externe d'un missile. Les résultats obtenus confortent l'Aérospatiale dans sa décision de poursuivre le développement de ce système.

REFERENCES

- 1 - CASSEL L.A., DURANDO N.A., BULLARD C.W., KELSO J.M.
"Jet Interaction Control Effectiveness for Subsonic and Supersonic Flight".
- AD 86 24 83 - September 1968
- 2 - F.W. SPAID and L.A. CASSEL
"Aerodynamic Interference Induced by Reaction Controls"
AGARD - AG-173 - 1973 -
- 3 - F. WILLIAM NESLINE and NORMAN C. NABEEFELD
"Design of Digital Autopilots For Homing Missile"
AGARD - CP.270 - 1979 -

SEEKER SYSTEMS SIMULATION, PRESENT CAPABILITY AND FUTURE TECHNOLOGY

by

Dr. K. V. GRIDER

Deputy Director

Systems Simulation and Development Directorate
US Army Missile Laboratory
US Army Missile Command
Redstone Arsenal, Alabama 35898

ABSTRACT

The US Army Missile Command's use of seeker-in-the-loop real-time simulation in the development of surface-to-air missile systems is discussed. Material is presented to show that seeker-in-the-loop simulation makes a very positive contribution in the context of the current constraints on weapon system development, such as limited resources, the requirement for convincing system demonstrations, and the requirement for evaluation in a realistic environment including electromagnetic countermeasures and counter-countermeasures. The present facilities and capabilities for such simulation in the radiofrequency, nonimaging infrared and electro-optical bands are described and discussed. Examples of recent simulation results and their contribution to cost-effective system development are presented. Finally, developing technology in this critical simulation area and the US Army's plans for future increased simulator capability are addressed. In particular, such topics as the development of multimode or multispectrum, imaging infrared, and millimeter wave simulators are discussed.

INTRODUCTION

Current procedures for acquiring and supporting weapon systems require that key program and technical decisions be made at specific milestones. Recent actions to streamline and shorten the acquisition process accentuate the need for reliable and timely data on which to base these decisions. An increasingly important and valuable source of information for making such decisions is seeker-in-the-loop simulation. In this type of simulation, the seeker is mounted on a computer controlled flight table and realistic target/environmental signals are radiated from a computer controlled target array in a scenario which closely emulates real world conditions. The seeker/target miss distance and detailed seeker and environmental/target data are observed in real-time and recorded for subsequent analysis for each engagement.

The US Army Missile Command has been a pioneer in providing state-of-the-art technology for such non-destructive simulation of missile systems and continues as a technology leader in this field. The Advanced Simulation Center, developed by the US Army Missile Laboratory, performs simulations across a wide band of the electromagnetic spectrum, including radiofrequency for weapons such as air defense systems, infrared for weapons such as man-portable and mobile air defense systems, and electro-optical for weapons involving fiber optics guidance and systems using tracer overlays.

The seeker-in-the-loop simulation evaluates critical hardware and software elements as well as the simulated components of the missile in realistic, dynamic environments. It increases the value of flight test programs by replicating the flight test scenario in preflight and postflight analyses. In turn, the flight test program is used to validate the seeker-in-the-loop simulation as well as digital or hybrid simulations. When properly integrated into an overall test and evaluation program, these simulations provide a cost-effective source of reliable data to reduce the risk and uncertainty in system performance and to improve management decision-making over the entire missile system life cycle.

Resource management and technical constraints in developing today's missile systems require that a set of simulations be established and used in developing and fielding each missile system. Many program development offices have recognized this requirement and provide funds at the beginning of the development program to establish the appropriate set of simulations as early as possible. The simulation set can then be used throughout the life of the weapon system. Requirements driving simulation use include the following:

- o Improved cost-effectiveness
- o Reduced risk and uncertainty
- o Convincing system demonstration
- o Confident performance evaluation to optimize warhead size and deployment strategies
- o On-schedule deployment
- o Quick response to threat changes.

Ideally, the set of system simulations are established during the technology-base or technology-transfer phases of each missile system life cycle and are maintained and used throughout system development, production, and deployment.

The simulations selected for a particular system supplement and complement the more traditional tools available for the assessment of weapon system performance. As a result of early guided missiles being tested primarily in the field, flight testing became a mature engineering discipline. However, for both scientific and fiscal reasons, the performance of today's multimode, multifunction guided missiles cannot be adequately assessed by flight tests alone. In particular, complex systems performing many functions

require testing in a controlled environment to determine response sensitivity to various stimuli. Acquiring such data in field testing is essentially impossible due to specific terrain features and system-to-system variation. Additionally, the high cost and technical complexity of flight testing today precludes the number of experiments required to exercise an adequate envelope of system parameters to collect statistical data, to demonstrate repeatability (an essential factor in system reliability), and to evaluate proof-of-concept. The cost-effective solution is a balanced mix of flight tests and simulation. This may include all-analytical digital, hybrid, seeker-in-the-loop, or man-in-the-loop simulations.

SEEKER-IN-THE-LOOP SIMULATION FACILITIES

Development of the Advanced Simulation Center capability was initiated in the late 1960's in response to a US Army Missile Command requirement for an Army-wide source of expertise and capabilities in large scale seeker-in-the-loop simulations. Since activation in 1975 the Advanced Simulation Center has developed over 150 large-scale all-digital, hybrid, hardware-in-the-loop, and man-in-the-loop system simulations. The primary user has been the US Army Missile Command, but users have included many other Army, Navy, and Air Force organizations. Simulations are accomplished by individual or combined use of the advanced simulation processor complex, the infrared simulation system, the electro-optical simulation system, and the radiofrequency simulation system in a real-time dynamic environment.

The advanced simulation processor complex, Figure 2-1, provides high-speed, large-memory processors to support hardware-in-the-loop simulations within the complex and seeker-in-the-loop simulations in the infrared, electro-optical, and radiofrequency simulators; to simulate large systems in all-digital or hybrid representation; and to conduct research on advanced processors. The advanced simulation processor complex consists of large scale digital and analog processors with capabilities of 500 million to one billion operations per second; a separate test bed for advanced processor research; direct digital and analog data links to the infrared, electro-optical, and radiofrequency simulators; and a highly effective special-design interconnection and setup subsystem. An advanced software operating system integrates the real-time digital processor, hybrid compiler, vector processors, high speed multivariant function generators, hardware and software interfaces and the high level simulation language required for seeker-in-the-loop system simulation.

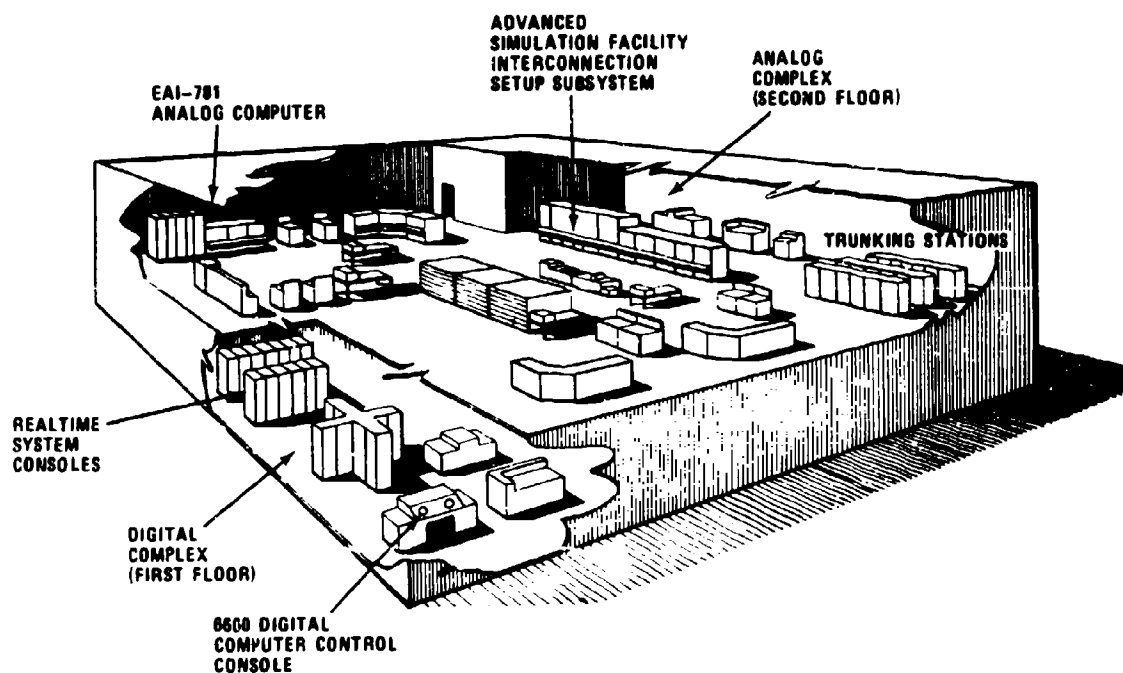


FIGURE 2-1 ADVANCED SIMULATION PROCESSOR COMPLEX

The infrared simulation system, Figure 2-2, provides a simulation tool for the design, development, and evaluation of infrared sensor systems applicable to surface-to-air, air-to-air, and air-to-surface missiles. Sensors in the 0.2 to 0.4 and 1.0 to 5.0 micron bands are hybrid computer controlled in six degrees-of-freedom during the target engagement sequence. A gimballed flight table provides pitch, yaw, and roll movements to the sensor airframe. A target generator simulates a variety of infrared target/background combinations which include tailpipes, plumes, flares, and fuselages in single or multiple displays against overcast or clear skies under various lighting conditions. These are displayed in azimuth, elevation, and range at the proper aspect by the target projection subsystem through a folded optical network, a display arm, and a display mirror. Simulation capability ranges from open-loop component evaluation to closed-loop total system simulation with countermeasures. The infrared simulation system capability is summarized in Figure 2-3.

The electro-optical simulation system, Figure 2-4, provides realistic and precisely controlled environments for the nondestructive simulation of a wide variety of ultraviolet, visible, and near infrared sensor systems. Actual sensors are hybrid computer controlled in six degrees-of-freedom while viewing targets under controlled illumination levels in an indoor simulation chamber and under ambient conditions on an outdoor simulation range. Three-dimensional target simulation is provided on a 32 foot by 32 foot terrain/target model/transporter which features a variety of topographical and man-made complexes at 600:1 and 300:1 scales, removable model sections, and fixed and moving targets. A moving projection subsystem provides two-dimensional representation. A gimballed flight table which provides pitch, yaw, and roll movements to the sensor airframe is attached to a transport which moves vertically and laterally. Either the terrain/target model or the two-dimensional projection subsystem is moved toward the flight table to provide the sixth degree-of-freedom. An adjacent high resolution TV/joystick console and helicopter crew station provide a means of evaluating man-in-the-loop guidance and target acquisition concepts. The electro-optical simulation system capability is summarized in Figure 2-3.

The radiofrequency simulation system, Figure 2-5, provides launch to intercept seeker-in-the-loop simulation of passive, semiactive, coherent and noncoherent active, command, beam rider, imaging and track-via-missile missile systems in surface-to-air, air-to-air, air-to-surface, and surface-to-surface engagements. Engagement scenarios include the use of multiple targets and jamming signals generated by actual jammers in the loop and the simulation of distributed clutter, targets distributed in range and angle, multipath, glint, and scintillation phenomena. Simulation in the radiofrequency simulation system is accomplished by radiating at operating wavelengths within a shielded anechoic chamber to a hardware seeker functioning in a dynamically simulated missile-target engagement. The electromagnetic environment for the seeker signal processor is simulated by means of a computer controlled radiofrequency signal generation system which feeds radiofrequency signals to the target and electromagnetic countermeasures antenna arrays. The targets, controllable in time, space, frequency, amplitude, polarization, phase, and number, are presented on a 534-element array of antennas representing a 42° field of view. Up to four

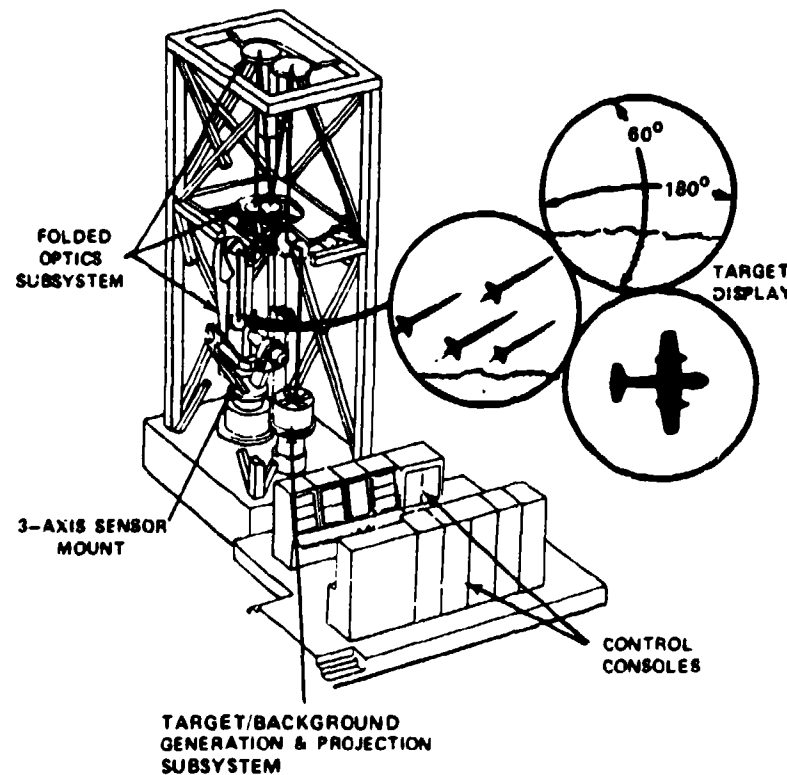


FIGURE 2-2 INFRARED SIMULATION SYSTEM

independent targets can be generated and displayed simultaneously in the 2- to 18-GHz range. By means of coaxial cable and wave guide paths between the radiofrequency signal generation system and the guidance sensor, simulated downlink, uplink and fusing signals may be passed between the guidance sensor and the radiofrequency generation system. In addition to the target antenna array, two denial electronic countermeasures channels feed 16 electromagnetic countermeasures antennas distributed among the target antennas to display up to two electromagnetic countermeasures signals for simulating stand-off jammers. Electromagnetic countermeasures signals, generated by actual jammers or emulated with a radiofrequency generation channel, can be dynamically colocated on the target signal through the use of a separate

PARAMETER	IRSS	EOSS	RFSS
WAVELENGTHS	0.2 TO 0.4μ , 1 TO 5μ	VISUAL, 2 TO 14μ , ULTRAVIOLET	1.7 TO 15 CM
MAX SEEKER DIAMETER	10 INCH	14 INCH	16 INCH
MAX SEEKER WEIGHT	26 LBS	150 LBS	150 LBS
FLIGHT TABLE FREQUENCY RESPONSE	15 TO 22 Hz	10 TO 23 Hz	13 TO 30 Hz
PHYSICAL EFFECTS SIMULATOR SIZE	27 X 12 X 10 FT (HIGH, WIDE, LONG)	CHAMBER, 38 X 40 X 120 FT (HIGH, WIDE, LONG) PLUS 200 FT OUTDOOR EXTENSION	CHAMBER: 48 X 48 X 48 FT (HIGH, WIDE, LONG)
TARGET RANGE	100 TO 10,000 FT	1,000 TO 144,000 FT	400 FT TO 94,000 FT (ACTIVE COHERENT) 40 FT TO MISSILE SENSITIVITY (OTHER)
MAX CLOSING VELOCITY	4,000 FT/SEC	9,000 FT/SEC	8,000 FT/SEC (ACTIVE COHERENT) 20,000 FT/SEC (OTHER)
MAX TARGET ANGULAR RATE	100°/SEC	200°/SEC	21,000°/SEC
TARGET DYNAMIC RANGE	3.6×10^{-4} TO 3.6×10^2 W/cm ² - μ	10^{-4} TO 10^3 FT CANOLES	MISSILE SENSITIVITY TO -17 dB m/m ²
UPDATE RATE	1 TO 2 MSEC	ANALOG	1 TO 5 MSEC
FIELD OF VIEW	$\pm 90^\circ$ Az, $\pm 30^\circ$ El	$\pm 120^\circ$ P, $\pm 40^\circ$ Y	42° CONICAL SECTOR
TARGET/CLUTTER TYPES	TAILPIPE/FLARE PLUME FUSELAGE BACKGROUND COUNTERMEASURES	GROUND TARGETS TERRAIN	GROUND RADAR AIRBORNE TARGETS CLUTTER ECM MULTIPATH JET ENGINE MODULATION RF IMAGING

FIGURE 2-3 ADVANCED SIMULATION CENTER CAPABILITIES SUMMARY

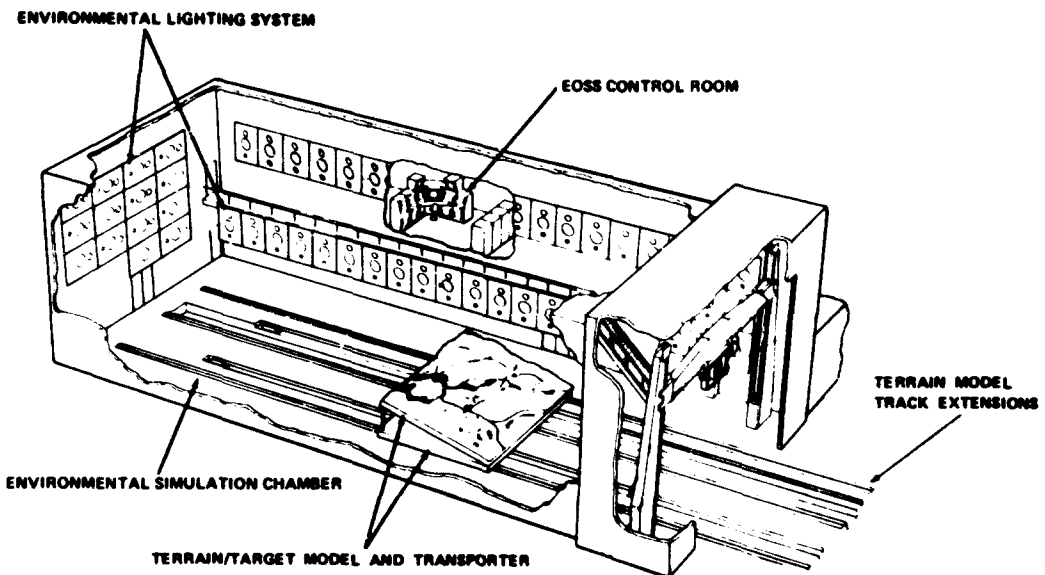


FIGURE 2-4 ELECTRO-OPTICAL SIMULATION SYSTEM

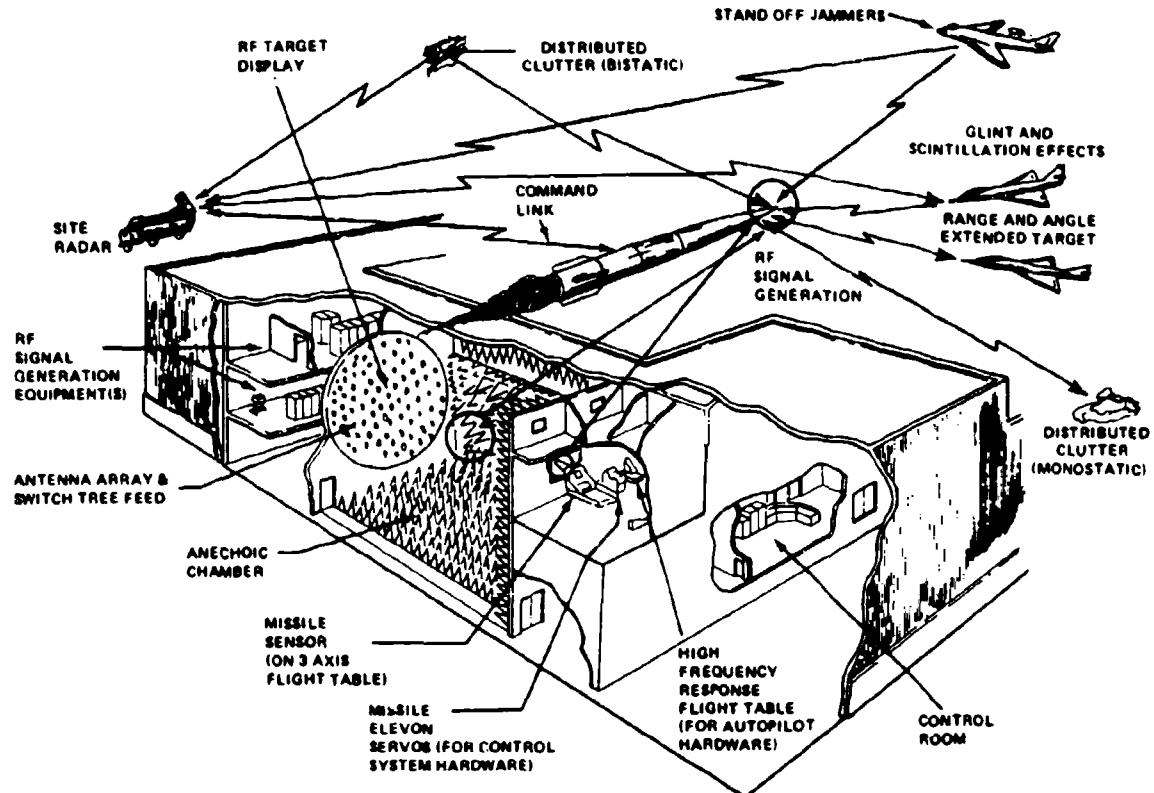


FIGURE 2-5 RADIOfREQUENCY SIMULATION SYSTEM

target channel to simulate an on-board self-screening or deceptive jammer. Expendable and escort screening jammers can be simulated in a similar manner with separate dynamic trajectory control. The missile-target relative motion is accomplished by controlling the target return signal in angle and range and by seeker angular motion provided by the flight table. The radiofrequency simulation system capability is summarized in Figure 2-3.

In addition to the Advanced Simulation Center laboratory hardware facilities, two other elements contribute to the simulation capability: The extensive software programs now available at the Advanced Simulation Center and the experienced technical staff, our most valuable asset. Some 250 major special-purpose software programs and techniques now exist at the Advanced Simulation Center. About one-fourth were developed prior to activation; the remainder evolved over eight to ten years of simulation operation as simulation experience increased and new equipment and capability were added. An example of a special-purpose software program is the computer-based path-loss/path-length program in the radiofrequency simulator. This program statuses the path length and path energy loss of the very large number of paths that the target signal may traverse from its crystal source to free space radiation from one of four ports of any of the 550 target array antennas. This statusing is required for many simulations because it is desirable to keep all path lengths to ± 1.5 wave lengths and the energy loss variation from antenna to antenna less than ± 1 db. Such a status is impossible to assess manually. The special-purpose program that handles this task automatically assess all possible path-loss/path-length measurements and indicates by a graphics display the antennas where the path-loss/path-length values fail to meet the specified value. Technicians then change out elements in the path identified (using sub-programs to identify the likely element) until all paths are within specification. Some 400 man years of development and checkout are now invested in such software programs. These programs provide laboratory control of all standard functions such as target motion, calibrations such as flight table readiness tests, diagnostics for complex systems such as the master/minicomputer interfaces, simulation aids such as real-time graphics, and simulation dependent software such as executive control, missile models and environmental models.

Simulation development, operations, maintenance, and system improvements at the Advanced Simulation Center are handled by a technical staff of over 100 engineers and technicians composed of Government and support contractor personnel. The principal engineering discipline is electronic engineering. The Advanced Simulation Center technical staff was developed over the past eight to ten years by careful selection and, as it now exists, is a national resource in seeker-in-the-loop simulation.

Planned expansion of the Advanced Simulation Center includes adding simulators to provide imaging infrared, multispectral, millimeter, additional radiofrequency and weapon system capabilities. The expansion is scheduled for incremental activation beginning in 1989. Prior to that time, an interim millimeter facility will be provided for use in the 1985-91 timeframe. These expansions are discussed in a later section of the paper.

SIMULATION DEVELOPMENT AND OPERATIONS

A successful simulation requires that the customer and simulation developers have a common definition and agreement as to simulation goals, objectives, and requirements. It is important that the customer understands what equipment and personnel he will provide and how they will interface with Advanced Simulation Center counterparts. A typical Advanced Simulation Center simulation program is conducted in five phases.

Phase I, the coordination and planning phase, starts through an initial contact between the potential customer and appropriate simulator personnel. The following goals and requirements are defined:

- 0 Simulation goals and benefits
- 0 Technical characteristics and requirements
- 0 Simulation scenario requirements
- 0 Application of simulation results.

These goals and requirements are reviewed against the capability of the Advanced Simulation Center. Simulation development and operational schedules are discussed and an initial cost estimate is made.

Phase II is the simulation development phase. During this phase, the environmental models, simulation scenarios, software, environmental model implementation and generation, interface controls, recording setup, display setup, and digital and/or hybrid missile models are developed. Particular emphasis is placed on the development, verification, implementation, and validation of environmental models using independent measurements and flight test data. These models are available in hierarchies of complexity, ranging from very simple to highly sophisticated. Model hierarchies allow the selection of the appropriate level of environmental complexity for each seeker, and permit the determination of seeker sensitivity to elements of the environment through systematic variation of model parameters. After selection of the appropriate generic model additional work is typically required to tailor the model for specific application, select and ready the specific data that the model will use, and check out the data/model in real-time.

Phase III, the simulation verification phase integrates the facility simulation configuration with the hardware and support equipment provided by the user. The user hardware is integrated with the facility using the missile/facility interface and control panels provided by joint Advanced Simulation Center/user design. The operational readiness of all software is verified, and baseline verification tests are performed, culminating in measurements of the propagated electromagnetic signal using both a test receiver and the seeker-under-test. Finally, the missile guidance loop is closed by a standard Advanced Simulation Center procedure in which software modules are replaced systematically by hardware elements and the overall simulation is verified.

The simulation operation phase usually involves both open- and closed-loop simulation. Open- or closed-loop simulation may be conducted with various missile hardware elements simulated by digital and/or analog models or with various elements of hardware-in-the-loop. Seeker-in-the-loop, as used in this paper, means an actual seeker operating in a closed guidance loop. In closed-loop simulations, all elements of the missile system and target are included either as hardware or as digital or analog models running in real-time. In open-loop simulation, where the objective is to characterize and evaluate the seeker as an independent element, the guidance loop is not closed. Seeker-in-the-loop simulations can vary from using only one missile hardware element in the loop (such as the seeker, guidance electronics, autopilot, or control system) to multiple missile elements plus actual jammers and elements of the ground radar. Open- and closed-loop simulations can be simple or complex depending on the fidelity required for the modeled element or phenomenon.

Phase IV, the simulation operations phase, begins with open-loop testing of the seeker. Periodic baseline tests are performed. Once the loop is closed, statistical sets of 5 to 50 runs are typically performed for engagement scenarios of interest. Total closed-loop runs for an average program vary from 1000 to 3000, with the number of runs conducted for a given program being determined by user requirements. The length of the simulation operations phase is usually estimated on the basis of a daily average of 50 to 100 closed-loop runs, based on the experience of more than 60 major simulations conducted to date. However, as many as 800 runs per day have been accomplished during exceptional simulation operations.

Phase V, the validation, analysis and documentation phase, accomplishes data collection, validation, reproduction, and distribution. A formal debriefing and an analysis or final report are provided to the customer.

A major and continuous activity, which is independent of specific simulation development, is hardware/software design to improve the overall simulation system and to add new capabilities to maintain a state-of-the-art capability. Without this well-planned and continuous modification and improvement activity, a simulator or facility would be obsolete in three to five years. One class of recently developed missiles, for example, requires a coherent active target to exercise the range gates of the missile. Two years of extensive hardware/software design and fabrication involving 10 to 15 engineers and technicians were required to provide that capability. Such an activity is analogous to a project development task requiring many engineering disciplines as well as parts procurement, subsystem fabrication, configuration control, and a check out/integration phase.

The hardware/software design activity consists of design of advanced processor hardware/software, simulator computer configuration and interfaces, missile electronic/electrical/mechanical interfaces, simulator software, missile models, environmental models, and target generation. Design of advanced processor hardware/software involves processor research on combined hardware/software capabilities with

the goal of designing/selecting optimum simulator processing systems for future simulation needs. A similar task is design and selection of current simulator computers and interfaces for immediate, specific simulation needs. The design of electronic/electrical/mechanical interfaces to interface and control the generic missile in the simulator system requires research and application of electromechanical, hydraulic, and control theory. Simulator software design involves writing software for developmental processors and for controlling various laboratory functions such as target generation and data display and recording systems. Environmental modeling involves the development of math models and the implementation of environmental models through target source generation equipment under computer control. This task often involves adapting a new computer configuration and writing highly specialized software. The environmental modeler must work closely with the target source generation engineer to recommend an implementable source generation configuration. The development of a generic missile model requires layout of the system into working math modules, development of the motor and aerodynamic/atmospheric modules, and development of the servo-loop and control system modules. Target generation involves the design of the electromagnetic sources for implementing the target model.

Simulation planning and operations as an overall task, require technical interface with the customer; the defining of requirements for facility modification or new capabilities; designing the missile simulation and control, recording and displays interface; defining environmental model requirements with attendant target generation requirements; defining facility software requirements; defining the missile model requirements; and writing the simulation plan and procedure. The appropriate hardware/software design engineer then takes the requirements and implements them. The operations engineer then conducts the simulation and assists the data analysis engineer in analyzing the data.

Maintenance and calibration of the target source generation system, the target display system, the processing system, and the interface and control system requires a separate, planned effort that is conducted in part during first and third shifts, which is an added engineering management and cost consideration in running a simulator.

SEEKER-IN-THE-LOOP SIMULATION EXPERIENCE

Seeker-in-the-loop simulation activity at the Advanced Simulation Center began in the early 1970's. Experience has been with infrared, optical and radio/frequency guided missiles in passive, semiactive, and active modes.

Experience at the infrared simulator has focused on a man-portable heat-seeking air defense system and on a major infrared air defense system. At the electro-optical simulator, emphasis has been on fiber optics guided systems and systems guided by tracer overlays. Electro-optical simulation is currently being conducted on application and demonstration of a fiber optics guided system. The first and most frequent user of the radiofrequency simulator has been a major semiactive surface-to-air air defense system and its derivatives sponsored by various organizations. Other important simulation work done in

the radiofrequency simulator includes ground-to-air missile site countermeasures against anti-radiation missiles, several classified programs, cruise missile evaluations, active coherent missiles, and various jammers. In the digital and hybrid advanced processor, we have supported all Army missile programs.

The simulation work performed in the radiofrequency simulator has been particularly impressive in both quality and quantity: Since activation in March 1975, the facility has been continuously scheduled averaging 15 simulations and 13,000 closed-loop runs per year.

Significant simulation work has been performed in the radiofrequency simulator in electromagnetic countermeasures and electromagnetic counter-countermeasures evaluation in three categories:

- o Jammer systems
- o Radiofrequency missile systems
- o Antiradiation countermeasure programs.

A large number of different jammers and various jamming techniques in breadboard form have been evaluated against various missile simulations. The jammers are operated out of a separate, shielded electromagnetic countermeasure room located behind the array. These signals can be colocated on the moving radar target being acquired/tracked by the missile seeker on the flight table in a closed-loop simulation. The effect of the electromagnetic countermeasure signal on acquisition, track, and engagement sequence is evaluated. Subsequent runs are often made where the missile has been modified by an electromagnetic counter-countermeasure technique and then the jammer is run in another mode or is modified in the continuing countermeasures/counter-countermeasures loop.

Over twenty missile systems and variations have been evaluated against various jammers for electromagnetic countermeasures vulnerability and electromagnetic counter-countermeasure effectiveness. Our experience has shown that once a valid missile simulation is established, jammer development offices and air force tactical commands are eager to test their jammers against the simulation, particularly against systems or techniques which offers a challenge or threat to their jammer. The missile program offices are likewise eager for their missiles to be evaluated against state-of-the-art jamming techniques. Both missile and jammer development offices benefit from this joint effort through cost savings and improved missile and jammer performance evaluation.

Considerable simulation work has been done in the radiofrequency simulator to assess the vulnerability of major U.S. surface-to-air missile system sites to an attack by an anti-radiation missiles. The effects of various countermeasures employed by the site have been evaluated. Seeker-in-the-loop simulation is by far the most cost effective approach to this analysis.

The eight to ten years simulation experience accrued by the Advanced Simulation Center has shown that simulation is very cost effective in addition to providing the simulation services which are mandatory in today's and tomorrow's environment. An example of cost savings/cost avoidance through simulation is the radiofrequency air defense system simulation work accomplished at the Advanced Simulation Center. Continuous seeker-in-the-loop simulation support has been provided to a major radiofrequency air defense system since the radiofrequency simulator became operational in 1975. This support consisted of evaluation of design changes, system upgrades, and evaluation of the system against advanced electronic countermeasures and postulated threats. Heavy emphasis was placed on electromagnetic counter-countermeasures modifications to the missile and included investigations and evaluations to assure that the modifications had no adverse impact on total system performance. The project office of this air defense system thereby significantly reduced the number of flight tests required to support program decisions. A precedent was established in the air defense community when a major system modification was released to production on the basis of seeker-in-the-loop simulation results. Subsequent flight tests verified the modification. Continuing support provided to this project has ensured an indepth and current knowledge of capabilities of this fielded system and has resulted in large cost savings.

FUTURE SEEKER-IN-THE-LOOP SIMULATOR DEVELOPMENT PLANS

Two seeker-in-the-loop simulator expansion programs are underway at the US Army Missile Command: an interim millimeter simulation facility and a larger permanent expansion, the millimeter/microwave simulation facility. Since seeker-in-the-loop simulation has proven to be a cost-effective critical management and technical measurement tool for weapon system acquisition and readiness, these simulators will greatly enhance the ability of the US Army and DOD to confidently field new weapon systems. A survey of planned seeker development, projected seeker/system fielding, and support of systems now in the field has dictated the type and spectrum of simulators being planned.

Planning for the future simulators is driven by the following considerations:

- o Army and Department of Defense weapon system development
- o Survey-determined requirements for hardware-in-the-loop simulators: Radiofrequency, millimeter, imaging infrared, multispectral, and weapon system
- o Requirements for passive, semiactive, and active (coherent/noncoherent) simulation modes
- o A need for realistic multiple target and clutter models at operational frequencies
- o Ability to comparatively evaluate missile systems in benign, electromagnetic countermeasures, electromagnetic counter-countermeasures environments
- o Ability to evaluate actual electromagnetic countermeasures hardware against seeker-in-the-loop simulations in a covert environment
- o Provision of a cost-effective mix of seeker-in-the-loop simulation with flight test programs
- o Provision of seeker-in-the-loop simulation support throughout weapon system life.

The first simulator expansion program, the interim millimeter simulation facility, will require a separate building adjacent to the Advanced Simulation Center, Figure 5-1. This facility is being sized for 30-100 GHz and small aperture seekers. The chamber will be 32 feet wide, 30 feet high and 50 feet long. The targets and environmental effects will be displayed by an array of antennas under computer control in a manner similar to the existing RF system previously discussed. The facility will be operational in late 1985 and is expected to be used into the 1990's. Early use of this facility will provide a needed interim millimeter wave simulator capability for millimeter systems as well as a test bed for millimeter simulator techniques to be employed in subsequent millimeter simulators.

The millimeter/microwave simulator facility will be a three-story, 285 foot by 185 foot building adjacent and to the north of the Advanced Simulation Center, Figure 5-2. It will contain seven simulators, the required support equipment, and the office support space to be self-contained. A major feature of this facility is the construction of the six simulation chambers for seeker-in-the-loop simulation and the set of three chambers for the weapon system simulator. The chambers are multistoried rooms, with the largest being 60 feet long by 50 feet high by 50 feet wide. The chambers are shown in Figure 5-3.

The construction of the millimeter/microwave simulator facility will begin in 1986 with first use in 1989. Of the seven simulators planned, three will be implemented initially:

- o Radiofrequency simulator: 4-12 GHz - operational 1989
- o Millimeter simulator: 35-220 GHz - operational 1989
- o Weapon system simulator: 0.5-50 GHz - operational 1990.

Two additional radiofrequency simulators, an imaging infrared simulator, and a second millimeter simulator will be fitted out with equipment in an incremental sequence beginning in 1989 and ending with all chambers operational in 1993/94.

In the use of the new simulators, the US Army Missile Command will provide the basic facility, the staff for developing the specific user simulation, and the operations staff. The user, as in the current simulators, will fund unique simulation hardware/software, development of his specific simulation, and the operational cost of running his simulation. The user will define his requirements and participate in the simulation development and operations. The US Army Missile Command will develop and operate the simulation and participate in the data/system evaluation as requested by the user.

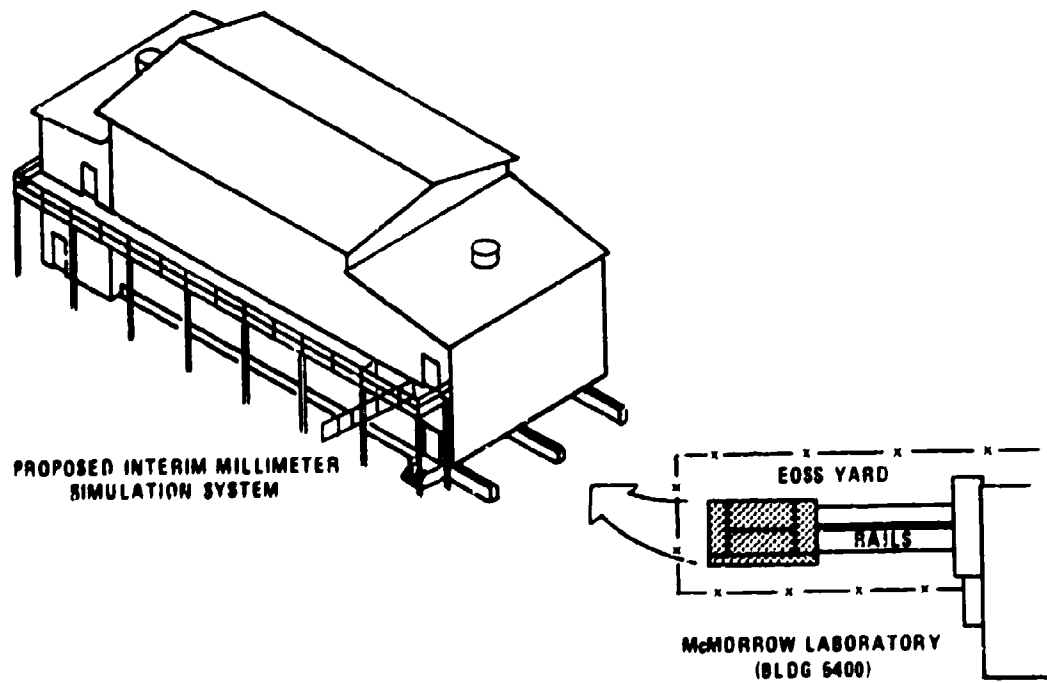


FIGURE 5-1 INTERIM MILLIMETER SIMULATION SYSTEM

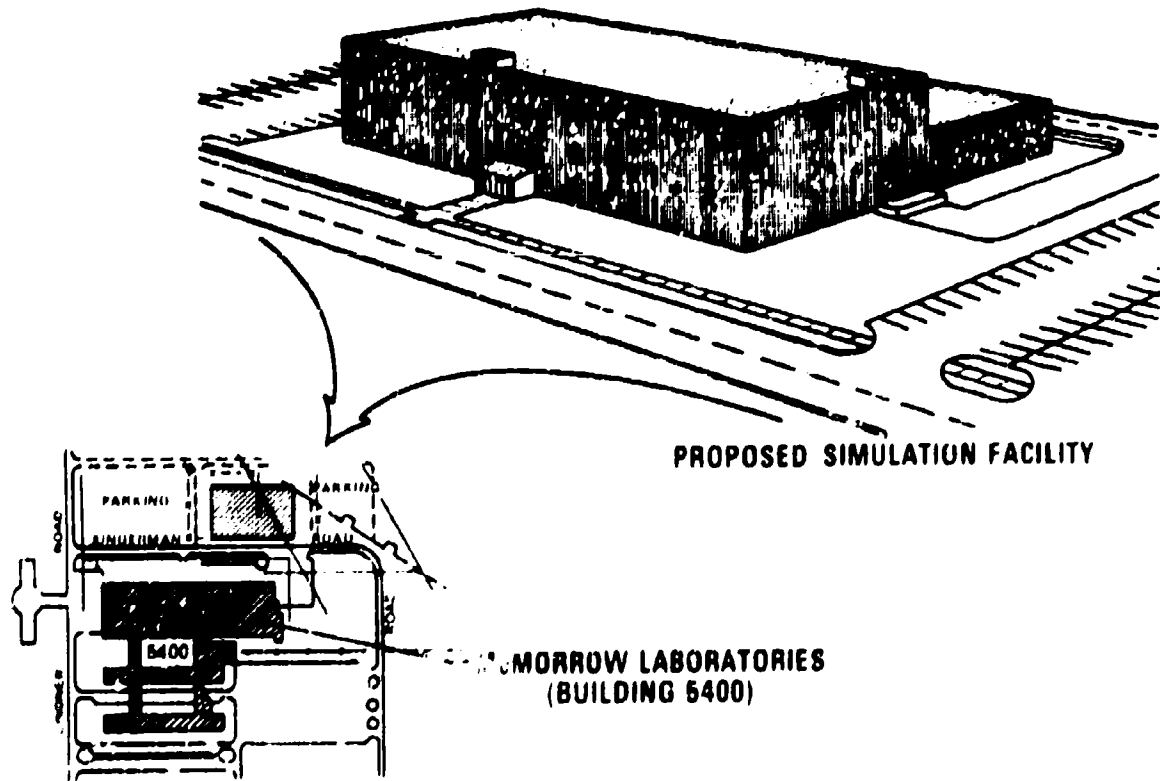
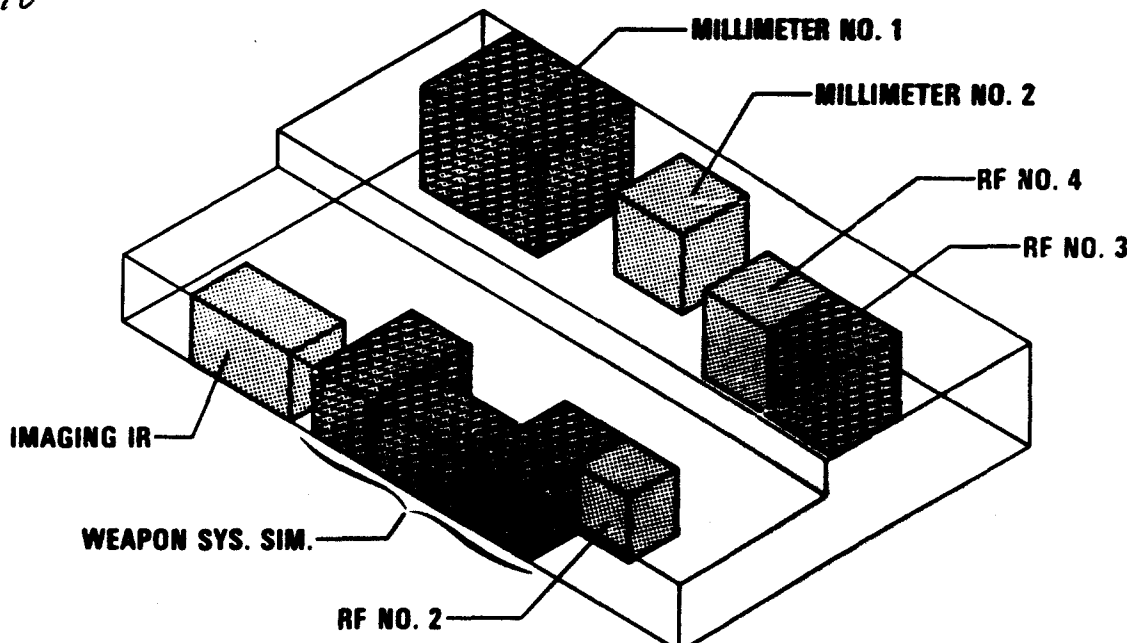


FIGURE 5-2 MILLIMETER/MICROWAVE SIMULATION FACILITY



CHAMBERS TO BE COMPLETED INITIALLY

VIEWED FROM REAR (NORTHWEST) OF BUILDING

FIGURE 5-3 MILLIMETER/MICROWAVE SIMULATION FACILITY CUTAWAY SHOWING CHAMBER VOLUMES

SUMMARY

Seeker-in-the-loop simulation is a valuable and mandatory source of information for management and technical decision making in developing and fielding today's sophisticated guided missile systems. The US Army Missile Laboratory has been a pioneer in providing state-of-the-art technology and capability in seeker-in-the-loop simulators. This activity was initiated in the late 1960's and has seen the successful development and use of the Advanced Simulation Center, which provides three major simulators and a central advanced simulation processor complex. The simulators operate in the infrared, electro-optical and infrared spectrum. All simulators provide realistic, controlled, dynamic targets in realistic mission/engagement scenarios.

Development and operation of the seeker-in-the-loop simulations require a multidisciplined staff who interface with the simulation customer in defining and establishing his simulation. Participation by the simulation customer in developing and running the simulation is required. A typical simulation development is conducted in five phases: Coordination and planning, development, verification, operation, and validation, analysis and documentation. A major activity in operating a seeker-in-the-loop simulator is design and provision of hardware/software to maintain the simulator as a state-of-the-art facility. This design and build-up is best provided by the resident staff because of the uniqueness of the technical requirements. Software design, electronic/electrical/mechanical interfaces under computer control, environmental models, and the electromagnetic implementation/display of the models are the major tasks involved.

The simulators have been used extensively for the past eight to ten years by US Army and DoD air defense system and jammer development offices. Over 150 major simulations have been accomplished to date at the Advanced Simulation Center. Combined missile system evaluation and jammer evaluation are often accomplished simultaneously in a very cost-effective manner. Cost-effective benefits of seeker-in-the-loop have been repeatedly demonstrated by using simulation in a mix with flight tests to substantially reduce the number of costly flight tests.

The US Army Missile Command is planning two seeker-in-the-loop simulator expansion programs: An interim millimeter simulation facility to be operational in 1985 and a larger permanent millimeter/microwave simulation facility which will begin initial operation in 1989 with full up operation in 1993/94. The permanent facility will provide seven new seeker-in-the-loop simulators: Three radiofrequency simulators, two millimeter simulators, an imaging infrared simulator, and a weapon system simulator. These simulators will provide long-term support to missile system development, deployment, and threat response modifications.

MISSILE SYSTEM FOR LOW ALTITUDE AIR DEFENCE

Mr Robert BROWN
Mr Gianfranco SANTI
Defence Systems Division
SELENIA INDUSTRIE ELETTRONICHE ASSOCIE S.P.A.
Via Tiburtina Km. 12,400 00131 ROMA ITALY
Telephone 06/43601
Telex 613649 SEL ROM

SUMMARY

The contribution of simulation techniques adopted in the design and development phases of the low altitude surface to air missile system SPADA is here described.

This contribution was given in two distinct areas: one as a tool to validate system concepts, the other in conjunction with field tests to complete operational evaluation.

1. INTRODUCTION

A most demanding requirement which is common to most airforces worldwide is the defence of high value targets (typically airports), within friendly territory, from low level, high speed air raids.

The location of such defended targets is known to the enemy, and therefore attacks are pre-planned to take advantage of terrain contours and of electronic countermeasures (screening and deception) so as to avoid or to delay detection by the defence systems and therefore narrow in to the target, reaching useful weapon release distances.

The Italian Air Force decided to develop a missile system specifically designed for airport defence, which should take particular regard for the identification and integrity of friendly A/C. The resulting system, named SPADA, should be redeployed rapidly by virtue of its modularization to enhance system survivability to attacks and to adapt to the change of objective to be defended.

2. PRELIMINARY DESIGN ACTIVITIES

By government decision, the three Italian Services were invited to adopt a single missile which could be employed in the A/A, S/A, shipborne and groundbased roles. Following this line of action, Selenia has developed the Aspide missile to satisfy this multirole requirement.

Further, Selenia was tasked to develop a system in the groundbased role, which could exploit fully the characteristics of the missile for the defence of airports and vital areas against low altitude attacks.

The preliminary analysis of this requirement implied the verification that suitable horizons for system deployment could be found in the vicinity of the areas to be defended.

In fact the useful range of the ASPIDE and the requirement for safe friendly A/C identification required extended visibility of low flying A/C, which seemed at first to be an almost impossible task.

This verification was a complex activity due to the large variety of terrain profiles which characterize the Italian territory. To expedite the exercise, a software facility named SITING was developed.

3. THE SITING PROGRAMME

As a first step, the terrain of interest was digitized in steps of 250 m on the basis of 25000 scale maps providing height lines every 5 meters. The maximum height per element was derived, and fed into an EDP system.

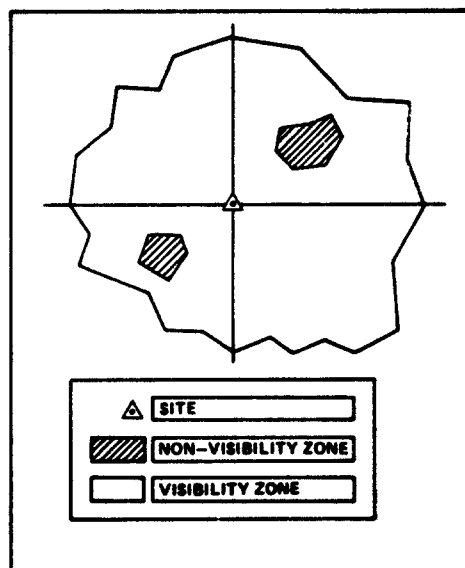


FIG. 5-1

The programme provides a terrain mask related to each site selected (See fig. 5-1). Here an example of digitized horizon is shown. The shaded areas are those where a flying A/C is masked, the white areas are those where the A/C is visible. The A/C is assumed to be flying in a theoretical terrain following mode at a preselected altitude. Amongst all the available horizons thus made available, those suitable for system siting were selected, and it was verified that for all areas of interest system siting did not offer any significant problem, solving all initial doubts. System design could therefore be initiated.

4. SYSTEM SIMULATION PROGRAM

As a design aid and as a verification of system concepts SELENIA relied upon a system simulation program based upon the theoretical siting of system units to defend real targets against simulated attacks. The obvious advantage which derives from the adoption of a simulation effort is that a large number of interactive parameters may be taken into account, and varied, to ascertain system acceptable behaviour under a complex and comprehensive set of conditions. Such effort is also highly cost effective.

4.1. SIMULATION ORGANIZATION

The block diagram in fig. 5-2 shows the main constituents of the simulation.

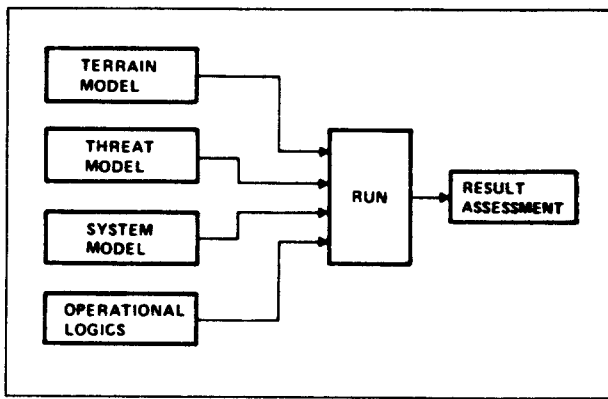


FIG. 5-2

Here the terrain model provides the search and tracking radar visibility areas as a function of flight altitude together with the coordinates of system units location.

The threat model provides the attack formation, A/C kinetics and ECM environment.

The attack formation may consist of any number of A/C flying in any configuration (wing, strimline, Vickers, etc.) and may be broken at any point in time. An A/C breaking away from a formation may continue its flight autonomously. Each A/C may change its altitude, heading and speed independently of the other aircraft.

4.2. SIMULATION TOOLS

Discrete and continuous events must be simulated. The former are sudden instantaneous changes which take place within the system or threat scenario (i.e. the destruction of an attacking A/C); the latter are events which last a certain time (i.e. the flight of the missile). Either events may be deterministic or probabilistic.

An ECM environment can be simulated, where techniques such as standoff, escort and self screening jamming may be adopted against the search radar, the tracking radars and against the missiles. Each A/C may be flying in self screening mode and resulting mutual screening is taken into consideration by the system.

The program takes into account also the jam strobe generation of the search radar, track on jam of the tracking radars and the home on jam of the missile.

The system model provides the system components performance parameters. These are contained in subroutines and may be modified by the operator.

The operational logics define the operational modes and characteristics of the system, these too may be varied by the operator.

The interaction of the operational logics with the models defined above produces the simulation of the events which characterize an attack on the defended target.

Such events have a probabilistic nature, therefore the selection of effective valuation criteria must be based upon statistics which are relevant to system assessment.

The attrition rate and the survival probability of the defended target are taken as merit figures in this validation process.

4.2.1. *Critical Events Method [1]*

The critical Events method has been adopted to process discrete events. The status of the system and that of the threat are taken into examination only when these Critical events take place.

Some Critical events take place at known times because known a priori. These are:

- the A/C entering the operational scenario
- the A/C manoeuvring
- the A/C exiting the scenario.

Other critical events happen at unknown times because they are triggered by other critical events.

These are:

- A/C detection by the search radars
- A/C designation
- A/C acquisition by a Firing Section (F.S.)
- A/C entering the firing area of a F.S.
- missile launch
- result of the launch (intercept or miss)
- F.S. disengagement.

The delay between the generating event and that which ensues may be calculated making use of deterministic or probability functions.

In other cases, such delay cannot be calculated because the event is itself probabilistic. A typical case is given by the detection of a target.

In this case, the delay may be evaluated by means of the "pseudo time stepping" technique. This technique consists in the performance of a test at programmable time instants to verify whether the critical event expected takes place and when. The test sequence stops only when the expected event has taken place.

4.2.2. *Time Stepping Method*

This method has been supplied for the simulation of continuous events (i.e. the flight of a missile). Such events are usually represented by differential equations which can be integrated through the usual stepped techniques (Runge Kutta). During the adoption of the time stepping method, the critical event time is stopped. The continuous event is followed through (i.e. missile flight to intercept) to completion. At this time, such event becomes a critical one. This time is memorized as a delay and simulation is restarted from the instant at which the continuous event began.

4.2.3. *The Monte Carlo Method*

This method has been applied to random events such as:

- a. Discrete events having a given probability to occur are dealt with by using a sequence of pseudo random numbers having a flat

distribution between 0 and 1. It is decided that the event has taken place if the pseudo number extracted is less or equal to the probability of the random event happening (i.e. the target kill).

- b. Discrete events which we are sure will take place following a random delay which starts from the generating event. This delay can be evaluated by selecting a pseudo random number out of sequence having an appropriate distribution law and taking such number as an estimate of the delay required (i.e. operator reaction time).
- c. Continuous events governed by random laws having a known distribution. Such events are simulated, with the appropriate distribution, at time intervals which are related to the correlation time of the random variables (i.e. target scintillation).

5. SIMULATION STAGES

The language adopted was Fortran V and the operational system was the UNIVAC EXEC-8. The programme consisted of 5500 statements contained in one Main, 37 subroutine and two additional procedures run on PDP processor. For convenience, the program was divided into stages.

The first simulation stage consists of data reading. The second consists of the running of the program and results recording.

The third stage is the processing of the data recorded to derive statistical data of interest.

5.1. STAGE 1 STRUCTURE

During this stage, data relevant to the following models is read:

- Terrain
- threat
- system

No data is assigned within the program.

The parameters which characterize each of these models can be modified by the operator to verify the impact on overall system performance.

5.2. STAGE 2 STRUCTURE

Here the program is run. The block diagram in figure 5-3 provides an outline of the flow of activities involved.

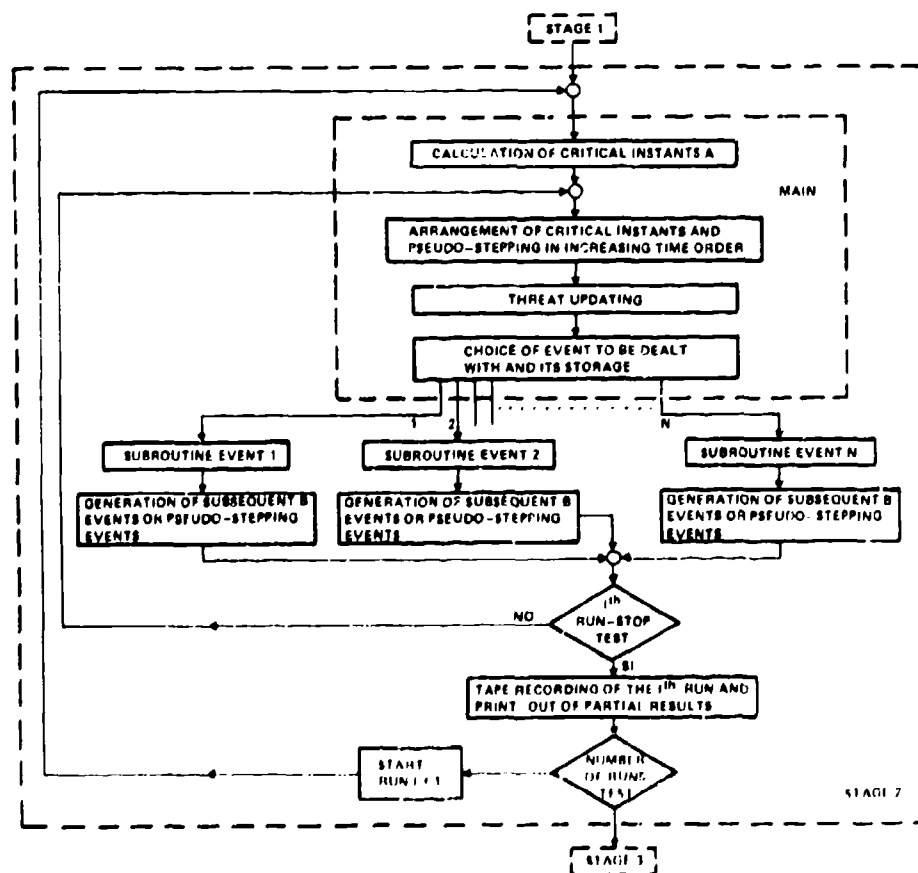


FIG. 5-3

5.3. STAGE 3 STRUCTURE

The data processed and recorded during stage 2 is here further processed and printed.

The main data consists of:

- attrition rate
- number of missiles fired by each F.S. and their total number
- mean, distribution function and cumulative probability of the following parameters:
 - . Detection Center reaction times
 - . F.S. reaction times
 - . intercept distances from the F.S.

6. UTILIZATION OF THE SIMULATION PROGRAM

6.1. PURPOSE

The simulation program served two main purposes. One was to validate the basic system design concepts, the other was to optimize some of the system components parameters, mainly those of the radars, and to choose the best suited system operational logics.

Validation of design concepts was carried out by taking into examination a large area of the Italian territory, containing airports, a naval base, a number of ports and other vital areas.

Through use of the program SITING, the best suited emplacement positions for system sensors were identified. Results were further checked on the field.

A number of suitable deployment configurations for the defence of the targets which matched the expected threat were found.

The threat model simulated attack raids which could be divided into two main groups:

- realistic Italian A.F. prepared raids
- raids prepared by the defence planners which exploited the weakest point of the defence without taking regard to the physical flight limitations of attack A/C.

6.2. RESULTS

The results of the simulation program were such as to convince the Italian A.F. that the adoption of the ASPIDE Missile in the groundbase configuration could result in an effective Air defence system and also convince the designers that the system could be implemented and that it satisfied the requirements.

A number of computer runs were further carried out to optimize some system parameters such as data rate, range and detection probabilities and the logics governing the threat evaluation and target designation.

At this stage system specs were frozen and approved by the A.F. and funding was made available by the government to commence development activities of the SPADA System.

7. SPADA SYSTEM OUTLINE

7.1. SYSTEM CONFIGURATION

The SPADA, in its basic configuration, consists of a Detection Centre (D.C.) and of up to four Firing Sections (F.S.).

The D.C. consists of an agile, phase coded, coherent chain search radar with integrated IFF and of a Command and Control Centre manned by three operators.

The tasks of the D.C. are those of automatic:

- target detection and track while scan
- target identification
- threat evaluation
- F.S. designation
- tactical management of F.S. reaction

The F.S. consists of a monopulse agile tracking radar combined with a CW illuminator, a Command and Control Centre manned by one operator and up to a maximum of three missile launchers, each containing up to six missiles.

The weapon adopted is the ASPIDE CW semiactive homing missile carrying a 30 kg fragmentation type warhead, having an effective range well in excess of 10 kms and maintaining, throughout its flight, manoeuvrability sufficient to take on rapidly manoeuvring attacking A/C.

Task of the F.S. is to engage the designated target.

It is also worth mentioning that the SPADA D.C. can be integrated in the NADGE network.

7.2. FEATURES UNIQUE TO SPADA

The specific characteristics of the SPADA missile system, which make it unique among SHORAD systems, may be summarised as follows:

- a. possibility to deploy system units so that defence extends from small areas such as an airport to vast areas, up to 900 Sq kms, such as towns and industrial plants.
- b. possibility to exploit terrain contour to maximise radar horizons by siting system units up to relative distances of the order of a few kms.
- c. system modularity to cope with defence requirements which may differ because of threat density, target value and terrain contour.
- d. choice of a search radar having a useful range, also in high density ECM environment, which is well in excess of the needs of the weapon employed. This provides a desirable lead time for unambiguous friendly A/C identification even in those cases where damage upon mission reentry has occurred. Because of the extended range of such radar, a large flexibility of system component siting is made possible.
- e. automatic track initiation and TWS, down to very low altitudes and automatic identification process which takes into account IFF reply and rules of behaviour of incoming A/C.
- f. automatic performance of all basic functions and transmission of all operational data (instructions, commands and reports) via digital link to minimize reaction times.
- g. choice of a missile having an effective range in excess of 10 kms to assure flexibility in F.S. siting, consistent with points a, b and c above.

8. POST DEVELOPMENT SYSTEM SIMULATION

Once the system components hardware and SW development had been completed in accordance with the specifications defined during the design phase, Selenia was faced with the problems of system test and evaluation.

To optimize the management of related test and evaluation activities, it was decided to make recourse to a comprehensive simulation facility.

Such decision came from a company policy aimed at the use of simulators for the whole military product line of systems in the field of Air Defence using interceptors or missiles.

Through the introduction of simulators as specific tools for operational SW development and maintenance, the even more valuable tasks of system evaluation, optimization and ease of operational spec modification were achieved.

9. SIMULATOR CONFIGURATION

9.1. GENERAL

The System Simulator, abbreviated for convenience to SIM, carries out on line and in real time the simulation of the environment within which the SPADA may be called to operate.

The SIM is made up of dedicated hardware and environment simulation software.

Upon request, any of the sensors simulated may be replaced by a real component without the need for any modification.

The dedicated HW consists of a radar simulator (sync + video) and a processing unit.

The rest of the SIM HW consists of the real units such as computers, consoles etc which make up the real Command and Control Part.

The dedicated SW consists of as many modules as the number of units to be connected to the post to be simulated and of the operational scenario.

The operational SW is the real operational software running on the fielded system.

The SIM is divided into two main constituents:

a D.C. SIM and a F.S. SIM.

Each one of these may operate alone or, when interconnected, they give way to the SPADA SIM.

9.2. THE DETECTION CENTRE SIM

This facility consists of a System section, which includes a processing unit and equipment units identical to those making up the real detection centre i.e. the NDC-160 processor, the 3 MDU consoles, the magnetic tape unit etc, and of an Environment simulator, which includes a processor, a search and interrogation radar simulator and system input output interfaces.

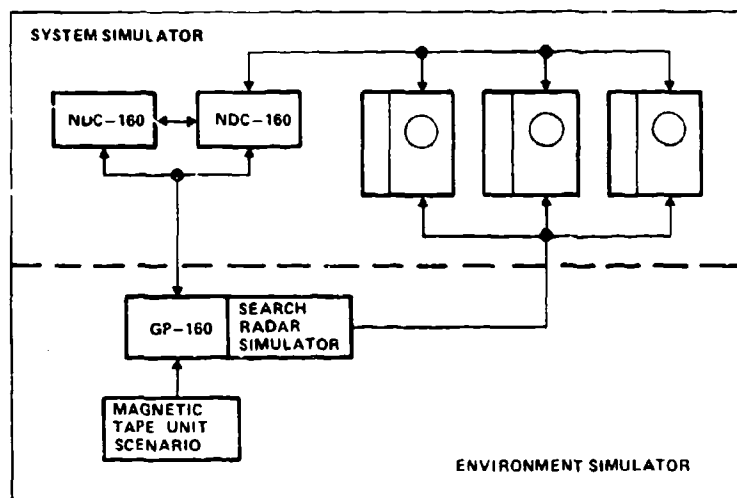


FIG. 5-4 - THE D.C. SIM

System SIM and Environment SIM are interconnected only through those interfaces and links which can be found in the SPADA; i.e. the search radar, the four F.S.s, the NADGE link.

The data rates in the SIM are those which can be found in real life.

The SW is organized in system section SW and environment section SW.

The system section SW is the SW normally operating in real life.

The environment section SW includes six packages: the search radar, the four firing sections, the NADGE link.

The operational scenario SW will be described further ahead.

9.3. THE FIRING SECTION SIM

The F.S. SIM follows a similar organization as the DC SIM.

The F.S. SIM System section consists of one NDC-160, one MDU console and one Magnetic Tape Unit.

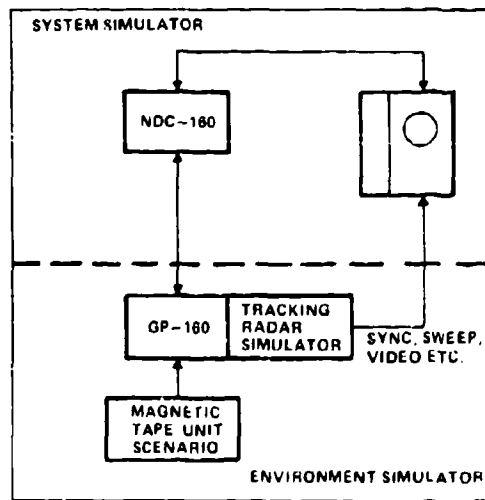


FIG. 5-5 FS SIM

The F.S. SIM environment simulator consists of a processor, a tracking radar simulator and system I/O interfaces.

The interconnection of these sections is through the tracking and illuminator radar, three launchers and the Detection centre.

System SW is the one governing real life operation. The environment section SW includes the tracking/illuminator radars, the launchers and the Detection centre.

9.4. THE OPERATIONAL SCENARIO DEDICATED SW

In order to stimulate the Environment Simulator and activate the system operational SW, a software module has been introduced which simulates the tactical scenario.

The scenario in subject is the one which would be seen by the SPADA system through its radars. It therefore includes target plots, clutter maps, IFF replies and ECM environment in the case of the DC. The same holds true for the FCS, where the external world is seen through the acquisition and tracking radar and includes target plots, clutter and in particular noise and deception jammers.

The tactical scenario module is easily programmed off line due to the adoption of an interactive man machine set of instructions and is contained within the SIM.

A further facility is given by the possibility of live recording of real trials in the field, and of reducing the data provided by the search and tracking radars onto the tactical scenario.

10. UTILIZATION OF THE SIM

During the first half of 1983, the SPADA system, in its full asset, was deployed at the military airport of Pratica di Mare, near Rome, to verify through preplanned flight missions, the performance of the system components and of the system as a whole.

This test phase was meant to identify and perform those adjustments to the systems which were necessary to harmonize the sensors performances operating in a real environment with the overall system performance required.

The flight test program was also meant to complete acceptance by the Italian Air Force of individual system components and their integration.

The SIM proved to be effective in the identification of areas on which to intervene to bring system performance within specification and in finding the most acceptable compromises between sensor desensitizing and false plot generation, limiting the generation of false tracks (clutter tracks) to an acceptable level, as an aim to no more than one every half hour.

The algorithms governing A/C formation split and merge were further adjusted through analysis, on the SIM, of recorded field data based upon specially organized flight tests.

In particular, the SIM was used extensively in the selection of the best suited algorithm governing the dimensioning of the radar plot correlation gate.

In fact only through field testing of the radar was it possible to measure range and azimuth precisions with the accuracy required for the dimensioning of such gates, a critical factor which determines the rate at which false plots (i.e. plots associated with clutter returns) are generated.

Eight different flight tests were carried out during this initial phase, using small radar section A/C, in the main F104s or similar.

Flight scenarios were kept simple and were often repeated to ensure consistent results were given by the system. The orographic situation was also taken into account in optimizing system component siting. The Data and scenario related to system operation was recorded and utilized on the SIM to verify the following:

- detection
- track initiation
- track WS
- designation and acquisition
- track management capability

In the second half of 1983, having completed the initial test phase, the system was moved to the Grosseto Air Base utilizing truck and rapid attachment wheel pairs. The ease of transport of the system along a variety of road surfaces was most appreciated.

Here the tests were aimed at system operational evaluation making use of a high number of missions performed by the attack squadrons flying in from air bases throughout the Italian territory.

The missions relied heavily on ECM support to further test the SPADA ECCM characteristics and were also performed by high numbers of attacking A/C (up to 24), to verify system saturation.

The high costs associated with this essential and extensive flight trial program, were contained by making use of the SIM. Scenarios were in fact recorded and rerun at the factory.

The perfect match between system responses in the real scenario and in the same scenario run on the SIM, convinced the user that the simulator was an effective tool in all the evaluation processes adopted.

Even more demanding scenarios were created on the SIM to explore system extreme performance boundaries exhaustively.

In particular all the problems related to friendly A/C identification were analysed and resolved.

At present the system, fully refurbished, is allocated to the defence of a high value strike airport in northern Italy.

Further systems are undergoing the relevant factory and field acceptance tests.

References:

HOMING HEAD IMPERFECTIONS ALTERING MISSILE GUIDANCE

M. DESMERGER - RESPONSABLE DES ETUDES AUTODIRECTEURS - DEPARTEMENT RCM - DIVISION AVIONIQUE
THOMSON-CSF - 178 Bd GABRIEL PERI - 92240 MALAKOFF - FRANCE

SUMMARY : Our purpose is to analyse the electromagnetic homing head imperfections which mainly alter the missile guidance. We will deal with problems connected with detection of the target (detection time, parasitic signals rejection, and with phenomena introducing errors on target parameters measurement (thermal noise, parasitic signals, nature of the target, radome aberrations ...).

1 - INTRODUCTION

A homing head is to be found in missiles of most surface to air systems to achieve good guidance even if the target is far from the launcher.

Here, we will only deal with electromagnetic homing heads. As the radar cross-section of targets is much less than that of spurious signals (around clutter for example), the homing head uses Doppler effect to get speed selection between target and spurious signal. Such homing heads can be semi-active, or active ones.

Though a homing head is mainly a tracking radar, it has, before tracking, to detect the target. That is the reason why we will deal with those two phases. But we will only deal with the homing head imperfections which may alter the performance of that radar and consequently the missile guidance.

Nevertheless the electronic counter measures are not taken into account here.

2 - DETECTION PHASE

The problem to solve is to detect the right target as quickly as possible.

In fact, specifications of the system impose a probability of acquisition to be reached in a given time.

In presence of thermal noise alone, detection theory shows that a matched filter has to be used.

Thus, if the target location (angular one, range one and velocity one) is perfectly known, just one matched filter is necessary. But it is never the case, and finding of the target is necessary. The best way to satisfy specifications would be to use as many matched filters as is necessary to cover all the possible locations of the target. This will lead to the lowest power to be radiated, but is it always reachable ?

Consider, first, the angular location of the target. As a homing head has only one antenna, it is impossible simultaneously to have several angular cells. That means that a compromise has to be found between the two following possibilities

- using a narrow antenna beam "matched" to the target and moving it until the target has been detected
- using a wide antenna beam so that the target is inside the beam whatever its angular location is.

As regards to the range and speed matched filters, it is theoretically possible to have all those resolution cells simultaneously. But we have to keep in mind that, during the tracking phase, only one cell is needed. Thus, if we consider the homing head cost, it is not obvious that using all those cells will lead to the best solution.

In fact, from the point of view of the homing head design, one of the most important parameters to be taken into account is the accuracy of target location (angular, range and velocity location), this location being sent by the system.

And the angular location accuracy will allow the choice of the homing head frequency to be taking into account :

- the missile diameter imposes the greatest antenna diameter thus the beam width versus frequency
- the atmospheric and transmission lines losses which increase with frequency
- the greatest power reachable at each frequency (for a given cost).

All that has been said before implies there is only thermal noise. In fact there are parasitic signals which may alter target detection. The most important of these are the spill over or transmitter leakage and ground clutter.

2.1. Spill-over

The spill-over signal is the fraction of the transmitted power which reaches the receiver.

It is physically impossible to make the power of spill-over less than that of thermal noise.

As, in most cases, it is not necessary to track targets whose radial velocity is zero, the spill-over signal may be rejected by filtering in the frequency domain. Thus the off-band attenuation of the Doppler filters is determined by the power of the spill-over signal. Often, this off-band attenuation can only be reached using cascaded filters.

Nevertheless Doppler filters can completely reject the spill-over signal only if this signal is monochromatic (or if the transmitter is noiseless). As this is not true, the spill-over power determines the amount of noise of the transmitter, that is to say the noise level which does not alter the homing head sensitivity.

2.2. Ground clutter

Ground clutter has very often a power higher than that of thermal noise and even that of the target echo. This means that, to detect the target, it is judicious to separate the target from the clutter using the difference of velocity between the two. This mean that, it is better to have no ambiguity in the velocity domain. To have no such ambiguity, this leads to choosing a high pulse repetition frequency if an active homing head is used. Therefore range measurement will be ambiguous and eclipsing losses are introduced. These phenomena are to be taken into account while determining homing head characteristics.

Even if target and ground clutter may be separated using velocity difference, that is to say using Doppler filtering, the same problem as for spill-over occurs : ground clutter carries the noise of the transmitter. In that case, the problem is more difficult due to decorrelation between the noise transmitted and received.

It means that some sensitivity problem may occur when the Doppler frequency of the target is near that of the ground clutter.

When Doppler frequency of the target lies in the Doppler range of ground clutter, the homing head sensitivity is imposed by ground clutter power and not by thermal noise. This is due to the fact that a ground clutter signal looks like a noise. Even if this noise is not absolutely white, no signal processing is able to completely eliminate ground clutter. Therefore the homing head sensitivity is not that given by thermal noise.

3 - TRACKING PHASE

The tracking phase is the most important one for the homing head. So we will try to point out all the phenomena which may alter the miss-distance between missile and target. We will deal with :

- thermal noise
- angular glint
- noises introduced by signal processing
- radome aberrations
- effect of parasitic signals.

But we will not deal with Electronic Counter Measure effects.

3.1. Thermal noise

Thermal noise affects all measurements made by the homing head, that is to say velocity measurement, range one and angular one. Of course angular measurement is the most important since guidance is mostly done using angular information. But, in the homing head, angular measurement cannot be made if the target's speed and range have not been selected.

According to Woodward formula, thermal noise induces a noise whose standard deviation is $\frac{\Delta x}{\sqrt{2R}}$

Where Δx is the measurement cell width and R the signal to noise ratio.

Therefore, in order to reduce noise measurement, cell width has to be reduced and signal to noise ratio increased.

Cell width cannot be made as narrow as wished. It is obvious that if during measurement time the target moves more than cell width this will lead to a signal loss. That is mainly true for range and velocity cells because they are the smallest. The same problem would occur if the target is sliced by the cells.

As for signal to noise ratio, we have said that a matched filter is always used. But the signal to noise ratio to be used in Woodward formula is that obtained after post-integration, that is to say the signal to noise ratio measured at the output of tracking loops. This leads to using tracking loops as narrow as possible.

The limits of that narrowing are :

- the angular tracking loop cannot have a time constant greater than the time constant requested for the whole missile
- the doppler tracking loop cannot have a time constant greater than the angular tracking loop time constant
- doppler and range tracking loops have to be consistent with target manoeuvres.

In fact tracking loops are often adaptative one in order to take into account power fluctuations of the target signal. Nevertheless, and in spite of the influence of thermal noise decreasing as missile to target range decreases, thermal noise introduces a noise on the miss-distance.

3.2. Angular glint

A target seen by a radar is neither made with only one reflector nor with an infinity. For a given angle aspect, only few reflectors have to be taken into account.

As a target fluctuates around its trajectory, the phase of each signal reflected by each reflector varies (the amplitude varies also but more slowly). Thus the signal received by the homing head is a fluctuating one. Some power distributions have been assumed by Swerling. This is true for all signals delivered by the homing head antenna.

Therefore the angular measurement is not a steady one. The point aimed at by the homing head fluctuates and can even be outside of the target span.

Such a fluctuation introduces noise on miss-distance.

It would be interesting to reduce the noise induced by angular glint.

Filtering that noise is not always compatible with the time constant requested for the whole missile. So that other signal processing have to be evaluated :

- by isolating each reflector of the target
- by finding angular signal processing which is less sensitive to angular glint than the usual one.

Notice that, when using antiglint, one has to be sure that the homing head is actually tracking only one target, otherwise the missile would fly exactly between the two targets !

3.3. Noise introduced by signal processing

We have said that thermal noise introduces noise which decreases as signal to noise ratio increases. This would lead to no noise when the missile is near the target (see the propagation formula). In fact, this is not true because the noise of the last IF amplifier is not attenuated when the signal increases and/or quantization noise have/has to be taken into account.

A good design of the homing head has to make that noise smaller than that induced by angular glint.

An other source of noise that induces miss-distance is the antenna pointing loop.

For simplification, antenna pointing may be split into a tracking loop and a stabilization loop.

The tracking loop has to point the antenna to the target using information given by the receiver. Thus its performance are imposed by angular measurement quality. The stabilization loop has to make antenna pointing independant of missile movements. Such a loop is necessary because guidance is made using angular information measured in absolute coordinates. This loop has a greater bandwidth than the tracking loop one.

All imperfections of these loops will induce miss-distance. Among these imperfections we can quote

- backlashes in antenna drive
- resonant frequency of antenna drive mechanism
- threshold of motor
- noises introduced by angular and/or angular rate pickoff
- imperfections in signal processing (for example quantization error and trigonometric approximations when it is digitally made).

3.4. Radome aberration

The shape of the radome is imposed by aerodynamic considerations. The choice of its material is determined by thermal and strength constraints resulting from aerodynamic stresses.

Unfortunately that does not lead to an electrically good radome. Radome introduces losses and an insertion phase. If the insertion phase was independant of the point considered on the radome, no modification on antenna beam would occur. This is not true, and the major effect is an angular deviation of the beam which is called radome aberration.

If radome aberration was the same whatever the antenna position was, no problem would occur during guidance. As radome aberration varies, de-stabilization of the missile may occur in some flight conditions if aberration slope is too high.

In order to make the aberration slope as low as possible, the thickness of the radome is not the same at every point and could be computed by specialized programs.

When the radome is manufactured some imperfections alter this theoretical result. First, thickness can only be obtained with a given tolerance (tolerance has to be compared with wavelength).

Secondly, the material used may not be homogenous and a dielectric constant change will occur inducing variations of electrical performance.

Thirdly, temperature causes dielectric constant variation. Here the problem is difficult to appreciate because, during flight, temperature is not constant throughout the thickness of the radome and is not constant along the radome (it depends also on the missile incidence).

So, the radome has to be made carefully, then it is measured at ambient temperature in order to be rectified or to be compensated. Compensation means taking into account the measured aberrations in the angular tracking loop.

But, even if this correction is perfect, it is not proven that this correction will be valid during all possible flights (low altitude ones, and high altitude ones).

The problem for the radome designer is thus to specify the aberration slope he can get within a given cost. At present, an aberration slope lying near 2 % seems to be reasonable.

The radome also has other imperfections but they do not react directly upon guidance. Side-lobes level of the antenna increase in presence of the radome. This is mainly due to reflections upon radome wall and diffraction by the radome tip. There is also creation of a side-lobe corresponding to reflection of the antenna main beam upon radome wall, and thus the angular position of that lobe depends on antenna angular position inside the radome.

3.5. Effect of parasitic signals

Parasitic signals can be defined as signals in presence of which a bias may occur in tracking loops. Thermal noise is, with that definition not a parasitic signal.

The most known parasitic signal is two targets instead of one ! If the homing head cannot discriminate and track only one of them, the missile will fly between the two targets.

In order to minimize that occurrence, the smallest gates are to be used. If it is possible for velocity and range one, the smallest angular gate is defined by antenna diameter and thus cannot be reduced as wished.

An other parasitic signal is ground clutter. If clutter was white noise, no bias would occur. For diffused clutter that is true. But for an isolated building, for example, it is not true and some precautions have to be taken to avoid tracking loops being captured.

4 - CONCLUSION

We have tried to point out most of the imperfections which can alter homing head working during the detection and tracking phases. A lot of them are inherent in radar theory (like noise, clutter), the others inherent in defects.

The result is that the homing head designer has to make compromises in order to obtain the "best" homing head. Fortunately progress in technology and specially in digital processing leads to building a more and more powerful homing head.

WARHEADS FOR SAM SYSTEMS

M. HELD
 Head of Research and Future Programmes
 for Warheads and Fuzes
 Messerschmitt-Bölkow-Blohm GmbH
 Hagenauer Forst
 8898 Schrottenhausen
 Germany

ABSTRACT:

The hits are differentiated between direct hits and near pass. In the case of near pass the fragmenting warheads transfer the HE-energy to the target much more effectively than blast warheads. With high hit densities special synergistic or cumulative effects can be achieved. This will be discussed in details. Special high fragment beam densities can be obtained by aimable warheads. The effectiveness of warheads will be described with the use of lethality models.

INTRODUCTION

The range of today's air targets is very multiform, both with regard to their size and to their speed. Apart from the large, but slow transport aircraft, air targets are considered mainly to be fighter bombers which constitute a direct threat to defence. Moreover, also the reconnaissance aircraft which usually fly at very high altitudes should be taken into consideration.

Also missiles pertain to the class of air targets, e.g. naval target missiles that attack close above the waterline and which are known as Sea Skimmers, or missiles that attack on the dive. Both have an especially small-area silhouette.

Furthermore, tactical and strategic missiles must be considered, too. These are particularly difficult to fight because they are relatively small and, on the other hand, they have a rather tough overall structure presenting only very few vulnerable components during the terminal flight phase.

In response to the great variety of air targets, the range of possible warheads is very wide, too (Annex 1: "Air Target Warheads"). It is not possible to describe all fundamental details within the scope of this paper, but an attempt is made to highlight the operating principles and to indicate a few trends of development which in the author's opinion are of particular interest.

With regard to the warhead it does not really matter whether the launch platform is surface-based (Surface-to-Air-Missiles - SAM) or whether it is airborne (Air-to-Air Missiles - AAM or AIM) (Fig. 2 - 9461). For the warhead, all targets are air targets, whereas the missile has to take the respective launch platform into consideration with regard to its seeker, guidance, controls, motor, look angle, direction of attack and range. Perhaps different engagement situations may occur, depending on the type of mission, and this must be taken into consideration for the design of a warhead (Fig. 3 - 9467).

DIRECT HITS

In the engagement of a missile with a target there are two basically different possibilities (Fig. 4 - 9465):

- direct hits
- near misses.

Small-caliber projectiles do normally not have a proximity fuze and therefore need a direct hit on the target in order to succeed. The high repetition rate of guns can well offer the opportunity of direct hits in a salvo, if the air target comes within the range of the weapon system.

With missiles, which usually are designed for longer ranges, direct hits are rather rare. The author knows of only one weapon system, namely BAE's Rapier in the UK, which has no proximity fuze but a semi-armor-piercing warhead for penetration into the air target (Fig. 5). The warhead alone, which has an overall weight of ... kg and a charge weight of ... kg, is certainly sufficient to incapacitate an air target.

A comparison of the kill probabilities for projectiles of from 20 to 56 mm caliber, based on a considerable number of literature references (Fig. 6 - 9433), shows that in the case of a direct hit the Rapier warhead should have a practically 100 % kill probability against fighter-bomber class air targets. It should be emphasized that neither the air target nor the direction of approach, nor the specific design of the projectile are exactly given in Fig. 6 - 9433, which explains the wide range of kill probabilities versus the caliber.

Mention should also be made of the fact that the structural weight of mediumrange systems (i.e., no shoulder weapons) is already so high that a direct hit on an air target with a relative velocity of from 300 to 1000 m/s will result in heavy damage on the target. Fig. 7 - 9445 gives an indication of the structural weights of a few SAM's, and of the possible range of relative velocities - or impact velocities - and the corresponding energies, as expressed in the equivalent kilogram weight of TNT.

When the warhead of a missile detonates before impact on the target, the missile structure near the warhead will be heavily damaged. However, the main mass of the missile, which consists of the motor, stabilization, etc., keeps flying in the same direction, at least over short distances of a few meters, and may therefore hit the target to produce considerable damage. Keeping this in mind, the usual severe requirement for the proximity fuze not to respond prematurely in the case of a direct hit may not appear so very important. The larger the missile, the less significant is this requirement.

EFFECT AT MISS DISTANCE

In general, the possibilities of guided control at long range, or the seeker accuracy - in particular in the case of counter-measures of the target to be attacked -, or, the control accuracy of the missile against highly maneuverable targets are not sufficient for direct hits to occur at high probability. Usually, the missile passes by the target at a rather close distance of only a few meters. A few meters mean almost a direct hit, when a typical target - a fighter bomber - about 20 to 30 m long and 5 to 10 m wide is being considered.

In such a near miss, or near pass, "energy" must be released at the right moment in order to fight the target efficiently (Fig. 8 - 9379). In general, this energy is stored in the warhead.

SOURCE OF ENERGY

Quite generally, the source of energy is the chemical energy stored in the high explosive charge. The particular performance of high explosive charges is not its extraordinarily high energy content, which is of the order of 5000 kJ/kg and, therefore, is only about one tenth of that of petrol or coal which use the oxygen of the air for combustion, whereas explosives and propellants have the oxygen necessary for the reaction (burning) stored in a molecular form. The specific feature of high explosives is their extremely high reaction rate, viz. their detonation velocity. This means that their "power" and gas production per unit time is greater by a factor of about 10^5 than any other chemical reaction (Fig. 9 - 9377).

The reason for this is that the reaction is set off and is maintained by a shock wave, namely, the detonation wave, which in high-energy military explosives propagates at 8000 to 9000 m/s instead of at only a few tens of meters per second, as in the case of the combustion of rocket propellants (Fig. 10 - 9376).

According to the German DIN 20 163 standard, explosives are generally classified as high explosives, propellants, primary explosives, and pyrotechnic mixtures (Fig. 11 - 9378). High explosives, in turn, are divided into military high explosives, which are designed for high energy content, environmental stability, low sensitivity and long in-service life, and commercial explosives, which above all have to be inexpensive. Commercial high explosives are again sub-classed as either blasting explosives or as permissibles (permissible high explosives; safety explosives for use in underground mining). The latter produce no toxic reaction products with NO and CO, and they are also not able to ignite firedamp.

The energy content of military high explosives for blast and fragment acceleration is today largely extracted to the ultimate. In the near future there will be no high explosives that have a higher energy content than RDX and HMX, which at present are the most widely used high explosives.

On the other hand, research and development for insensitive high explosives has made considerable progress. Today there are high explosives available which in practice resist to much higher temperatures, namely, to 200 to 300 °C, than do RDX (about 140 °C) or HMX (160/170 °C).

In particular, the hitherto preferably used "binding agent" TNT, which melts at about 80 °C, is being replaced by plastic binders. Such explosives are now mainly used in filling the warheads of air-to-air missiles which are liable to attain enhanced temperatures by aerodynamic heating. Moreover, insensitive explosive mixtures are being developed to be resistant to bullet attack and fuel fire hazards (Fig. 12 - 9436).

BLAST EFFECT

All warheads for stand-off effect are filled with a high explosive charge. On detonation of the latter, the latent chemical energy is released producing - in the case of military high explosives - about 1000 liters of high-pressure high-temperature gas (3000 °K - 5000 °K) per kilogram of explosive. Pressures are in the order of several 10 GPa. The gas attempts to expand, thus compressing the surrounding air which it pushes away. This results in what is known as a blast wave (Fig. 13 - 9381).

In general, the blast effect is considered to be easy to calculate. However, going into greater detail one will discover the complexity of the interaction between a blast wave that is characterized by peak overpressure p_{max} , positive phase duration t , and positive phase impulse I , and the target structure that may consist of many components having different strengths and natural frequencies of vibration (see the attached papers "Blast Waves in Free Air" (Annex 2) and "TNT-Equivalent" (Annex 3)).

For a rough estimate, a square-root law can be assumed for the charge weight in the D-versus-W plane (Fig. 14 - 9383):

$$D = K \cdot W,$$

where the value of K is in the range of 0,3 to 0,5 m/ kg, depending on the type of target. For smaller charges, however, the distances D from the air target must not be measured from a center of mass, but they must be taken from a line or surface of reference (Fig. 15 - 9384).

FRAGMENT WARHEADS / FRAGMENT EFFECTS

The high-pressure gases from a detonating high explosive charge are capable of accelerating the casing in which they are enclosed, and to impart it a high velocity that depends on the charge-to-casing mass ratio. A smooth casing will be broken up into so-called "natural fragments", that is into both small and large fragments. For a most efficient attack to a target, however, a favorable size of fragment is sought, which can be obtained by controlled fragmentation or by using preformed fragments. Fast and heavy fragments, though few in number, can be produced from multi-projectile warheads. Especially fast fragments can be obtained from the so-called multi-shaped-charge warheads with peak velocities of up to 4 - 5 km/s. A continuous, expanding rod can be obtained by a cleverly engineered arrangement of rods that surround the charge and which are welded together at their ends. Particularly high hit densities can be reached with "aimable warheads" (Fig. 16 - 9413).

While a blast wave so-to-say continuously covers the entire space, thus having a quite limited range of action, a detonating high explosive charge is able to bring a fragment casing to a high velocity so that the fragments transmit concentrated energy over long distances; however, this is done only along the discrete trajectories of the fragments between the warhead and the target (Fig. 17 - 9468).

The fragments are accelerated for one by the shock wave that is induced in the casing and which entails a material velocity of the casing, and, secondly, they suffer an after-acceleration by shock reverberations and by the expanding reaction gases of the detonation (Fig. 18 - 9382). Depending on the charge-to-casing mass ratio, velocities are from about 1000 to 2500 m/s. To a first approximation, which is actually valid only for an infinitely long cylinder, the fragment velocity can be calculated from the ratio of mass of the casing, m , to mass of the high explosive charge, c (usually termed "metal-to-charge ratio, m/c), by means of the Gurney formula:

$$v_0 = 2E (m/c + 0,5)^{-1/2}$$

where $2E$ is known as the Gurney energy constant, which is an experimental constant having a value of between 2.0 and 2.8 km/s, depending on the type of high explosive charge and on the design of the casing.

FRAGMENT KILL MECHANISMS

The call for an "optimum fragment" will imply the type of target components and on the kill mechanisms that are effective. If, however, optimization of the fragments is considered with vulnerability models, then it is rather the "kill criterion" that has been used than the kill mechanism that is of importance (Fig. 17 - 9462).

The following kill mechanisms can appear (Fig. 20 - 9415):

- penetration or perforation performance, P , which certainly is the fundamental quantity
- depth of penetration, combined with the diameter of the hole, $Px\phi$; this indirectly implies the hit probability against a large number of components, such as wire bundles, rods, hydraulic lines, etc.
- volume V as determined from depth of penetration times cross sectional area of the hole, $Px\phi$

- momentum, which is particularly significant for the plastic deformation of components
- energy, with energy meaning practically the same as volume, because the depth of penetration and the volume directly correlate with one another (Fig. 21 - 9447)
- structural kill, which is derived experimentally from the geometric mean of energy and energy density, which also involves specific cumulative or synergistic effects
- power P , which is given by energy per unit time.

All the quantities given above are usually valid not only for a single fragment but also for the sum of many fragments that hit a target. They must therefore be considered in context with the hit density, i. e., with the number of hits per unit area.

The dimension of the structural kill criterion is that of a force, which can be expressed in Newtons. The number of hits required to fulfill this criterion must be ≥ 50 . Practical values for the structural kill criterion are values of 1 MN and above (Fig. 22 - 9416).

The power or power density criterion has been little used up to now because the cumulative and synergistic effects have not yet been investigated experimentally to satisfaction (Fig. 23 - 9464).

Considering the critical components of a typical air target and the kill mechanisms that can destroy these, one will find that the entire range shown above plus the fragment velocity, which may be responsible for the reaction and/or for the initiation of propellants and high explosives, are involved (Fig. 24 - 9418).

CUMULATIVE AND/OR SYNERGISTIC EFFECTS

The question is: how can a higher kill probability against an air target be achieved (Fig. 25 - 9463)? Quite generally, this is possible by more energy, which in particular means higher fragment velocity, since this contributes to energy by its square, and by more mass, which appears in the energy term only linearly. However, more velocity and more mass for the fragments usually means heavier and bigger warheads.

The above example has shown that specific effects, such as structural kill and power density, go along with higher hit density, i. e. with narrower fragment beams.

It has also been mentioned that the efficiency can be increased by what is known as synergistic effects. Synergistic means that an effect A and B is not equal to the sum of A plus B, but is greater than A plus B.

We shall now briefly explain the mechanisms of action of the cumulative effects. If the individual impacts of fragments in a target are spaced widely in time, i. e. $t < t_{cr}$, they will cause no specific weakening of the target. If, however, the fragments impact at high area density and in rapid succession, i. e. when $t < t_c$, then cumulative effects will occur. In general, cumulative effects can be classed as mechanical, hydraulic, and vapourific effects (Fig. 26 - 6996 a).

Mechanical cumulative effects are due to the superimposition of the individual fragment impacts in the target, when the fragments are not independent penetrators, but when there are interconnected impacts by a concentrated fragment beam; this means, the fragments at high number density per unit area and within a very short interval of time (Fig. 27 - 9419).

The upper part of Fig. 28 - 3761 shows an x-ray flash radiograph of a fragment beam, the lower part shows the effect in a spaced target consisting of 4 mm thick DURAL plates spaced at 100 mm.

When a fragment hits a target plate and perforates it, both target and fragment material will partially vaporize. This vaporized metal is very susceptible to reaction with the oxygen of the surrounding air. The sequence of frames of a 7-mm steel sphere perforating a 2-mm DURAL plate at angles of 0°, 30°, and 60°, which were recorded as shadowgraphs from an argon flash bomb background illumination at a speed of 10⁶ frames per second, clearly show the formation of this fine dust cloud, in particular on the side of entrance of the sphere (Fig. 29 - Fig. 31, 3762, 3759, 3760). This vapour cloud of very fine metal with new and non-oxidized surfaces reacts with the oxygen of the air and in this way creates an additional pressure that acts on the target plate from outside. The smoke marks that can often be found on the impact side of the target plates are due to this phenomenon.

But also on the rear side there is fine target and fragment material which has a very high reactivity with the oxygen of the surrounding air. The pictures in Fig. 32 - 4117 show how the fragments increasingly shatter on impact with increasing velocity of impact; in this case it was a steel and a cadmium sphere with velocities ranging from 700 to 1600 m/s and fired against a 2 mm DURAL plate. Fig. 33 - 4127 shows the almost complete shattering of a 9 mm diameter steel sphere fired at velocities as a function of the impact velocities ranging from 300 m/s up to about 3000 m/s (Fig. 34 - R. Recht).

The reaction of the vapour cloud with the oxygen of the air occurring on impact in front of the target plate creates a very short external overpressure that acts on the target plate and which in the case of high hit densities may well crush a planking.

On the other hand, the reaction in the closed volume behind the target plate will heat the gas by reactions and/or by the hot and small fragment particles, thus creating a quasi-static internal overpressure. This overpressure can be measured and lasts for several milliseconds (Fig. 35 - 9437 and Fig. 36 - 3259).

A hydraulic shock effect is produced when liquid tanks are hit by fragments or projectiles. It seems surprising at first glance that the perforation performance of the fragments decreases again with increasing velocity (Fig. 37 - 7928). For 3.5 gram and/or 7 gram fragments, the highest penetration performance is obtained in the range of about 1200 - 1400 m/s. This is readily understood when the deformation of the fragments at different velocities is examined (Fig. 38 - 7944).

While they are only slightly shortened at 600 m/s, they are slightly eroded and deformed mushroom-like at 1000 m/s, and they are strongly eroded when they are shot into the water at a velocity of 1800 m/s. With increasing velocity, the fragment area is increasingly broadened and the mass is reduced by erosion so that the fragments velocities, in particular the first tanks are more and more damaged by the stronger hydraulic shock caused by the higher energy induced (Fig. 39 - 7942 and Fig. 40 - 7943). A considerably stronger destructive effect caused by addition and cumulation will of course occur when a greater number of fragments hit a hydraulic tank.

The critical time differences necessary for cumulative and synergistic effects can be derived from an analysis of the phenomena (Fig. 41 - 9420). In metals, the shock waves must superimpose and the hit density must be relatively close. Assuming, for simplicity, that the fragments have a distance of not more than 50 mm from one another and that the sound velocity is 5 mm/us, one will find a critical time difference of about 10 us for the hits of fragments. For the superposition of shock waves in a liquid with a typical sound velocity of 1.5 mm/us, a critical time of 100 us will result when the fragments impact at distances of 150 mm from one another.

For the quasistatic overpressure, produced by fragment impacts in a closed chamber, times will be in the range of 1000 us, or 1 ms.

In other words, this means that cumulative vapourific effects by internal pressure enhancement will practically always occur, if only the hit density is sufficient, i. e. when many fragments enter the same area or volume. Superimposed hydraulic shock effects require time intervals that are shorter by a factor of 10, and the mechanical cumulative effect requires a particularly "simultaneous" arrival of fragments.

Apart from hit density and hit rate, also the specific shape of the fragment plays its part in the cumulative effects, in particular in the vapourific effect.

AIMABLE WARHEADS

Warheads can be classed according to their fragment distribution (Fig. 42 - 4626 a). Sometimes, wide elevational fragment spray angles are required or provided in order to hit a larger area of an air target and/or in order to "compensate" for inaccuracies of fusing. However, this means that a large number of fragments will miss the target - depending on the miss-distance and on the size of the target.

Narrow fragment beams, down to parallel fragment trajectories, are required in order to achieve an enhanced cumulative effect. In this way, cumulative and synergistic effects can be obtained at least up to certain distances.

A very narrow beam is obtained with the continuous rod warhead, in which the rods, which are welded together at their ends, unfold as a continuous ring. However, this type of warhead is now less and less used at the higher relative velocities and more complex interceptions, because the expansion velocity of the ring from such a warhead is for various reasons limited, and because the targets have struts and reinforcements at certain places which eliminate a structural kill by such a warhead.

Aimable warheads give higher hit densities, i. e. fragments per unit area, which depend less on distance.

The dependence of the hit density on distance is evident from the following simplified formulas (Fig. 43 - 7932a). For a conical angle of aperture, the hit density n decreases as the square of the distance R ($n \sim 1/R^2$). In the case of parallel fragment trajectories it goes linearly with distance ($n \sim 1/R$), and for an aimable warhead with exactly parallel fragment trajectories it would be completely independent of distance, $n = \text{konstant}$).

Moreover, one should distinguish between directional and aimable warheads (Fig. 44 - 4472). "Directional" warheads always have a specific direction, e. g. the missile axis or transversely to it, that is, a radial direction or even multiple radial directions. In the case of radially "aimable", a radial specific direction of fragment of energy performance is created only immediately before detonation of the warhead, i. e. at target engagement so-to-say.

With today's high engagement velocities and high maneuverability of air targets and missiles, directional warheads cannot be used at present, at least not with the technology existing at present. Ideas to use e. g. elliptic warheads and to aim at the target with the wide side of the warhead by rotating the entire missile have repeatedly been abandoned.

However, several institutions have undertaken to study "aimable warheads". But also with these, "mechanical adjusting" or aiming of the warhead within the missile with the means available today has proven to be too slow in most of the cases. The space and weight required for control units that would permit fast rotations to be made are too much for to pay off.

In contrast to this, "steerable" warheads, i. e. such in which aiming is achieved by control of the detonation wave or "detonation wave aiming", can be put into action in almost no time, i. e. within a span of microseconds. However, the gain in fragment velocity is only 10 to 20 %, and the gain in energy at comparable hit densities is therefore about 20 to 40 %, which is rather moderate.

A "mechanical deformation", e. g. by pyrotechnically opening the warhead to present a large area, will also require too much time to be practicable.

Considerably higher hit densities can be achieved by "deforming the warhead", in particular by "detonative deformation" with which the entire sequence of functions is a matter of milliseconds.

For a better understanding, Fig. 45 - 7838a schematically shows a "steerable", a quadrant opening as a "mechanically deformable" and a "detonatively deformable" warhead.

The increase in efficiency of a warhead can be considered with regard to the increase in energy imparted to the target and, hence, to the increased kill probability (expressed in terms of a higher E/E_0) at constant distance R_0 and constant warhead mass M_0 , or with regard to the increase in distance, R/R_0 , at constant energy E_0 and constant warhead mass M_0 , or with regard to a reduction in mass, M/M_0 , at constant energy E_0 and constant miss-distance R_0 . Fig. 46 - 9438 gives a rough indication of the values for a warhead with detonation wave aiming and for a detonatively deformable warhead as compared to a conventional fragment warhead. The gain in energy of the warhead with detonation wave aiming is about 20 to 40 %, whereas the increase in range is only of the order of 10 to 20 %, or the reduction in weight is in the range of 0,8 to 0,7.

In the case of a detonatively deformable warhead the gain factors are much more favourable: the energy gain is about 2 to 4, which means a correspondingly higher kill probability, the factor of increase in permissible miss-distance or range is about 1.4 to 2, and the warhead mass can be reduced by a factor of 0.6 to 0.4.

The relative costs for a detonatively deformable warhead are higher by a factor of 2, the required more complex safety-and-arming unit by a factor of 10, and the specific sensor giving the required azimuthal resolution is by a factor of 1,5 more costly than a regular sensor of a conventional warhead, respectively (Fig. 47 - 9439). These relative costs can be quantified by multiplication by the fractional costs of the components; the warhead itself is in the range of 3 %, the safety-and-arming unit around 0,1 %, and a regular proximity fuze runs up to about 10 % of the overall costs of a missile. The total fractional costs for a conventional warhead including the SAU and the sensor amount to about 13,1 %.

By multiplying the increased costs for the detonatively deformable warhead by the fractional costs, one will find these to amount to about 1 % for the SAU, about 6,6 % for the warhead, and about 15 % for the sensor, which adds up to 23 %. This means that the fractional costs of these components rises from 13 to 23 % of the missile costs. This does not include the costs for the launcher, for the firing unit, for logistics, etc.

However, the highest gain by a detonatively deformable aimable warhead will have to be traded in for the highest costs and risks of development. At present, certainly not all components have already been developed for producibility; a development period of 5 to 6 years and an evaluation time of another 2 years will have to be taken into consideration. This means that the earliest in-service use of a detonatively deformable warhead could be in eight years' time from now (Fig. 48 - 9440).

On the other hand, the components for a warhead with detonation wave aiming are known. For a specific warhead geometry they would only have to be adapted and tested by an adaptation development, which appears to be feasible within a time of 3 years, including the required environmental proving. Evaluation would require another 2 years, so production could commence in about 5 years.

COMPARISON OF WARHEADS

With the SIDEWINDER warhead as an example, we shall now present the various principles of warheads, as they are used in practice or as they might evolve.

The Mk 9B warhead contains a cast aluminized HBX1 charge and has a smooth steel casing, which on detonation of the charge is broken up into controlled fragments by a sheet of plastic liner with a roof pattern (Fig. 49 - 8363 and Fig. 50 - 8373).

The Mk 9L warhead contains a plastic-bonded high explosive charge with 2 layers of rod fragments. A very narrow fragment cone is produced by double-end ring-initiation (Fig. 51 - 8362).

A detonation wave aiming warhead with an 8-fold simultaneous initiation along a cylinder generating line by means of a detonative logic is sketched in Fig. 52 - 8360. It has been mentioned above that the technological details do in principle exist. They need only to be adapted to the given warhead mass and geometry.

Finally, a detonatively aimable warhead with its deformation charges, an attenuation layer, the main charge, etc. is schematically shown in Fig. 53 - 8361.

Quite generally, the costs of the warhead proper of surface-to-air missiles are of the order of 3 % (Fig. 54 - 9441).

The continually increasing costs, in particular those of seekers and sensors make it possible to introduce also more efficient and, hence, also more expensive warheads; the fractional costs of the warhead and of the safety-and-arming unit would in this case not change at all. This becomes evident from a look at the trend of the costs of new missile systems quite generally (Fig. 55 - 9442).

MODELS OF EFFECTIVENESS

The statements usually made about the effectiveness of warheads are based mainly on model calculations. Quantitative measurements at modern air targets are relatively rare. Trials are usually conducted against older components of aircraft or against entire older aircraft. Owing to the exorbitant costs of such trials, their number is rather limited. The uncertainties of a correct extrapolation become still higher, because modern targets of the potential enemy are not available.

Calculations of the encounter probabilities in azimuthal and polar (elevational) directions, and of the relative speeds to be expected present no problem (Fig. 56 - 9443). More critical are the ways of calculating the fusing times by means of fuze models, because the complex physical phenomena, in particular the ones involved in radar sensors, are only difficult to describe. In general one determines one trajectory and makes the warhead detonate on this line at constant distances in order to calculate subsequently the locations of the hits in the target. With the type of warhead known, the velocity, mass etc. of the fragments hitting the target can be given exactly. On the other hand, also the material thicknesses to be perforated, the fragment residual velocities, the hits, and the depth of penetration in critical components can be calculated exactly if the target is known.

Statements as to whether components that have been hit will really be incapacitated should be regarded critically. As was mentioned above, the component kill criteria are critical per se and, on the other hand, they depend to a considerable extent on the velocity, mass, density and shape of the fragments as well as on the real number of hits, on the hit density, on the pyrophoricity of the fragments, and so on.

Statements as to the behavior of the target when one or several components have been damaged will usually present no problems.

Usually, a quite simple damage prediction criterion, namely energy density, is employed because the kill criteria and the kill mechanisms for the individual components are in most of the cases not known with sufficient accuracy (Fig. 57 - NWC). Energy involves mass and velocity in terms of the known relationship, which for many components may be not absolutely correct, but which, on the other hand, should not be too far from reality. This criterion is correct at least in the case when, so-to-say, gauge firings have been made within the ranges of the applicable and given fragment masses and velocities. The more the fragment velocities and masses depart from the gauge firings, the greater will be the deviation from reality.

Several other examples of trial firings against aircraft components are presented, in which synergistic effects have occurred, owing mainly to very high fragment velocities and high rate of impact.

SUMMARY

Direct hits are certainly the most effective ones. When an SAP warhead of a missile detonates inside a target, a very high kill probability can be expected owing to the relatively high warhead mass and charge weight as compared to those of a medium-caliber projectile. When the missile is not too small, its weight alone will suffice for a considerable damage to be done in an air target in the case of a direct hit.

When a missile is likely not to hit the target, it will have to carry a warhead that transfers energy from the missile's trajectory into the target. By a suitable proximity fuze, the warhead must be initiated at the "right" moment, as the missile passes by the target, and the energy stored in the high explosive charge will then be released.

The blast wave acts to all sides, but it has a comparatively short range as compared to a fragment warhead. Fragments are much more efficient in transporting energy from the missile, or warhead, to the target, but they can do this only along their discrete trajectories. The possible range depends in this case on the weight of the warhead and, hence, on the number and velocity of the fragments as well as on the size and hardness of the target, on the engagement situation, and on the type of fragments and on the density of the hits.

As to aimable warheads, a moderate gain in the range of 20 to 40 % can be obtained, with a relatively small development and production effort, through steerable warheads, and a gain by a factor of 2 to 4 can be obtained by detonatively deformable warheads, though only with greater effort in development (Fig. 58 - 7496).

The advantages and disadvantages of the various types of warheads, and a relative cost comparison with a natural-fragment warhead are shown in Fig. 59 - 9469.

Today, conventional fragment warheads have more or less reached a technological limit that permits only insignificant improvements, or rather adaptations to missile systems and optimizations for modern air targets, to be made. Aimable warheads, however, constitute a considerable potential which does not yet seem to approach a technological limit of development (Fig. 60 - 7868 a). Therefore, considerable effort should be directed towards developing and productionizing this type of warhead. This could bring about a real technological progress in air target defence.

Air Targets

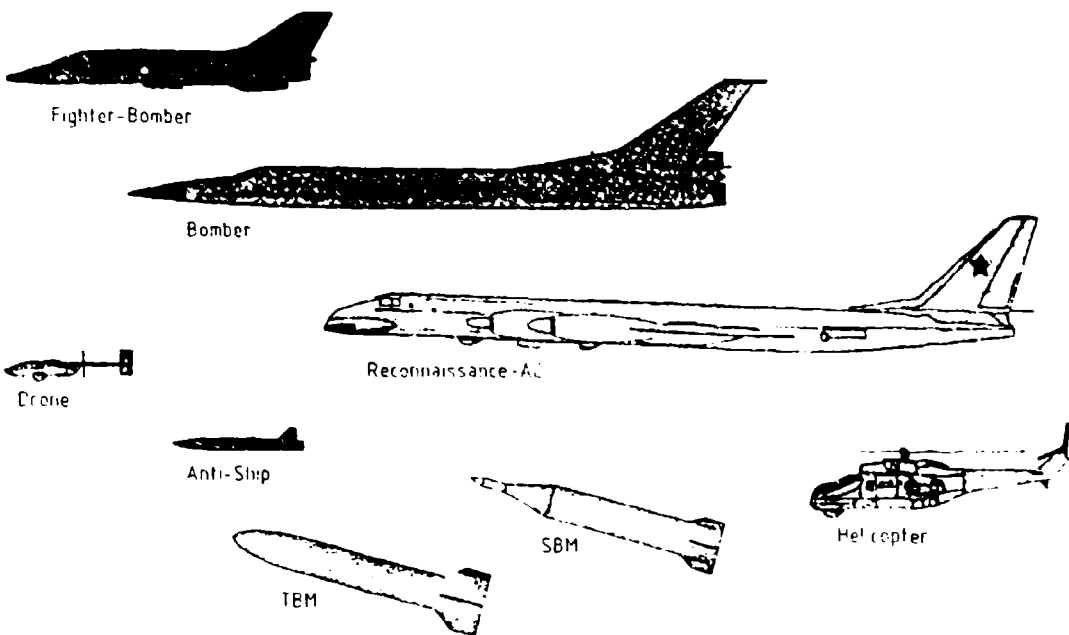


Fig. 1

Direct Hits against Air Targets

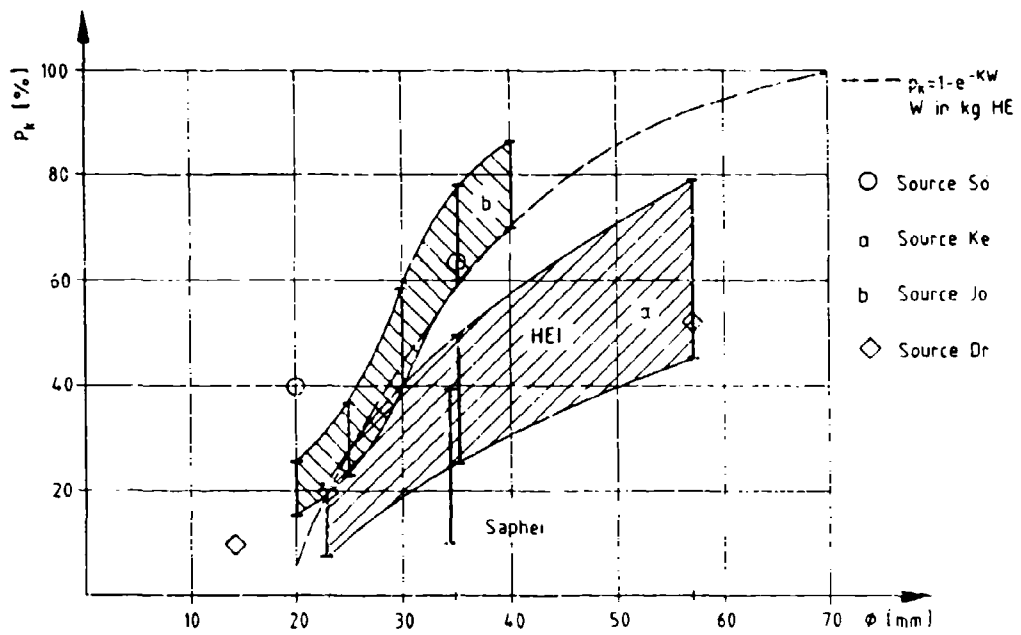


Fig. 6

Surface-to-Air Missiles

Designation	Launch Mass kg	Speed	Kinetic E kg TNT
Rapier	43	Ma 2,0	1,8
Crotale	80	Ma 2,3	4,5
Indigo	121	Ma 2,5	8,1
Roland	63	Ma 1,6	1,7
Chaparral	84	Ma 2,5	5,6
SA 2 (Guideline)	2300	Ma 3,5	302,0
SA 3 (Goa)	950	Ma 3,5	125,0
SA 4 (Ganef)	2500	Ma 2,5	168,0
SA 6 (Gainful)	550	Ma 2,8	46,0
SA 7 (Grail)	9,2	Ma 1,5	0,2
SA 8 (Gecko)	190	Ma 2,0	8,1
SA 9 (Gaskin)	30	Ma 2,0	1,3
SA 10	1500	Ma 6,0	580,0

Fig. 7

Near Pass

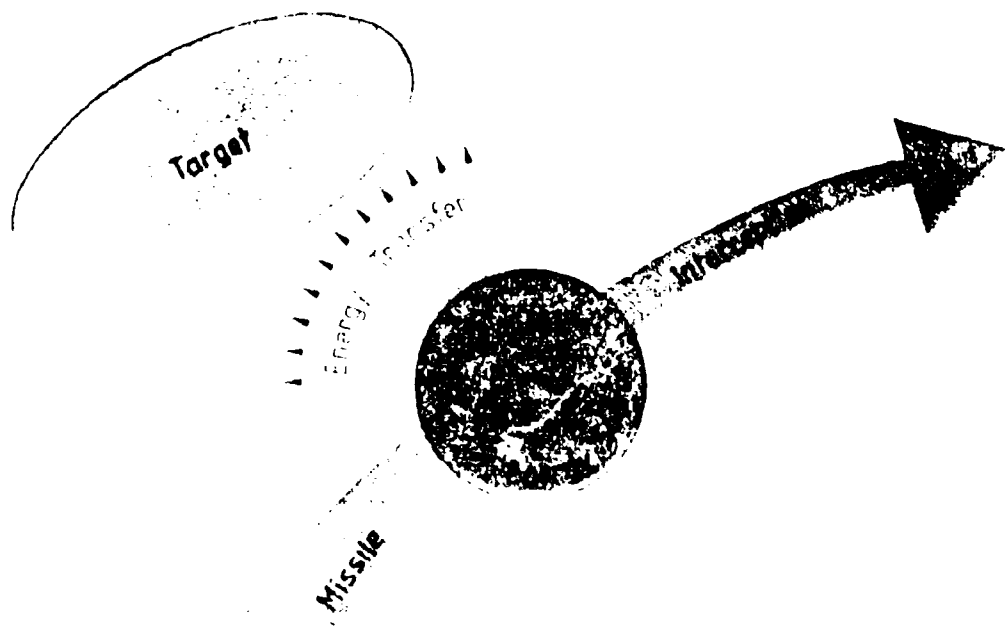


Fig. 8

High Explosives

Detonation = 8×10^3 m/s
 Energy (only) = 5×10^6 J/kg
 Power (10 μ s) = 5×10^{11} W/kg
 Gaseous Products = 10^3 ltr/kg
 Temperature = 10^3 °K

Reaction Rate

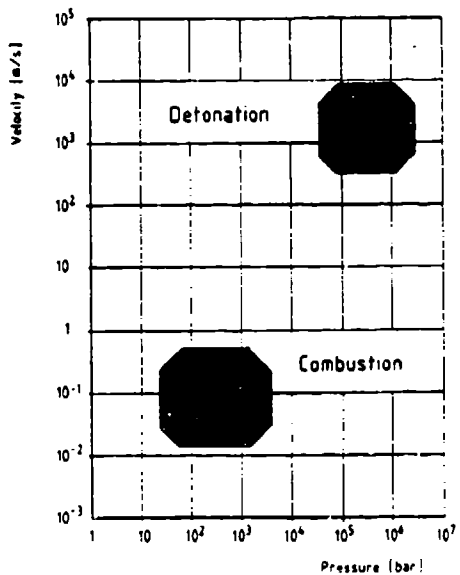


Fig. 9

Fig. 10

DIN 20163

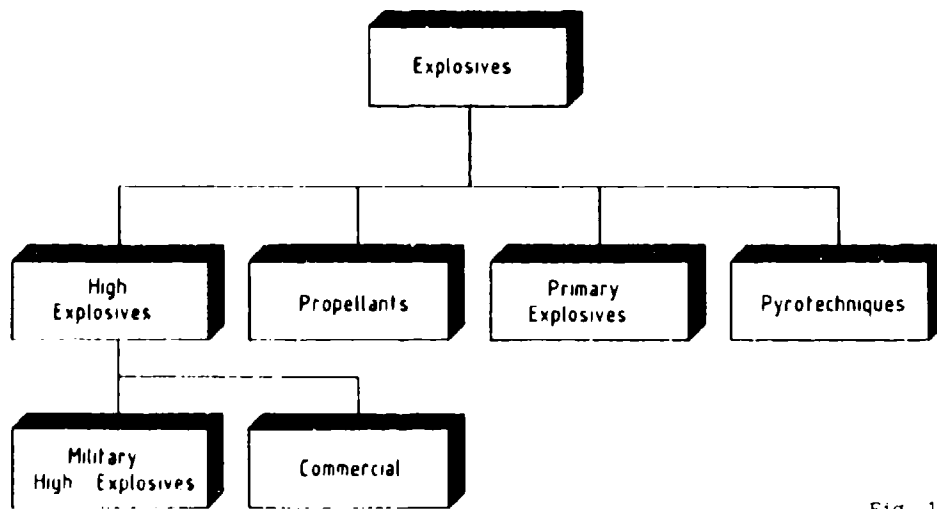


Fig. 11

Warhead-Types for Anti-Air Targets

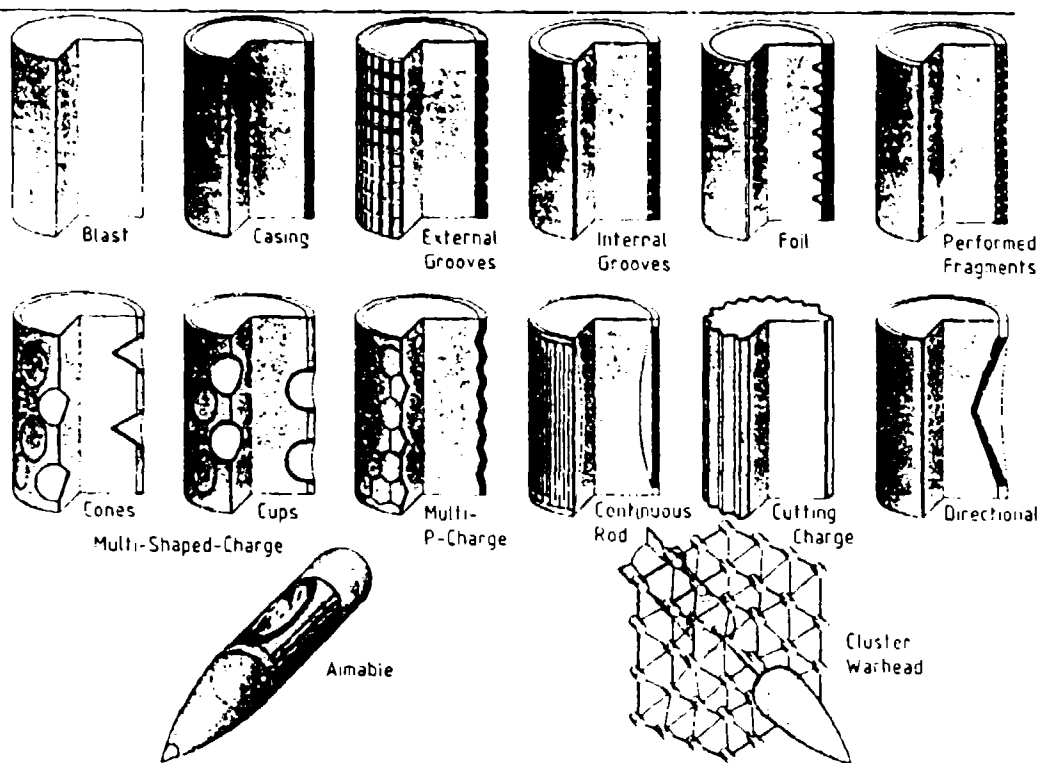
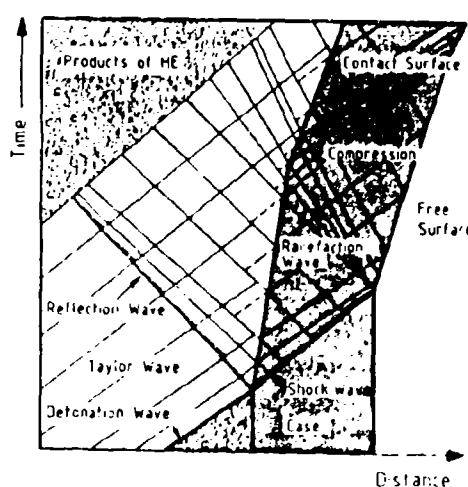


Fig. 16

Fragment Acceleration

Shock Load



Expanding Products of HE

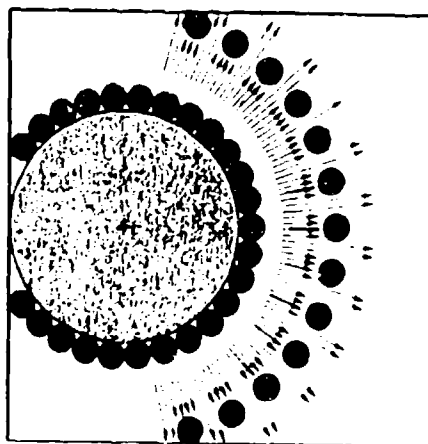


Fig. 18

Structural Kill Criteria

✓ Energy - Energydensity

$$K_s = \sqrt{E \cdot (E/A)} = E/\sqrt{A}$$

$$\text{Dimension - Force } N = \frac{N \cdot m}{\sqrt{m}}$$

$$K_s = \frac{n \cdot m \cdot v_{cr}^2}{2 \cdot \sqrt{A}}$$

$$n = \frac{2K_s \cdot \sqrt{A}}{m \cdot v_{cr}^2}$$

$$m = \frac{2K_s \cdot \sqrt{A}}{n \cdot v_{cr}^2}$$

$$v_{cr} = \sqrt{\frac{2K_s \cdot \sqrt{A}}{m \cdot n}}$$

Fig. 22

Power-Density-Criterium

$$\frac{P}{A} = \frac{E / \Delta t}{A} = \frac{n \cdot E_n}{A \cdot \Delta t}$$

$$\text{from } r = \frac{R}{v} \text{ follows } \Delta t / v = \frac{R}{v^2} \cdot \Delta v$$

$$\frac{n \cdot E_n \cdot v^2}{A \cdot R \cdot \Delta v} = \frac{n \cdot E_n}{A \cdot R} \cdot \frac{v}{\Delta v / v} = \frac{n}{A} \cdot \frac{m \cdot v^3}{2R \cdot \Delta v / v}$$

$$\text{with } \frac{n}{A} = \hat{n}$$

$$\frac{P}{A} = \hat{n} \cdot \frac{m \cdot v^3}{2R \cdot \Delta v / v}$$

Fig. 23

Critic...

s and Kill Mechanisms

Crit. Component	Crit. Parameter	Velocity	Res Pen	Φ Hole	Momentum	Energy	Energy Density	Force	Power
Crew			x						
Electronics			x	x					
Cable Trees				x					
Controls				x					
Actuator				x					
Fuel Line				x					
Fuel Tank				x		x			(x)
Rotor Blades				x					
Engine				x					
Structure					x	(x)	x		(x)
Gearing									
Propellant		(x)							
HE		x							

Fig. 24

Definitions

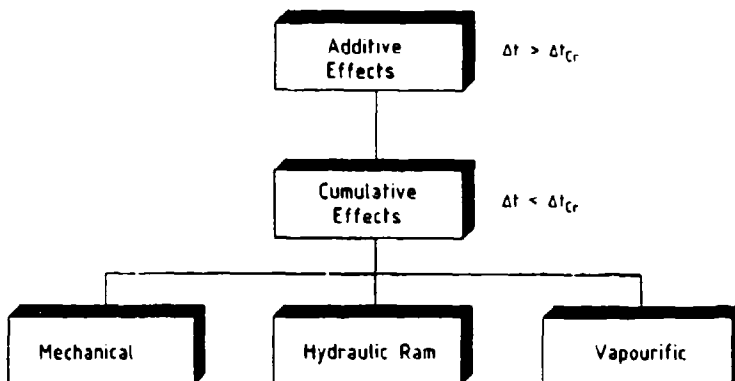


Fig. 26

Multiple Fragment Impacts

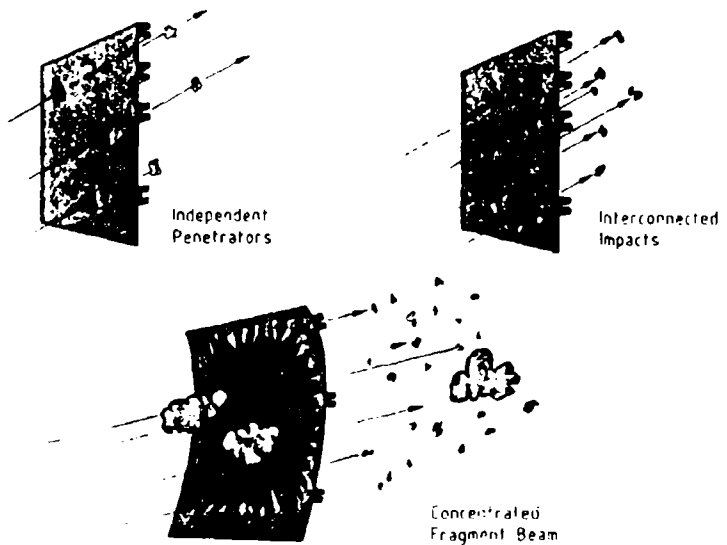


Fig. 27

$\Delta t_{\text{critical}}$?

- Shock Wave in Metal

$$\Delta t < 10 \text{ } \mu\text{sec} \quad (150 \text{ mm } 5 \frac{\text{mm}}{\mu\text{sec}})$$

- Shock Wave in Liquids

$$\Delta t < 100 \text{ } \mu\text{sec} \quad (150 \text{ mm } 1,5 \frac{\text{mm}}{\mu\text{sec}})$$

- Internal Blast (vapourific effect)

$$\Delta t < 1 \text{ msec}$$



Fig. 41

Different Possible Fragment Distributions

Conical

Fragment Distribution



Parallel

Fragment Distribution



Continuous

Rad



Aimable

Fragment Distribution

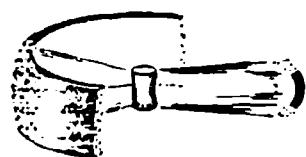
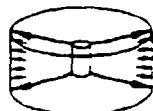


Fig. 42

Hit Densities \bar{n}

$$1: \frac{\text{Number of Fragments } n}{\text{Area } A}$$

$$n = \frac{A}{2\pi R (R \cdot l_1 \cdot c_1 + l_2 \cdot c_2) + L_{WH}}$$



$$1: R \cdot l_1 \cdot c_1 + l_2 \cdot c_2 + L_{WH}$$

$$A = \frac{A}{2\pi R^2 (l_1 \cdot c_1 + l_2 \cdot c_2)}$$

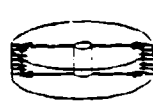
$$n \sim 1/R$$



$$2: c_1 = c_2 = 0$$

$$A = \frac{A}{2\pi R^2 \cdot \pi n}$$

$$n \sim 1/A$$



$$3: c_1 = c_2 = 0 \quad \alpha = 0$$

$$\delta = n_0 / n = \text{const}$$

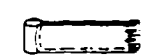


Fig. 43

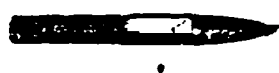
Orientation of Effectiveness



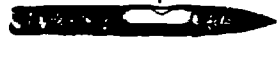
Omni-Directional

Elevational Directional-
Planar Focussing

Radial-Aimable



Axial-Directional



Radial-Directional

Multi-
Radial-Directional

Fig. 44

Aimable Warhead



STEERABLE



OPENING



DEFORMABLE

Fig. 45

Warhead / Missile Costs

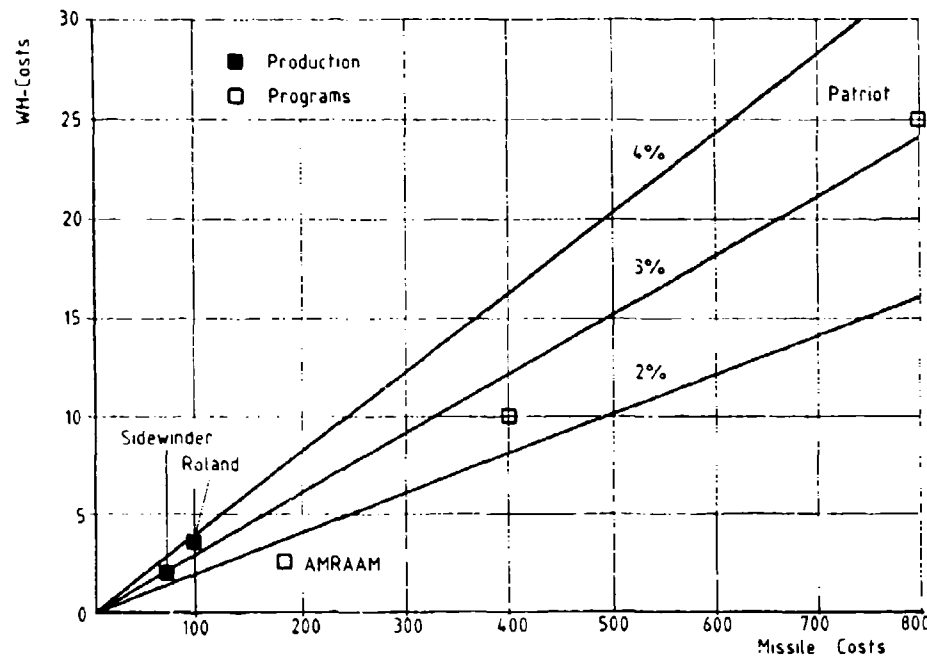


Fig. 54

AAM's and SAM's

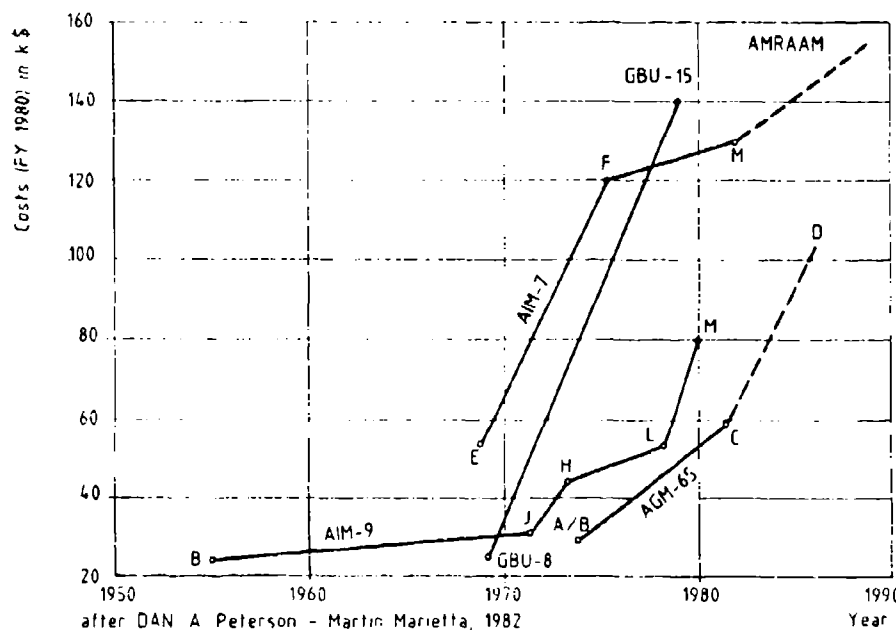


Fig. 55

Vulnerability Model Structure

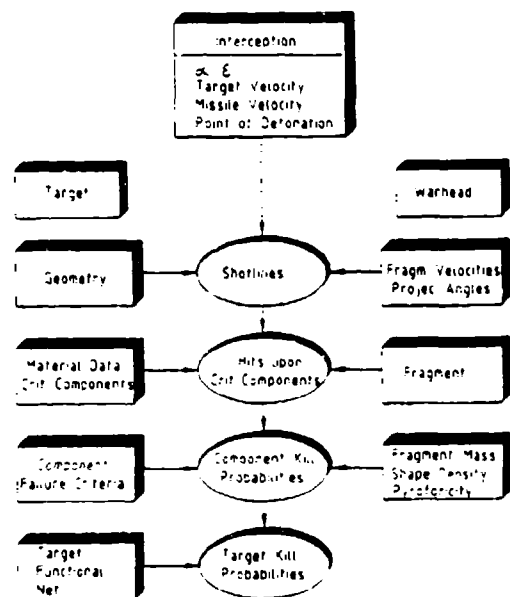


Fig. 56

Effectiveness in Respect to Aerial Targets

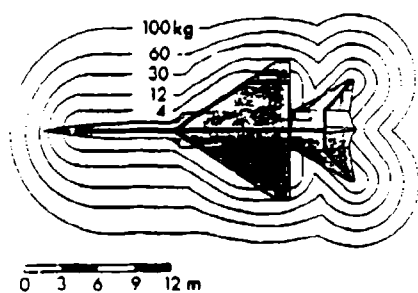
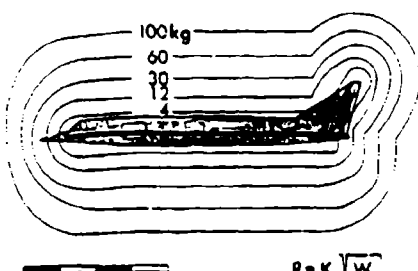


Fig. 15

Kill - Mechanisms

Perforation	P
P x Diameter	P x ϕ
$P \times \phi^2 \approx V$	V
Impuls I	I
Energy	E
Structure	N
Power	P ₀

All values also correlated to hit density

Fig. 20

Energy-Volume Relationship

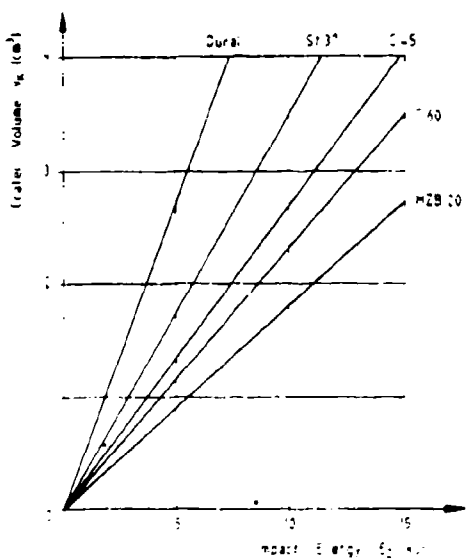


Fig. 21

Performance of anti-aircraft Warheads

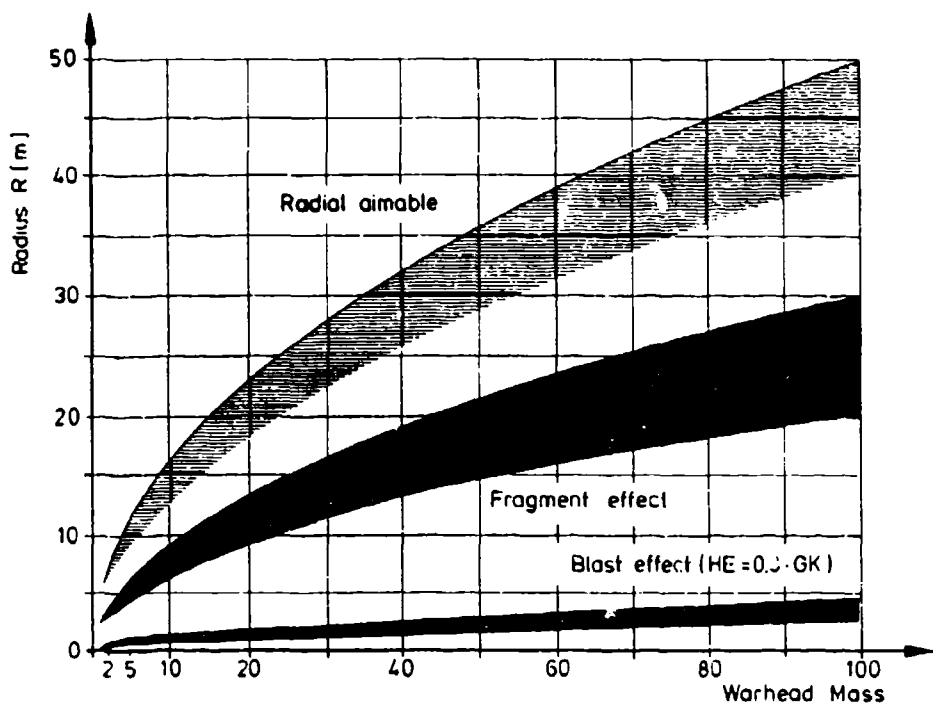


Fig. 58

Air Target Warheads—advantages, disadvantages, cost comparison and examples of use

Warhead type	Advantages	Disadvantages	Approximate cost per kg of explosive	Example of use
Pressure warhead	inexpensive	low effective radius (direct hit necessary)	0.6	None
Fragmentation warhead with smooth frag casing	simple structure, cheap, high structural rigidity	non-explosive area of large and small fragments	1	AA 1, 2, 3, 4, 5, 6, 7, 8, 9, 10, 11, 12, 13, 14, 15, 16, 17, 18, 19, 20, 21, 22, 23, 24, 25, 26, 27, 28, 29, 30, 31, 32, 33, 34, 35, 36, 37, 38, 39, 40, 41, 42, 43, 44, 45, 46, 47, 48, 49, 50, 51, 52, 53, 54, 55, 56, 57, 58, 59, 60, 61, 62, 63, 64, 65, 66, 67, 68, 69, 70, 71, 72, 73, 74, 75, 76, 77, 78, 79, 80, 81, 82, 83, 84, 85, 86, 87, 88, 89, 90, 91, 92, 93, 94, 95, 96, 97, 98, 99, 100, 101, 102, 103, 104, 105, 106, 107, 108, 109, 110, 111, 112, 113, 114, 115, 116, 117, 118, 119, 120, 121, 122, 123, 124, 125, 126, 127, 128, 129, 130, 131, 132, 133, 134, 135, 136, 137, 138, 139, 140, 141, 142, 143, 144, 145, 146, 147, 148, 149, 150, 151, 152, 153, 154, 155, 156, 157, 158, 159, 160, 161, 162, 163, 164, 165, 166, 167, 168, 169, 170, 171, 172, 173, 174, 175, 176, 177, 178, 179, 180, 181, 182, 183, 184, 185, 186, 187, 188, 189, 190, 191, 192, 193, 194, 195, 196, 197, 198, 199, 200, 201, 202, 203, 204, 205, 206, 207, 208, 209, 210, 211, 212, 213, 214, 215, 216, 217, 218, 219, 220, 221, 222, 223, 224, 225, 226, 227, 228, 229, 230, 231, 232, 233, 234, 235, 236, 237, 238, 239, 240, 241, 242, 243, 244, 245, 246, 247, 248, 249, 250, 251, 252, 253, 254, 255, 256, 257, 258, 259, 260, 261, 262, 263, 264, 265, 266, 267, 268, 269, 270, 271, 272, 273, 274, 275, 276, 277, 278, 279, 280, 281, 282, 283, 284, 285, 286, 287, 288, 289, 290, 291, 292, 293, 294, 295, 296, 297, 298, 299, 300, 301, 302, 303, 304, 305, 306, 307, 308, 309, 310, 311, 312, 313, 314, 315, 316, 317, 318, 319, 320, 321, 322, 323, 324, 325, 326, 327, 328, 329, 330, 331, 332, 333, 334, 335, 336, 337, 338, 339, 340, 341, 342, 343, 344, 345, 346, 347, 348, 349, 350, 351, 352, 353, 354, 355, 356, 357, 358, 359, 360, 361, 362, 363, 364, 365, 366, 367, 368, 369, 370, 371, 372, 373, 374, 375, 376, 377, 378, 379, 380, 381, 382, 383, 384, 385, 386, 387, 388, 389, 390, 391, 392, 393, 394, 395, 396, 397, 398, 399, 400, 401, 402, 403, 404, 405, 406, 407, 408, 409, 410, 411, 412, 413, 414, 415, 416, 417, 418, 419, 420, 421, 422, 423, 424, 425, 426, 427, 428, 429, 430, 431, 432, 433, 434, 435, 436, 437, 438, 439, 440, 441, 442, 443, 444, 445, 446, 447, 448, 449, 450, 451, 452, 453, 454, 455, 456, 457, 458, 459, 460, 461, 462, 463, 464, 465, 466, 467, 468, 469, 470, 471, 472, 473, 474, 475, 476, 477, 478, 479, 480, 481, 482, 483, 484, 485, 486, 487, 488, 489, 490, 491, 492, 493, 494, 495, 496, 497, 498, 499, 500, 501, 502, 503, 504, 505, 506, 507, 508, 509, 510, 511, 512, 513, 514, 515, 516, 517, 518, 519, 520, 521, 522, 523, 524, 525, 526, 527, 528, 529, 530, 531, 532, 533, 534, 535, 536, 537, 538, 539, 540, 541, 542, 543, 544, 545, 546, 547, 548, 549, 550, 551, 552, 553, 554, 555, 556, 557, 558, 559, 560, 561, 562, 563, 564, 565, 566, 567, 568, 569, 570, 571, 572, 573, 574, 575, 576, 577, 578, 579, 580, 581, 582, 583, 584, 585, 586, 587, 588, 589, 589, 590, 591, 592, 593, 594, 595, 596, 597, 598, 599, 600, 601, 602, 603, 604, 605, 606, 607, 608, 609, 610, 611, 612, 613, 614, 615, 616, 617, 618, 619, 620, 621, 622, 623, 624, 625, 626, 627, 628, 629, 630, 631, 632, 633, 634, 635, 636, 637, 638, 639, 640, 641, 642, 643, 644, 645, 646, 647, 648, 649, 650, 651, 652, 653, 654, 655, 656, 657, 658, 659, 660, 661, 662, 663, 664, 665, 666, 667, 668, 669, 669, 670, 671, 672, 673, 674, 675, 676, 677, 678, 679, 680, 681, 682, 683, 684, 685, 686, 687, 688, 689, 689, 690, 691, 692, 693, 694, 695, 696, 697, 698, 699, 699, 700, 701, 702, 703, 704, 705, 706, 707, 708, 709, 709, 710, 711, 712, 713, 714, 715, 716, 717, 718, 719, 719, 720, 721, 722, 723, 724, 725, 726, 727, 728, 729, 729, 730, 731, 732, 733, 734, 735, 736, 737, 738, 739, 739, 740, 741, 742, 743, 744, 745, 746, 747, 748, 749, 749, 750, 751, 752, 753, 754, 755, 756, 757, 758, 759, 759, 760, 761, 762, 763, 764, 765, 766, 767, 768, 769, 769, 770, 771, 772, 773, 774, 775, 776, 777, 778, 779, 779, 780, 781, 782, 783, 784, 785, 786, 787, 788, 789, 789, 790, 791, 792, 793, 794, 795, 796, 797, 798, 799, 799, 800, 801, 802, 803, 804, 805, 806, 807, 808, 809, 809, 810, 811, 812, 813, 814, 815, 816, 817, 818, 819, 819, 820, 821, 822, 823, 824, 825, 826, 827, 828, 829, 829, 830, 831, 832, 833, 834, 835, 836, 837, 838, 839, 839, 840, 841, 842, 843, 844, 845, 846, 847, 848, 849, 849, 850, 851, 852, 853, 854, 855, 856, 857, 858, 859, 859, 860, 861, 862, 863, 864, 865, 866, 867, 868, 869, 869, 870, 871, 872, 873, 874, 875, 876, 877, 878, 879, 879, 880, 881, 882, 883, 884, 885, 886, 887, 888, 889, 889, 890, 891, 892, 893, 894, 895, 896, 897, 898, 899, 899, 900, 901, 902, 903, 904, 905, 906, 907, 908, 909, 909, 910, 911, 912, 913, 914, 915, 916, 917, 918, 919, 919, 920, 921, 922, 923, 924, 925, 926, 927, 928, 929, 929, 930, 931, 932, 933, 934, 935, 936, 937, 938, 939, 939, 940, 941, 942, 943, 944, 945, 946, 947, 948, 949, 949, 950, 951, 952, 953, 954, 955, 956, 957, 958, 959, 959, 960, 961, 962, 963, 964, 965, 966, 967, 968, 969, 969, 970, 971, 972, 973, 974, 975, 976, 977, 978, 979, 979, 980, 981, 982, 983, 984, 985, 986, 987, 988, 989, 989, 990, 991, 992, 993, 994, 995, 996, 997, 998, 999, 999, 1000, 1001, 1002, 1003, 1004, 1005, 1006, 1007, 1008, 1009, 1009, 1010, 1011, 1012, 1013, 1014, 1015, 1016, 1017, 1018, 1019, 1019, 1020, 1021, 1022, 1023, 1024, 1025, 1026, 1027, 1028, 1029, 1029, 1030, 1031, 1032, 1033, 1034, 1035, 1036, 1037, 1038, 1039, 1039, 1040, 1041, 1042, 1043, 1044, 1045, 1046, 1047, 1048, 1049, 1049, 1050, 1051, 1052, 1053, 1054, 1055, 1056, 1057, 1058, 1059, 1059, 1060, 1061, 1062, 1063, 1064, 1065, 1066, 1067, 1068, 1069, 1069, 1070, 1071, 1072, 1073, 1074, 1075, 1076, 1077, 1078, 1079, 1079, 1080, 1081, 1082, 1083, 1084, 1085, 1086, 1087, 1088, 1089, 1089, 1090, 1091, 1092, 1093, 1094, 1095, 1096, 1097, 1097, 1098, 1099, 1099, 1100, 1101, 1102, 1103, 1104, 1105, 1106, 1107, 1108, 1109, 1109, 1110, 1111, 1112, 1113, 1114, 1115, 1116, 1117, 1118, 1119, 1119, 1120, 1121, 1122, 1123, 1124, 1125, 1126, 1127, 1128, 1129, 1129, 1130, 1131, 1132, 1133, 1134, 1135, 1136, 1137, 1138, 1139, 1139, 1140, 1141, 1142, 1143, 1144, 1145, 1146, 1147, 1148, 1149, 1149, 1150, 1151, 1152, 1153, 1154, 1155, 1156, 1157, 1158, 1159, 1159, 1160, 1161, 1162, 1163, 1164, 1165, 1166, 1167, 1168, 1169, 1169, 1170, 1171, 1172, 1173, 1174, 1175, 1176, 1177, 1178, 1179, 1179, 1180, 1181, 1182, 1183, 1184, 1185, 1186, 1187, 1188, 1189, 1189, 1190, 1191, 1192, 1193, 1194, 1195, 1196, 1197, 1197, 1198, 1199, 1199, 1200, 1201, 1202, 1203, 1204, 1205, 1206, 1207, 1208, 1209, 1209, 1210, 1211, 1212, 1213, 1214, 1215, 1216, 1217, 1218, 1219, 1219, 1220, 1221, 1222, 1223, 1224, 1225, 1226, 1227, 1228, 1229, 1229, 1230, 1231, 1232, 1233, 1234, 1235, 1236, 1237, 1238, 1239, 1239, 1240, 1241, 1242, 1243, 1244, 1245, 1246, 1247, 1248, 1249, 1249, 1250, 1251, 1252, 1253, 1254, 1255, 1256, 1257, 1258, 1259, 1259, 1260, 1261, 1262, 1263, 1264, 1265, 1266, 1267, 1268, 1269, 1269, 1270, 1271, 1272, 1273, 1274, 1275, 1276, 1277, 1278, 1279, 1279, 1280, 1281, 1282, 1283, 1284, 1285, 1286, 1287, 1288, 1289, 1289, 1290, 1291, 1292, 1293, 1294, 1295, 1296, 1297, 1297, 1298, 1299, 1299, 1300, 1301, 1302, 1303, 1304, 1305, 1306, 1307, 1308, 1309, 1309, 1310, 1311, 1312, 1313, 1314, 1315, 1316, 1317, 1318, 1319, 1319, 1320, 1321, 1322, 1323, 1324, 1325, 1326, 1327, 1328, 1329, 1329, 1330, 1331, 1332, 1333, 1334, 1335, 1336, 1337, 1338, 1339, 1339, 1340, 1341, 1342, 1343, 1344, 1345, 1346, 1347, 1348, 1349, 1349, 1350, 1351, 1352, 1353, 1354, 1355, 1356, 1357, 1358, 1359, 1359, 1360, 1361, 1362, 1363, 1364, 1365, 1366, 1367, 1368, 1369, 1369, 1370, 1371, 1372, 1373, 1374, 1375, 1376, 1377, 1378, 1379, 1379, 1380, 1381, 1382, 1383, 1384, 1385, 1386, 1387, 1388, 1389, 1389, 1390, 1391, 1392, 1393, 1394, 1395, 1396, 1397, 1397, 1398, 1399, 1399, 1400, 1401, 1402, 1403, 1404, 1405, 1406, 1407, 1408, 1409, 1409, 1410, 1411, 1412, 1413, 1414, 1415, 1416, 1417, 1418, 1419, 1419, 1420, 1421, 1422, 1423, 1424, 1425, 1426, 1427, 1428, 1429, 1429, 1430, 1431, 1432, 1433, 1434, 1435, 1436, 1437, 1438, 1439, 1439, 1440, 1441, 1442, 1443, 1444, 1445, 1446, 1447, 1448, 1449, 1449, 1450, 1451, 1452, 1453, 1454, 1455, 1456, 1457, 1458, 1459, 1459, 1460, 1461, 1462, 1463, 1464, 1465, 1466, 1467, 1468, 1469, 1469, 1470, 1471, 1472, 1473, 1474, 1475, 1476, 1477, 1478, 1479, 1479, 1480, 1481, 1482, 1483, 1484, 1485, 1486, 1487, 1488, 1489, 1489, 1490, 1491, 1492, 1493, 1494, 1495, 1496, 1497, 1497, 1498, 1499, 1499, 1500, 1501, 1502, 1503, 1504, 1505, 1506, 1507, 1508, 1509, 1509, 1510, 1511, 1512, 1513, 1514, 1515, 1516, 1517, 1518, 1519, 1519, 1520, 1521, 1522, 1523, 1524, 1525, 1526, 1527, 1528, 1529, 1529, 1530, 1531, 1532, 1533, 1534, 1535, 1536, 1537, 1538, 1539, 1539, 1540, 1541, 1542, 1543, 1544, 1545, 1546, 1547, 1548, 1549, 1549, 1550, 1551, 1552, 1553, 1554, 1555, 1556, 1557, 1558, 1559, 1559, 1560, 1561, 1562, 1563, 1564, 1565, 1566, 1567, 1568, 1569, 1569, 1570, 1571, 1572, 1573, 1574, 1575, 1576, 1577, 1578, 1579, 1579, 1580, 1581, 1582, 1583, 1584, 1585, 1586, 1587, 1588, 1589, 1589, 1590, 1591, 1592, 1593, 1594, 1595, 1596, 1597, 1597, 1598, 1599, 1599, 1600, 1601, 1602, 1603, 1604, 1605, 1606, 1607, 1608, 1609, 1609, 1610, 1611, 1612, 1613, 1614, 1615, 1616, 1617, 1618, 1619, 1619, 1620, 1621, 1622, 1623, 1624, 1625, 1626, 1627, 1628, 1629, 1629, 1630, 1631, 1632, 1633, 1634, 1635, 1636, 1637, 1638, 1639, 1639, 1640, 1641, 1642, 1643, 1644, 1645, 1646, 1647, 1648, 1649, 1649, 1650, 1651, 1652, 1653, 1654, 1655, 1656, 1657, 1658, 1659, 1659, 1660, 1661, 1662, 1663, 1664, 1665, 1666, 1667, 1668, 1669, 1669, 1670, 1671, 1672, 1673, 1674, 1675, 1676, 1677, 1678, 1679, 1679, 1680, 1681, 1682, 1683, 1684, 1685, 1686, 1687, 1688, 1689, 1689, 1690, 1691, 1692, 1693, 1694, 1695, 1696, 1697, 1697, 1698, 1699, 1699, 1700, 1701, 1702, 1703, 1704, 1705, 1706, 1707, 1708, 1709, 1709, 1710, 1711, 1712, 1713, 1714, 1715, 1716, 1717, 1718, 1719, 1719, 1720, 1721, 1722, 1723, 1724, 1725, 1726, 1727, 1728, 1729, 1729, 1730, 1731, 1732, 1733, 1734, 1735, 1736, 1737, 1738, 1739, 1739, 1740, 1741, 1742, 1743, 1744, 1745, 1746, 1747, 1748, 1749, 1749, 1750, 1751, 1752, 1753, 1754, 1755, 1756, 1757, 1758, 1759, 1759, 1760, 1761, 1762, 1763, 1764, 1765, 1766, 1767, 1768, 1769, 1769, 1770, 1771, 1772, 1773, 1774, 1775, 1776, 1777, 1778, 1779, 1779, 1780, 1781, 1782, 1783, 1784, 1785, 1786, 1787, 1788, 1789, 1789, 1790, 1791, 1792, 1793, 1794, 1795, 1796, 1797,

<p>AGARD Lecture Series No.135 Advisory Group for Aerospace Research and Development, NATO ADVANCED TECHNOLOGY FOR SAM SYSTEMS ANALYSIS SYNTHESIS AND SIMULATION Published May 1984 118 pages</p>	<p>AGARD-LS-135 Surface to air missiles Missile control Missile guidance Homing</p> <p>The Lecture Series considers the introduction of new technologies and techniques in the analysis, synthesis and simulation of SAM systems seen from the point of view of Guidance and Control.</p> <p>It covers:— methodology for conception of advanced systems P.T.O.</p>	<p>AGARD Lecture Series No.135 Advisory Group for Aerospace Research and Development, NATO ADVANCED TECHNOLOGY FOR SAM SYSTEMS ANALYSIS SYNTHESIS AND SIMULATION Published May 1984 118 pages</p> <p>The Lecture Series considers the introduction of new technologies and techniques in the analysis, synthesis and simulation of SAM systems seen from the point of view of Guidance and Control.</p> <p>It covers:— methodology for conception of advanced systems P.T.O.</p>	<p>AGARD-LS-135 Surface to air missiles Missile control Missile guidance Homing</p> <p>The Lecture Series considers the introduction of new technologies and techniques in the analysis, synthesis and simulation of SAM systems seen from the point of view of Guidance and Control.</p> <p>It covers:— methodology for conception of advanced systems P.T.O.</p>
---	--	--	--

REPRODUCED FROM
BEST AVAILABLE COPY

<p>new concepts for missile control, and in particular for terminal control</p> <ul style="list-style-type: none">- present capability and future technology for seeker systems simulation- warhead technologies- homing head imperfections altering missile guidance- terrain bounce countermeasures against monopulse seeker system. <p>The material in this publication was assembled to support a Lecture Series under the Sponsorship of the Guidance and Control Panel and the Consultant and Exchange Programme of AGARD presented on 25-26 June 1984 at Porz-Wahn (Cologne), Germany; on 28-29 June 1984 in Rome, Italy and on 2-3 July 1984 in London, UK.</p>	<p>new concepts for missile control, and in particular for terminal control</p> <ul style="list-style-type: none">- present capability and future technology for seeker systems simulation- warhead technologies- homing head imperfections altering missile guidance- terrain bounce countermeasures against monopulse seeker system. <p>The material in this publication was assembled to support a Lecture Series under the Sponsorship of the Guidance and Control Panel and the Consultant and Exchange Programme of AGARD presented on 25-26 June 1984 at Porz-Wahn (Cologne), Germany; on 28-29 June 1984 in Rome, Italy and on 2-3 July 1984 in London, UK.</p>
<p>ISBN 92-835-0353-8</p>	<p>ISBN 92-835-0353-8</p>

AGARD
 NATO  OTAN
 7 RUE ANCELLE · 92200 NEUILLY-SUR-SEINE
 FRANCE
 Telephone 745.08.10 · Telex 610176

**DISTRIBUTION OF UNCLASSIFIED
 AGARD PUBLICATIONS**

AGARD does NOT hold stocks of AGARD publications at the above address for general distribution. Initial distribution of AGARD publications is made to AGARD Member Nations through the following National Distribution Centres. Further copies are sometimes available from these Centres, but if not may be purchased in Microfiche or Photocopy form from the Purchase Agencies listed below.

NATIONAL DISTRIBUTION CENTRES

BELGIUM

Coordonnateur AGARD · VSL
 Etat-Major de la Force Aérienne
 Quartier Reine Elisabeth
 Rue d'Evere, 1140 Bruxelles

CANADA

Defence Science Information Services
 Department of National Defence
 Ottawa, Ontario K1A 0K2

DENMARK

Danish Defence Research Board
 Østerbrogades Kaserne
 Copenhagen Ø

FRANCE

O.N.E.R.A. (Direction)
 29 Avenue de la Division Leclerc
 92320 Chatillon sous Bagneux

GERMANY

Fachinformationszentrum Energie,
 Physik, Mathematik GmbH
 Kernforschungszentrum
 D-7514 Eggenstein-Leopoldshafen 2

GREECE

Hellenic Air Force General Staff
 Research and Development Directorate
 Holargos, Athens

ICELAND

Director of Aviation
 c/o Flugrad
 Reykjavik

UNITED STATES

National Aeronautics and Space Administration (NASA)
 Langley Field, Virginia 23365
 Attn: Report Distribution and Storage Unit

THE UNITED STATES NATIONAL DISTRIBUTION CENTRE (NASA) DOES NOT HOLD
 STOCKS OF AGARD PUBLICATIONS. AND APPLICATIONS FOR COPIES SHOULD BE MADE
 DIRECT TO THE NATIONAL TECHNICAL INFORMATION SERVICE (NTIS) AT THE ADDRESS BELOW.

PURCHASE AGENCIES

Microfiche or Photocopy

National Technical
 Information Service (NTIS)
 5205 Port Royal Road
 Springfield
 Virginia 22161, USA

Microfiche
 ESA Information Retrieval Service
 European Space Agency
 10, rue Mario Nikis
 75015 Paris, France

Microfiche or Photocopy

British Library Lending
 Division
 Boston Spa, Wetherby
 West Yorkshire LS23 7BQ
 England

Requests for microfiche or photocopies of AGARD documents should include the AGARD serial number, title, author or editor, and publication date. Requests to NTIS should include the NASA accession report number. Full bibliographical references and abstracts of AGARD publications are given in the following journals:

Scientific and Technical Aerospace Reports (STAR)
 published by NASA Scientific and Technical
 Information Branch
 NASA Headquarters (NIT-40)
 Washington D.C. 20546, USA

Government Reports Announcements (GRA)
 published by the National Technical
 Information Services, Springfield
 Virginia 22161, USA



**REPRODUCED FROM
 BEST AVAILABLE COPY**